

24

15/2-7

DET NORSKE VIDENSKAPS- AKADEMI I OSLO

Vol. 28  
1970-72

**GEOFYSISKE PUBLIKASJONER**  
**GEOPHYSICA NORVEGICA**

Vol. XXVIII. No. 1

December 1970

HÅKON MOSBY

Atlantic water in the Norwegian Sea

OSLO 1970

UNIVERSITETSFORLAGET

DET NORSKE METEOROLOGISKE INSTITUTT

BIBLIOTEKET

BLINDERN, OSLO 3

# G E O F Y S I S K E P U B L I K A S J O N E R

## G E O P H Y S I C A N O R V E G I C A

VOL. XXVIII

NO. 1

### ATLANTIC WATER IN THE NORWEGIAN SEA

BY HÅKON MOSBY

FREMLAGT I VIDENSKAPS-AKADEMIETS MØTE DEN 29DE MAI 1970

#### CONTENTS

SYMBOLS and CONSTANTS . . . . .	2
SUMMARY . . . . .	2
INTRODUCTION . . . . .	2
I. HYDROGRAPHY	
1. Stations 1935 . . . . .	3
2. Vertical distribution . . . . .	3
3. Horizontal distribution . . . . .	3
4. Dynamical computations . . . . .	7
5. Bottom and deep water . . . . .	8
6. Upper water . . . . .	13
7. Atlantic water . . . . .	17
II. THE NORWEGIAN ATLANTIC CURRENT	
1. The Atlantic water . . . . .	18
2. Continuity conditions . . . . .	19
3. Empirical model . . . . .	20
4. Thermohaline model	
a. The surface . . . . .	24
b. The sub-surface . . . . .	26
c. In the west . . . . .	27
d. In the east . . . . .	30
e. The Atlantic current . . . . .	30
f. Balance . . . . .	32
g. Summer surface layer . . . . .	32
h. Intermediate layer . . . . .	35
i. Evaporation . . . . .	37
j. Precipitation . . . . .	37
k. Fresh water . . . . .	38
5. Seasonal variations . . . . .	39
6. Winter conditions . . . . .	41
7. Vertical convection . . . . .	49
8. Final balance . . . . .	54
REFERENCES . . . . .	58
APPENDIX . . . . .	60

## SYMBOLS AND CONSTANTS

- $L \approx$  length across Atlantic current  
 $H \approx$  average depth of water layer  
 $E = 0.8 \text{ m year}^{-1}$  = evaporation  
 $P = 1.0 \text{ m year}^{-1}$  = precipitation  
 $F = 1.1 \text{ m year}^{-1}$  = fresh water supply  
 $L = 50 \text{ m year}^{-1}$  = vertical motion of deep water  
 $v = 2.1 \text{ cm sec}^{-1}$  = average speed of Atlantic current  
 $v_M = 2.74 \text{ cm sec}^{-1}$  = average speed of Atlantic current at St. M  
 Summer surface water  
 $g_t = 1.5 \cdot 10^{-7} \text{ }^\circ\text{C cm}^{-1}$ ,  $D_\sigma = 30 \text{ m}$ ,  $H = 39 \text{ m}$ ,  $L = 350 \text{ km}$  (west)  
 $g_s = 0.17 \cdot 10^{-7} \text{ } \text{‰ cm}^{-1}$ ,  $D_\sigma = 30 \text{ m}$ ,  $H = 60 \text{ m}$ ,  $L = 300 \text{ km}$  (west)  
 $g_s = 0.07 \cdot 10^{-7} \text{ } \text{‰ cm}^{-1}$ ,  $D_\sigma = 60 \text{ m}$ ,  $H = 60 \text{ m}$ ,  $L = 300 \text{ km}$  (east)  
 Intermediate water  
 $g_t = 0.9 \cdot 10^{-7} \text{ }^\circ\text{C cm}^{-1}$ ,  $g_s = 0.135 \cdot 10^{-7} \text{ } \text{‰ cm}^{-1}$ ,  $\Delta D_\sigma = 50 - 43 = 7 \text{ m}$  (west)  
 Atlantic water  
 $g_t = 1.25 \cdot 10^{-7} \text{ }^\circ\text{C cm}^{-1}$ ,  $g_s = 0.135 \cdot 10^{-7} \text{ } \text{‰ cm}^{-1}$ ,  $D_\sigma = 80 \text{ m}$ ,  $H = 330 \text{ m}$ ,  
 $L = 400 \text{ km}$   
 $G_t = 0.40^\circ\text{C}$  and  $G_s = 0.03 \text{ } \text{‰}$  per degree latitude (north-south)  
 $A = A_z / \rho =$  vertical eddy diffusivity  
 $A = 3.2 \text{ cm}^2 \text{ sec}^{-1}$  at  $d\sigma/dz = 10^{-5}$   
 $A = 0.4 \text{ cm}^2 \text{ sec}^{-1}$  at  $d\sigma/dz = 10^{-4}$   
 $B = A_x / \rho = A_y / \rho =$  horizontal eddy diffusivity  
 $B = 3 \cdot 10^7 \text{ cm}^2 \text{ sec}^{-1}$

**Summary.** The hydrography of the southern part of the Norwegian Sea was studied further on the basis of the data from the *Armauer Hansen* 1935, supplementing in particular the earlier results concerning the deep and bottom water (MOSBY 1959).

On the basis of five parallel hydrographic sections across the Norwegian Atlantic current, an average section was constructed and used for the establishment of a thermohaline model, into which were introduced the various factors influencing the Atlantic water near  $66^\circ \text{N}$ . Supported by knowledge of the seasonal variations as obtained from long time series of measurements at Weather Station M ( $66^\circ \text{N}$ ,  $2^\circ \text{E}$ ), and introducing probable values of the mentioned factors, a reasonable heat and salt balance was obtained from December to September. This led to the collection of additional data in March and December in 1965, and to a model of the effect of the vertical convection in autumn by which the heat and salt balance could be established for the whole of the year.

**Introduction.** In preparation of the International Gulf Stream investigations 1939 (HELLAND-HANSEN 1937a, 1939, 1940), an intensive survey of the southern part of the Norwegian Sea was carried out in the research vessel *Armauer Hansen* in the summer of 1935. With an approximate distance of only 20 n. miles between the stations, and with sections in each degree of latitude, HELLAND-HANSEN (1935) had hoped to

get at least "a more correct picture of the hydrographic conditions" and of the Norwegian Atlantic current up to Lofoten at  $69^{\circ}$  N. The idea was to continue similar detailed investigations farther north towards Spitsbergen. Due to the many irregularities encountered and the probable formation of large eddies the plan was changed and the area east of  $3^{\circ}$  W between  $64$  and  $67^{\circ}$  N was covered with an even denser net of stations in the summer of 1936; the distance between stations was only about 10 n. miles, and sections were taken in each half degree latitude (HELLAND-HANSEN 1936). Some general features appeared to be similar in the two years, but there were also considerable differences. This led HELLAND-HANSEN to even more concentrated investigations in 1937 (HELLAND-HANSEN 1937b, 1938), but his studies of the data from 1935 and 1936 were not finished.

In 1948 regular hydrographic investigations were started at Ocean Weather Station M (MOSBY 1954). For the study of the long time series of data collected, the surveys from 1935 and 1936 form a valuable background; they have so far been utilized for an analysis of the deep water (MOSBY 1959), and will be used here for study of the upper layers also.

## I. Hydrography

1. *The stations from 1935* are shown in Fig. 14 which corresponds to Fig. 2 of the paper from 1959, in which also the stations from 1936 are shown in Fig. 3.

2. *The vertical distribution* of temperature and salinity in the section in  $66^{\circ}$  N in 1935 was also illustrated in the paper from 1959, Figs. 6 and 7. They clearly demonstrate the wedge-shaped profile of the Norwegian Atlantic current, with its highest salinities above  $35.30\text{‰}$  together with temperatures near  $8^{\circ}\text{C}$  east of  $2^{\circ}\text{E}$  at about 75 m depth contrasting to the deep water of  $34.92\text{‰}$  and temperatures below  $0^{\circ}\text{C}$ . Similar conditions are found in the other east-west sections both in 1935 and in 1936, and all of them show the "puzzling wave-forms" discussed 60 years ago by HELLAND-HANSEN and NANSEN (1909) and which are still not fully understood. In this area they form an important part of the complex of phenomena studied in later years under the name of "variability". They may be due to internal waves, but such waves are not easily identified in the sea; they may also be due to quasi-stationary eddies. We shall return to them below.

3. *The horizontal distribution* of temperature and salinity has also been illustrated in the mentioned paper from 1959: salinity at 100, 200, 400 and 600 m in Fig. 9, temperature at 400, 600, 800, 1000, 1200, 1500, 2000 and 2500 m in Figs. 10 and 11. Within the upper layers the drawing of the isolines is made difficult by the "puzzling waves" as well as by the fact that the observations are not simultaneous. For an orientation on the general stratification, however, the following maps have been prepared. In Fig. 1 (top) the density distribution in the surface layer is illustrated by isolines of  $\sigma_t$ , drawn at some liberty on the basis of the observations at 0, 10 and 25 m depth; due to wind and waves this layer is relatively well mixed within most of the area.

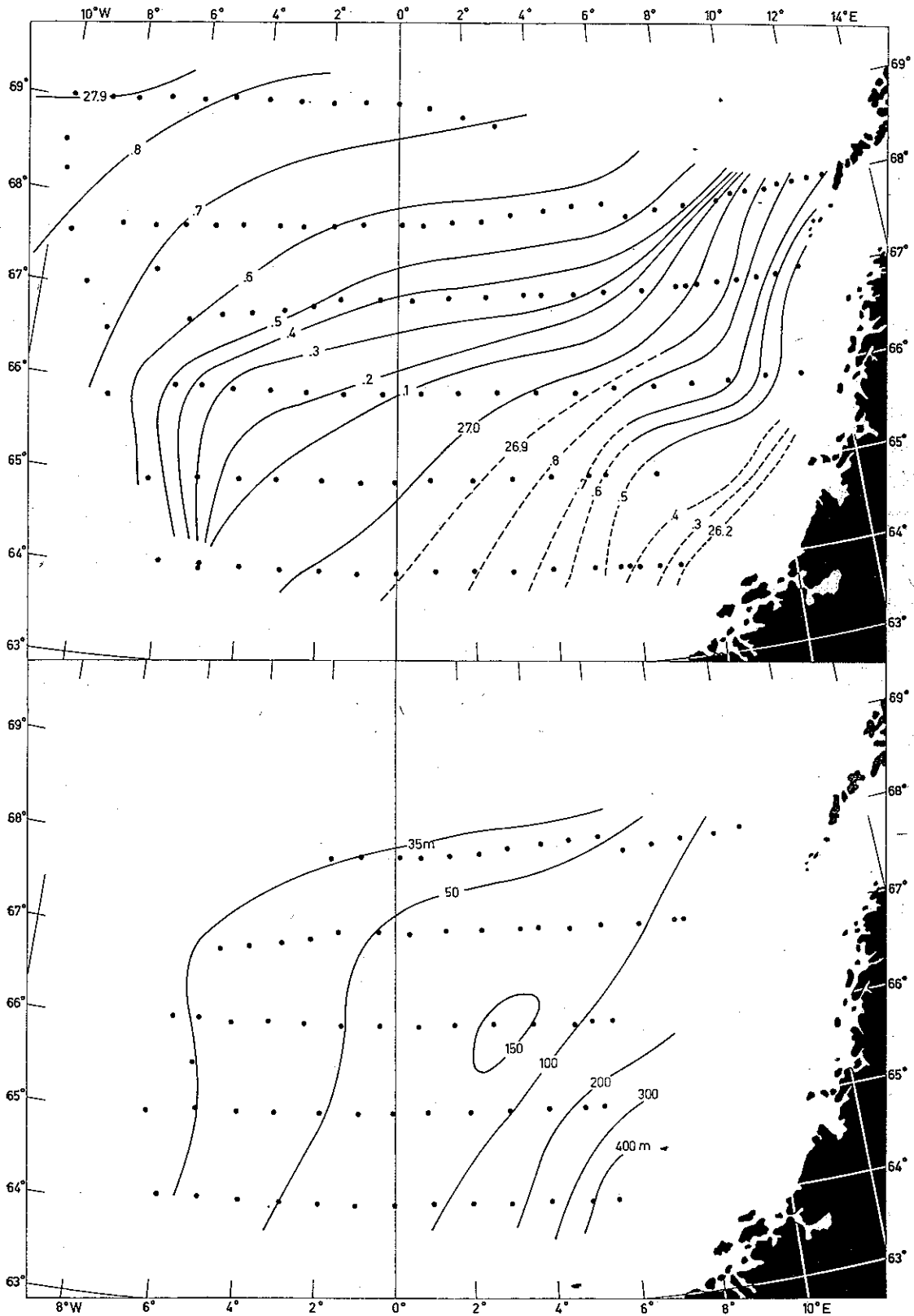


Fig. 1. Approximate  $\sigma_t$  at 0, 10 and 25 m (top) and depth of  $\sigma_t = 27.6$  (bottom).

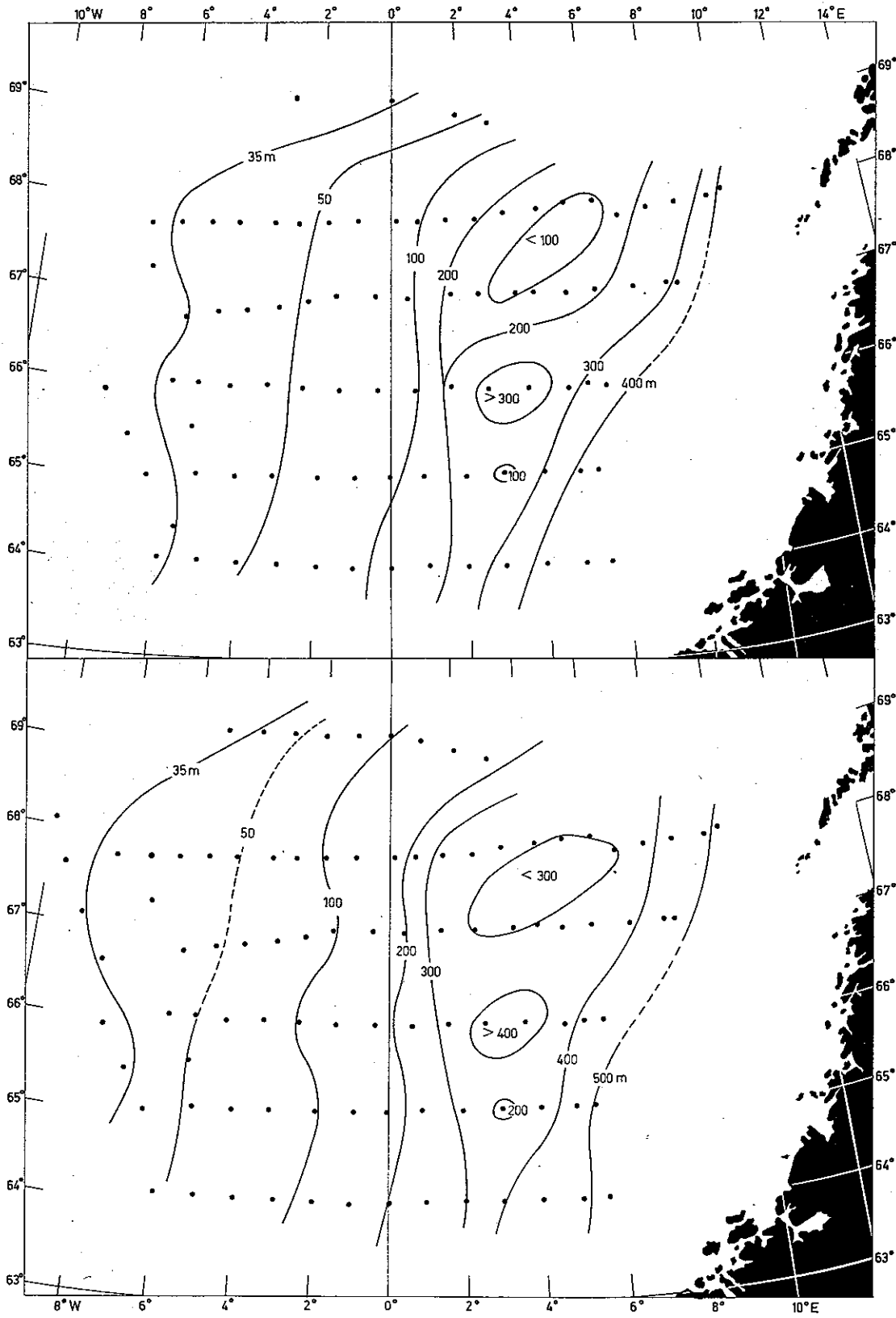


Fig. 2. Depth of  $\sigma_t = 27.7$  (top) and  $\sigma_t = 27.8$  (bottom).

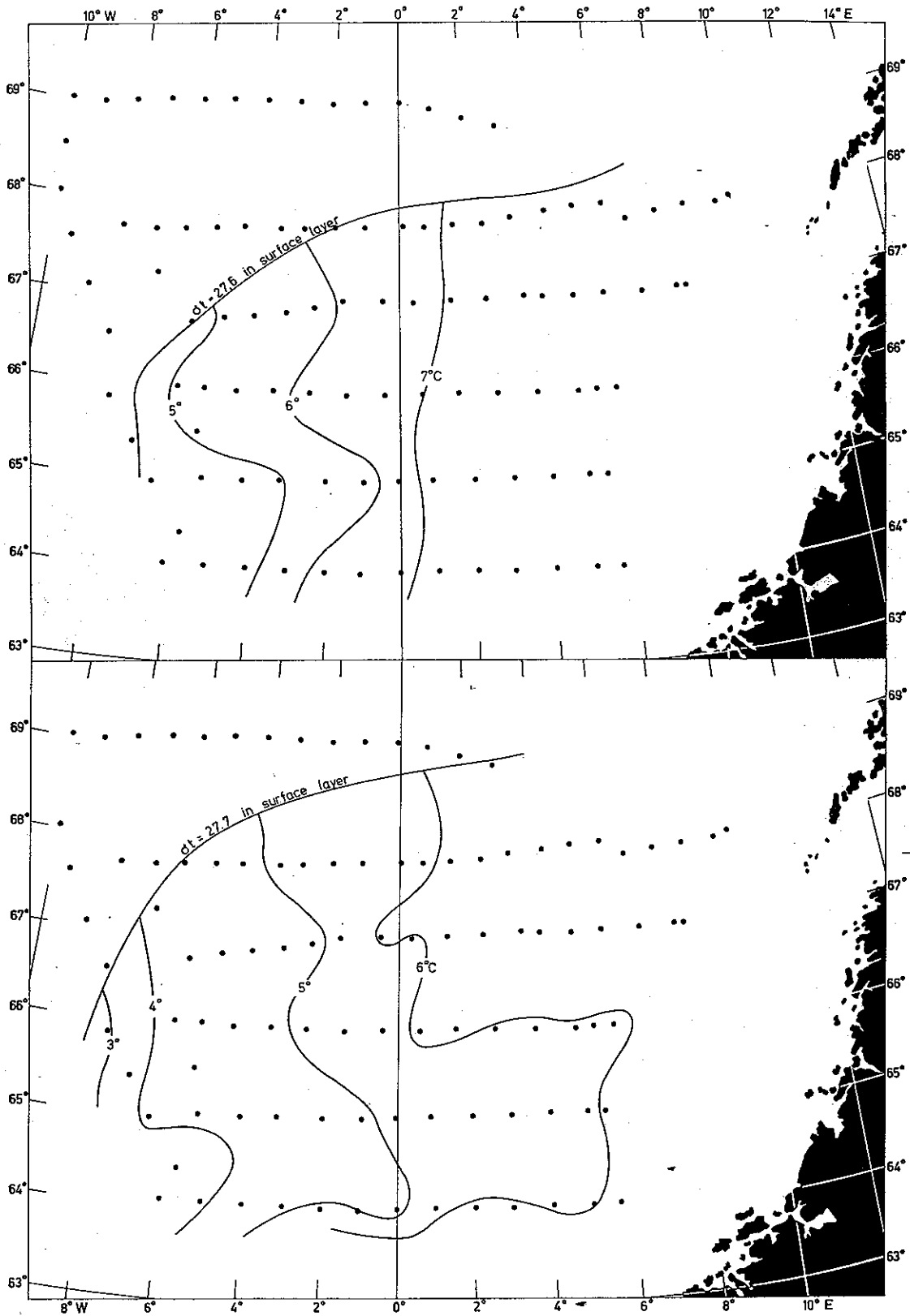


Fig. 3. Temperature at  $\sigma_t = 27.6$  (top) and  $\sigma_t = 27.7$  (bottom).

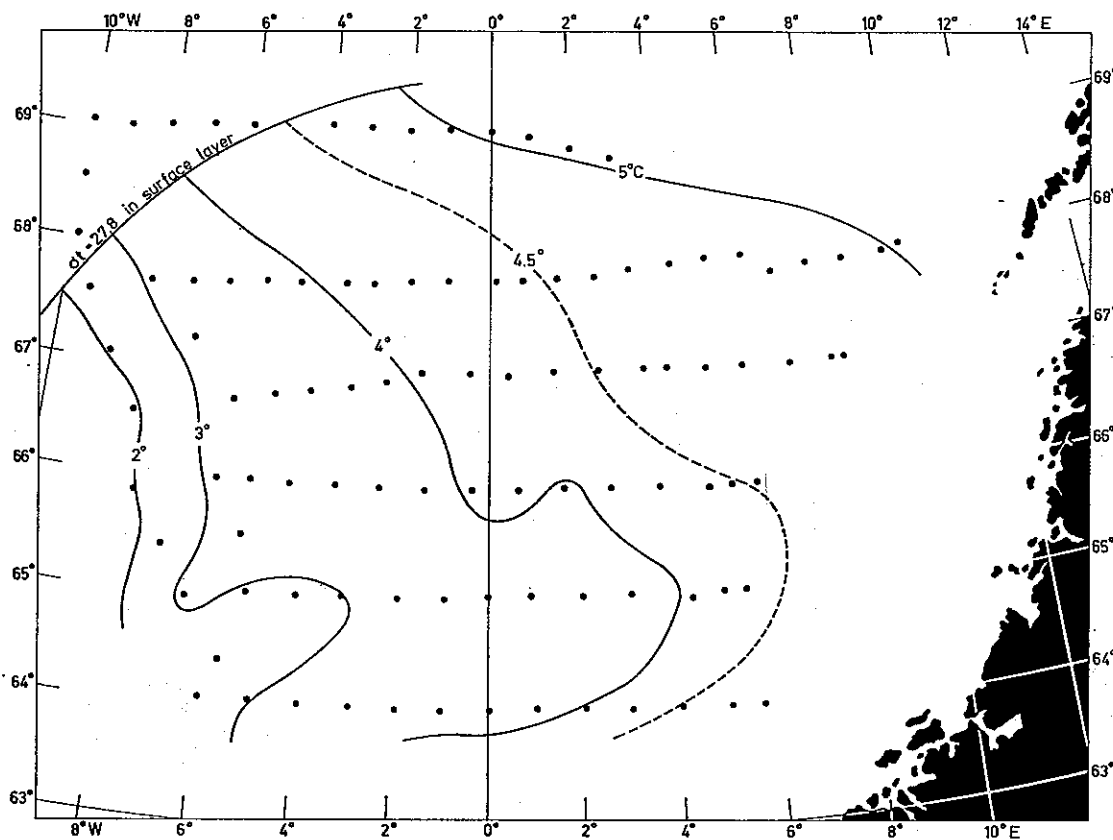


Fig. 4. Temperature at  $\sigma_t = 27.8$ .

Stations south of  $64^\circ\text{N}$  have not been taken into consideration. The dotted curves in the south-east are the most simplified. The heaviest water, with  $\sigma_t$ -values up to 27.9, is found in the north-west, the lightest with  $\sigma_t$ -values down to 26.2 in the south-east.

Within the Atlantic current the value  $\sigma_t = 27.6$  is usually found rather near to the surface, 27.7 occurs in the middle of the Atlantic water and 27.8 nearly indicates the lower limit of the latter. From Fig. 1 (bottom) it is seen that the surface of  $\sigma_t = 27.6$  reaches 400 m of depth in the south-east, rising gradually towards the north-west. The surface of  $\sigma_t = 27.7$  is seen from Fig. 2 (top) to rise from below 400 m in the east towards the west, and the surface of  $\sigma_t = 27.8$  is seen from Fig. 2 (bottom) to reach more than 500 m in the east. The highs and lows in the eastern part of the area indicate large irregularities to which we shall return below.

In Figs. 3 and 4 the temperature distribution on the same  $\sigma_t$ -surfaces is demonstrated. Within the Atlantic water, i.e. along the surfaces of  $\sigma_t = 27.6$  and 27.7, the temperature is seen to be nearly constant within a considerable area in the east, decreasing towards the west.

4. *Dynamical computations* were carried out many years ago under HELLAND-HANSEN'S very careful supervision. When the anomalies  $\Delta D$  of the dynamic depth are plotted against the depths of observation, the resulting very regular curves show a maximum



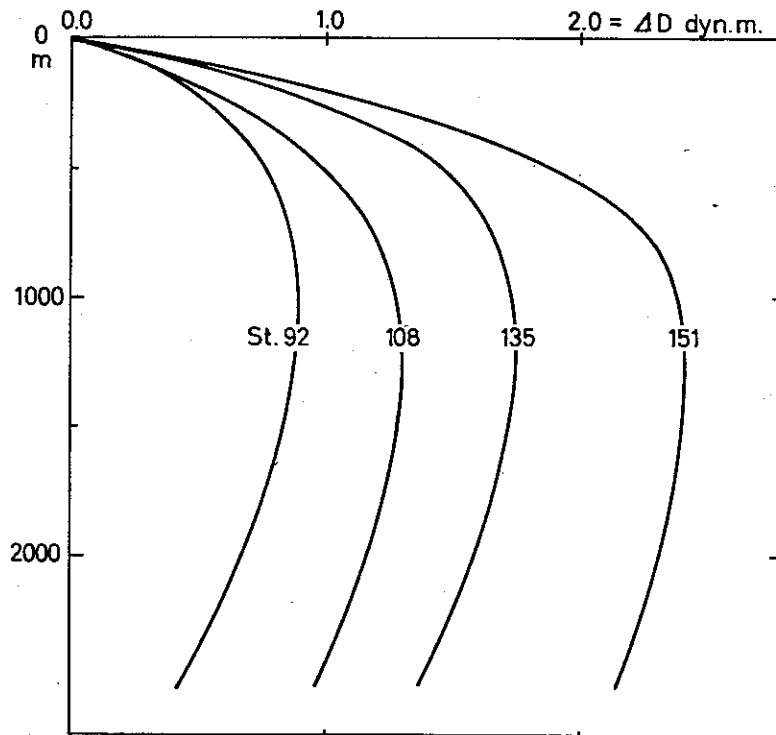


Fig. 5. Anomalies of dynamic depths in 1935.

of  $\Delta D$  at about 1200 m; a selection of these curves is reproduced in Fig. 5. Similar features were found in 1936. For our further studies it appears natural to choose a reference level within the maximum layer.

5. *Bottom and deep water.* The resulting currents at 2500, 2000 and 1500 dcb. relative to 1000 dcb. are seen on Figs. 6 and 7. At 2500 dcb. there is an axis running roughly NW-SE through stations 110 and 151, to the south of which the motion is towards the SE, while the stations to the north indicate a current in the opposite direction. At 2000 and 1500 dcb. this picture is reflected with contrasts decreasing upwards. When projecting the values from each station into a vertical plane at right angles to the axis mentioned, the average speed of motion relative to the 1000 dcb. surface is found at

2500 dcb. from 0.00040 dyn. cm per km to be  $0.30 \text{ cm sec}^{-1}$   
 2000 dcb. from 0.00017 dyn. cm per km to be  $0.13 \text{ cm sec}^{-1}$   
 1500 dcb. from 0.00009 dyn. cm per km to be  $0.07 \text{ cm sec}^{-1}$

In Fig. 7 a picture is also reproduced of the current at the sea-surface relative to the 1000 dcb. surface as found on the basis of the 2500 m stations only. In sharp contrast to the others it shows a general motion towards the north, along the eastern part of the basin; we here find at

0 dcb. from 0.044 dyn. cm per km  $33.01 \text{ cm sec}^{-1}$

or more than a hundred times the speed at 2500 dcb.

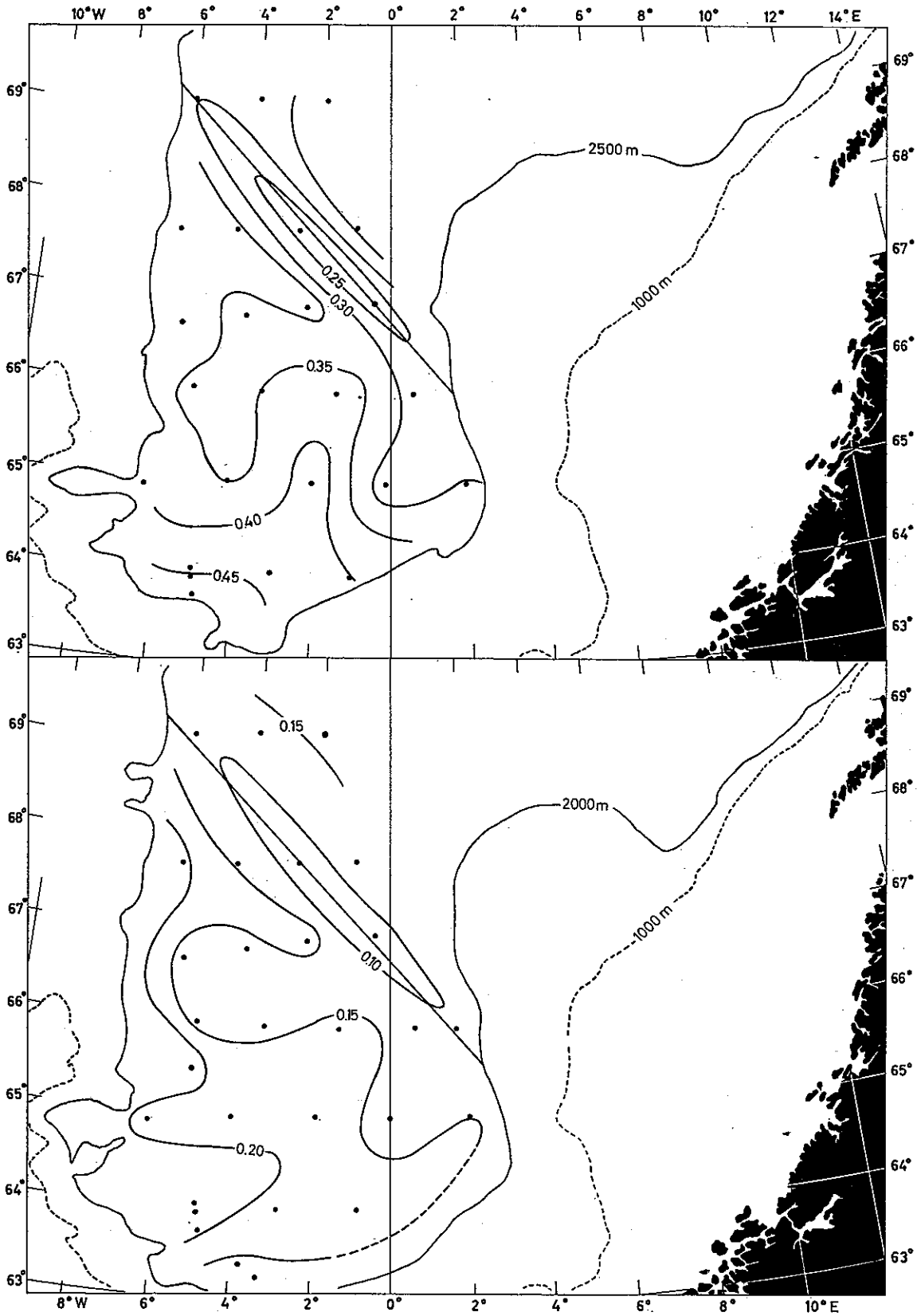


Fig. 6. Geostrophic currents at 2500 (top) and 2000 dcb. (bottom) in 1935.

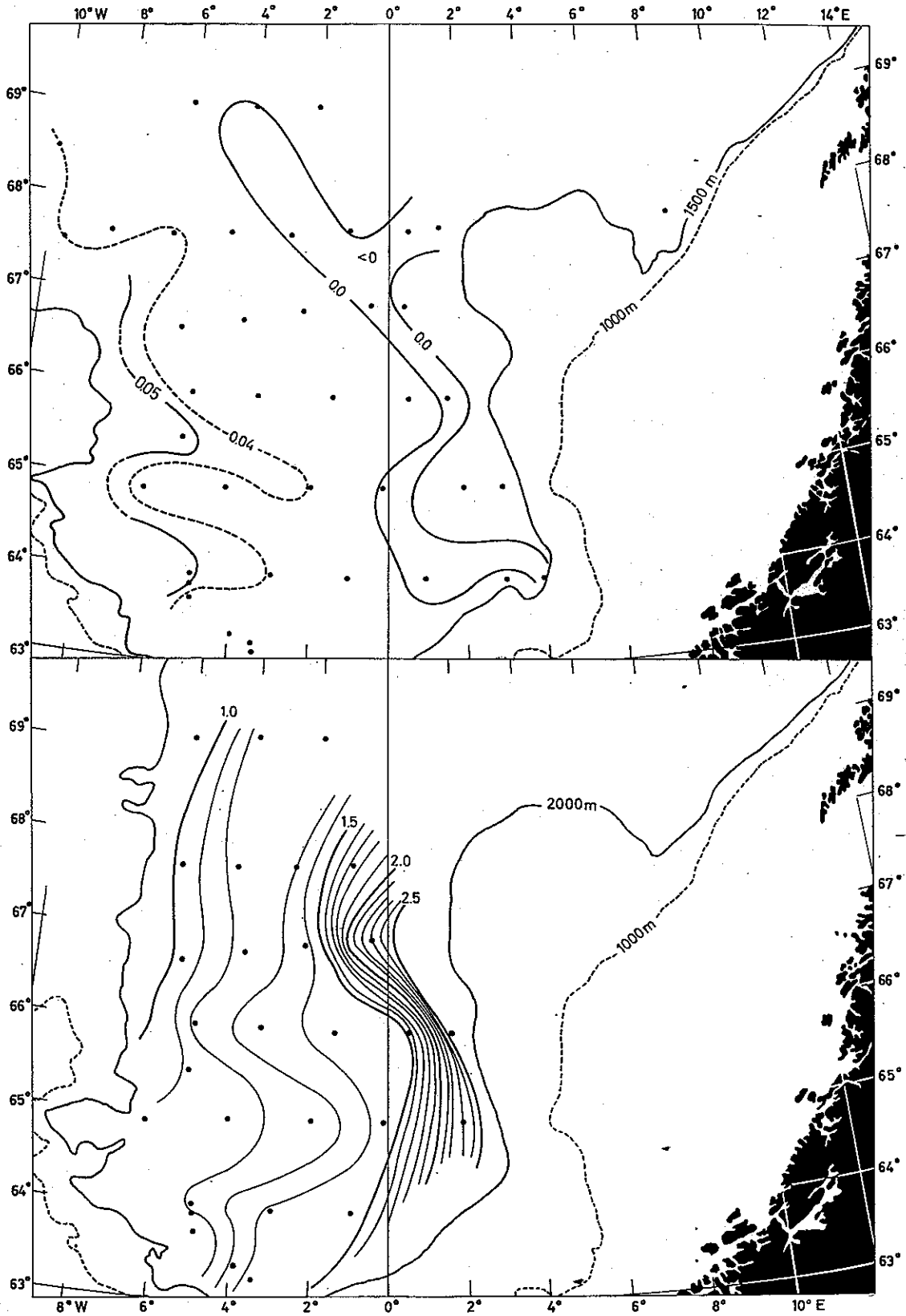


Fig. 7. Geostrophic currents at 1500 (top) and 0 dcb. (bottom) in 1935.

In Fig. 11 of an earlier paper (Mosby 1959) the individual temperature readings at 2500 m are given. The accuracy of these determinations is illustrated by the differences between the coupled thermometers being  $\bar{\approx} 0.01^\circ$  in 18 cases,  $0.02^\circ$  in 2,  $0.03^\circ$  in 1, and  $0.05^\circ$  in 1 case. The averages of the double determinations vary between  $-0.995$  and  $-1.035^\circ$ , and differ from  $-0.995^\circ$  by  $\bar{\approx} 0.02^\circ$  in 15 cases, by  $0.025^\circ$  in 3, by  $0.03^\circ$  in 3 and by  $0.04^\circ$  in 1 case. No tendency towards a systematic geographical distribution of these values is apparent, and the only possible conclusion is that the water at 2500 m was in this case homothermal, with a temperature of  $-1.015^\circ$ . For the 2000 m level the  $-1^\circ$  isotherm in the figure mentioned indicates a slightly higher temperature in the north-east and perhaps also in the south; the extreme values are  $-0.96$  and  $-1.04^\circ$ ; for the stations reaching 2500 m the extreme values at 2000 m are  $-0.98$  and  $-1.04^\circ$ . The average temperature at 2000 m was  $-1.015^\circ$  or exactly the same as at 2500 m. At 1500 and 1200 m the same figure shows increasing contrasts, the extreme values being  $-0.87$  and  $-0.98^\circ$  at 1500 m and  $-0.67$  and  $-0.87^\circ$  at 1200 m.

The observations from 1936 do not cover the north-eastern part of the same area. At 2500 m the average temperature was  $-1.00^\circ$  and the extreme values  $-0.98^\circ$  and  $-1.01^\circ$ ; at 2000 m the average temperature was  $-1.01^\circ$  and the extreme values  $-0.97$  and  $-1.03^\circ$ . At 1500 and at 1200 m similar features are indicated as in 1935.

These empirical results seem to agree nicely with the conception discussed in the following. From the recently finished bathymetric map by Eggvin (1963), it is seen that down to a depth of 2500 or 2600 m below the surface there is, at about  $72^\circ\text{N}$ ,  $1^\circ\text{W}$ , an opening for communication between the Spitsbergen Deep and the Norwegian Deep (terminology according to Helland-Hansen and Nansen, 1909).

For further estimates this map was used to determine by planimeter the areas enclosed by every 100 m contour line from 3900 to 1000 m depth. This was done for the southern basin, the Norwegian Deep, limited in the north by a broken line drawn from Jan Mayen via the banks to Bear Island, and for the Spitsbergen Deep, limited in the north by the 79th parallel. The resulting volumes below each 100 m contour line were plotted against depth. The rather smooth curves thus obtained gave the following figures:

Norwegian Deep	Area	Volume	
2500 m	0.466 mill km <sup>2</sup>	0.2524 mill km <sup>3</sup>	542 m
2600 m	0.429 mill km <sup>2</sup>	0.2076 mill km <sup>3</sup>	484 m
Spitsbergen Deep			
2500 m	0.274 mill km <sup>2</sup>	0.1496 mill km <sup>3</sup>	546 m
2600 m	0.246 mill km <sup>2</sup>	0.1236 mill km <sup>3</sup>	502 m

from which the average depths below the same surfaces were found (last column). Below the approximate threshold depth of 2500–2600 m we thus have about 0.23 and 0.14 mill km<sup>3</sup>, i.e. a total of 0.37 mill km<sup>3</sup>. The average depths from the surface are between 3042 and 3084 or 3063 m and between 3046 and 3102 or 3074 m respectively, or near 3070 m for both.

When bottom water is formed in the Spitsbergen Deep, for instance as illustrated in an earlier paper (Mosby 1967, Fig. 8), it will fill the deeper parts of the Deep and flow into the Polar Basin through the more than 3000 m deep trench in the Nansen Ridge (BALAKSHIN 1959). But this takes time, and part of the bottom water must therefore be expected to penetrate through the mentioned opening into the Norwegian Deep. It may also be that the process of bottom water formation will occur on the ridge between the two deeps. Due to the earth's rotation it will tend to follow the western slope of the bottom. Homogeneous and rich in oxygen it will fill the lower parts of the Norwegian Deep. The observations from 1935 show that the content of oxygen was approximately the same at 2500 and 2000 m (6.95–7.00 ml/l) as at 1500 and 1200 m. (As to the accuracy of the oxygen determinations in 1935 see Appendix). The inflow may be expected to last for several months, as shown in an earlier paper (Mosby 1961), in which the effects near Weather Station M in 66°N, 2°E are assumed to be observed until the month of July. If in 1935 the inflow was still going on at the time of observation, this might explain the stratification and the currents calculated above.

In the above-mentioned paper (Mosby 1967) some rough, quantitative estimates on the bottom water formation were made. The observations of the *G. O. Sars* in April 1958 showed nearly homogeneous water from the surface to the bottom within wide areas. Values of the expression  $\sum_0^{1200\text{m}} (28.100 - \sigma_t) \Delta z$  were used to illustrate the distribution of light water in the upper layers, and after plotting these values on a map (Mosby 1967, Fig. 8) the areas within the curves for the values 30, 40 and 50 of the said expression, extrapolating by free hand so as to close the curves in the south, we arrived at an area of some 0.15 mill km<sup>2</sup>. On the assumption of an average depth of about 3000 m we then found that the nearly homogeneous water present in April 1958 was about 0.45 mill km<sup>3</sup>. As seen above this is more than the total volume of both Deepes below the threshold separating them, which was 0.37 mill km<sup>3</sup>.

The 1958 observations were made in April, but the process of bottom water formation must have started in winter, probably several months earlier. The estimate of 0.45 mill km<sup>3</sup> must therefore be considered as only part of the bottom water formed that year. In the Norwegian Deep this volume is found below about 2130 m of depth. Imagine the basin to be closed while this deeper part of it is filled with fresh bottom water. The water at 1500 m would then be raised nearly to the 1000 m level. If both basins, considered as closed, are to receive the same amount of bottom water, the water particles at 1300 m would be raised to a little less than 1000 m of depth. As the basins are not closed, such effects will be much smaller, but the above figures may still serve as an illustration of the effects to be expected from inflowing bottom water upon the stratified water of the upper layers.

At Weather Station M the long time series of observations permit a study of annual variations of the interface between the Atlantic water and the deep water. This has lead (Mosby 1961) to an estimate of the vertical motion of approximately 50 m year<sup>-1</sup> under average conditions. As this interface, or the 35‰ isohaline surface, at St. M

is found at depths from 300 to 400 m, our planimeter results were supplemented above 1000 m with those of HELLAND-HANSEN and NANSEN (1909). It appeared that between the 300 m level and that of 400 m there is an approximate volume of 0.2 mill km<sup>3</sup>, and the average vertical motion of 50 m a year would then, in a closed basin, be produced by the introduction of only 0.1 mill km<sup>3</sup> of bottom water. However, the basins are not closed, and as far as the order of magnitude is concerned it must be said that a vertical motion of 50 m year<sup>-1</sup>, as "recorded" at St. M, may well be considered as a reasonable effect of the formation of some 0.45 mill km<sup>3</sup> of bottom water or even much more.

6. *Upper water.* When trying in the conventional way to construct maps of currents for the upper levels, we may as before use the 1000 dcb. surface as a reference level, but here we run into more serious difficulties with the construction. In Fig. 8 (top) an attempt has been made for the surface (1000-0 dcb.) by demanding a complete continuity of each contour line. In order to avoid the uncertainties in extrapolating into shallow waters, only stations reaching 1000 m of depth have been taken into consideration. The result is not encouraging, the picture obtained being at any rate too complicated to represent a stationary current system.

For a better understanding the anomalies of dynamic depth were plotted against longitude along each section. The result obtained for the 67th parallel is shown in Fig. 9 (top). Again we find the "puzzling waves"; the distance between crests and troughs appears to vary greatly, being of the order of some 100 km. The variations are similar for all levels, but the "amplitudes" are decreasing downwards. In the different sections the irregularities are different, but the general trend is the same: that of an increasing anomaly towards the east. Starting in the west, approximately where  $\Delta D_{1000-0 \text{ dcb.}} = 1$  (in fact 300 km west of the Greenwich meridian), we have now computed simple average values for the five sections in 64 to 68°N. The result is shown in Fig. 9 (bottom), where the slope of the curves indicates the average speed of the north-going current; the strongest current is found between 300 and 400 on the kilometre scale. With this as a guide we have, in Fig. 8 (bottom) tried to draw the isobaths of the surface (1000-0 dcb.) so as to represent a main current towards the north, allowing for irregularities by introducing isolated minima and maxima by isobaths corresponding to cyclonic and anticyclonic eddies. Most of these are seen to depend on one or very few stations within one section. Following the same pattern similar maps were drawn for the 75, 150 and 300 decibar surfaces; the map for 150 dcb. is reproduced in Fig. 10. At the 600 dcb. surface only very faint traces of the corresponding contrasts were found, as can be understood from Fig. 9. From the latter it will also be understood that the maps would have appeared more similar if isolines had been drawn not for every 0.25 dyn.cm, but for values proportional to the average values of  $\Delta D$  for each level.

The quasi-static condition for dynamic computation of the currents does not hold good for a system as that obtained here, since in the formula of HELLAND-HANSEN (1905) the acceleration has been neglected. Nevertheless the picture obtained may give an idea of the motions occurring within a water volume with a hydrographic structure as given by the observations. But it must also be borne in mind that the observations are

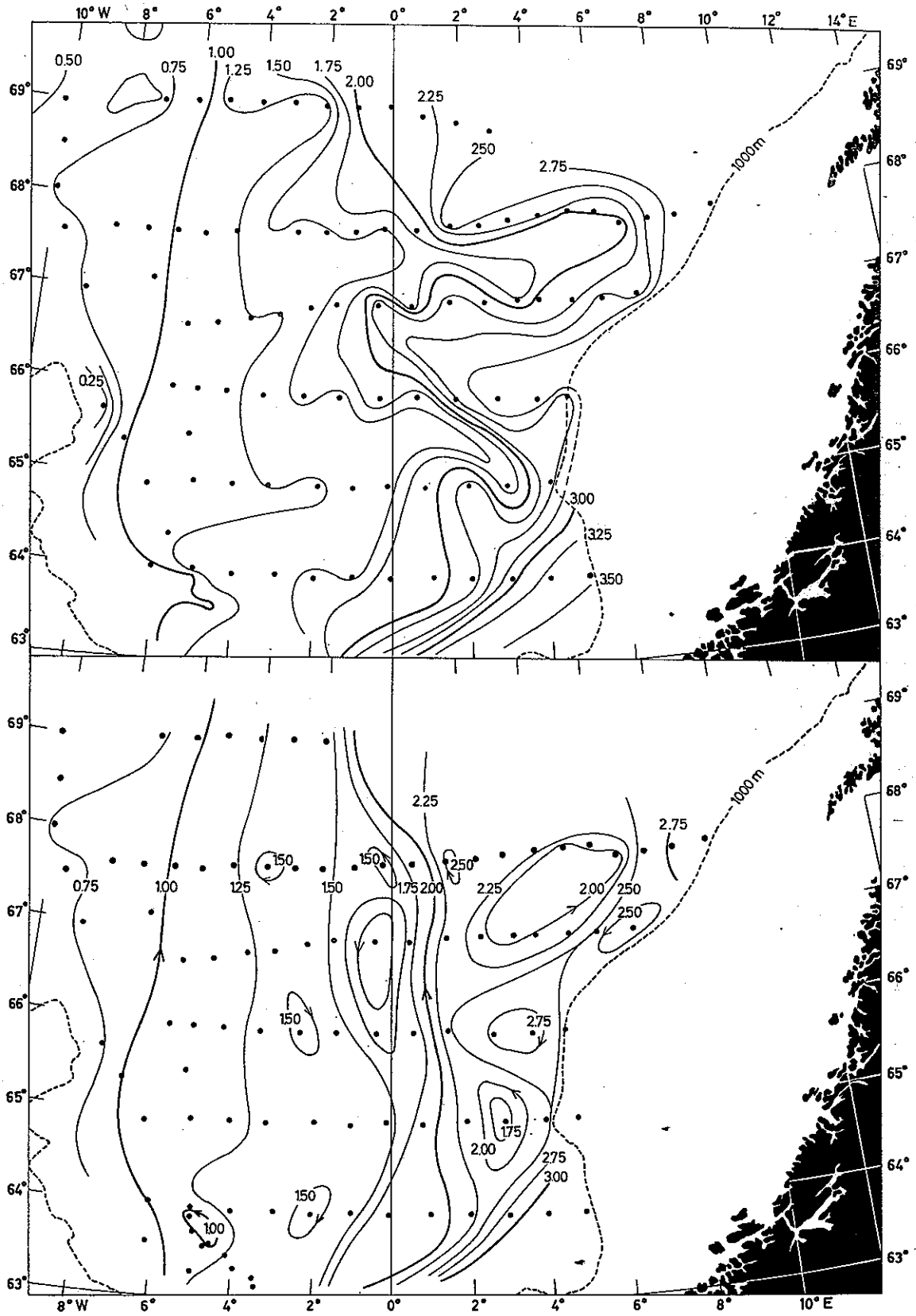


Fig. 8. Two interpretations of the surface currents in 1935.

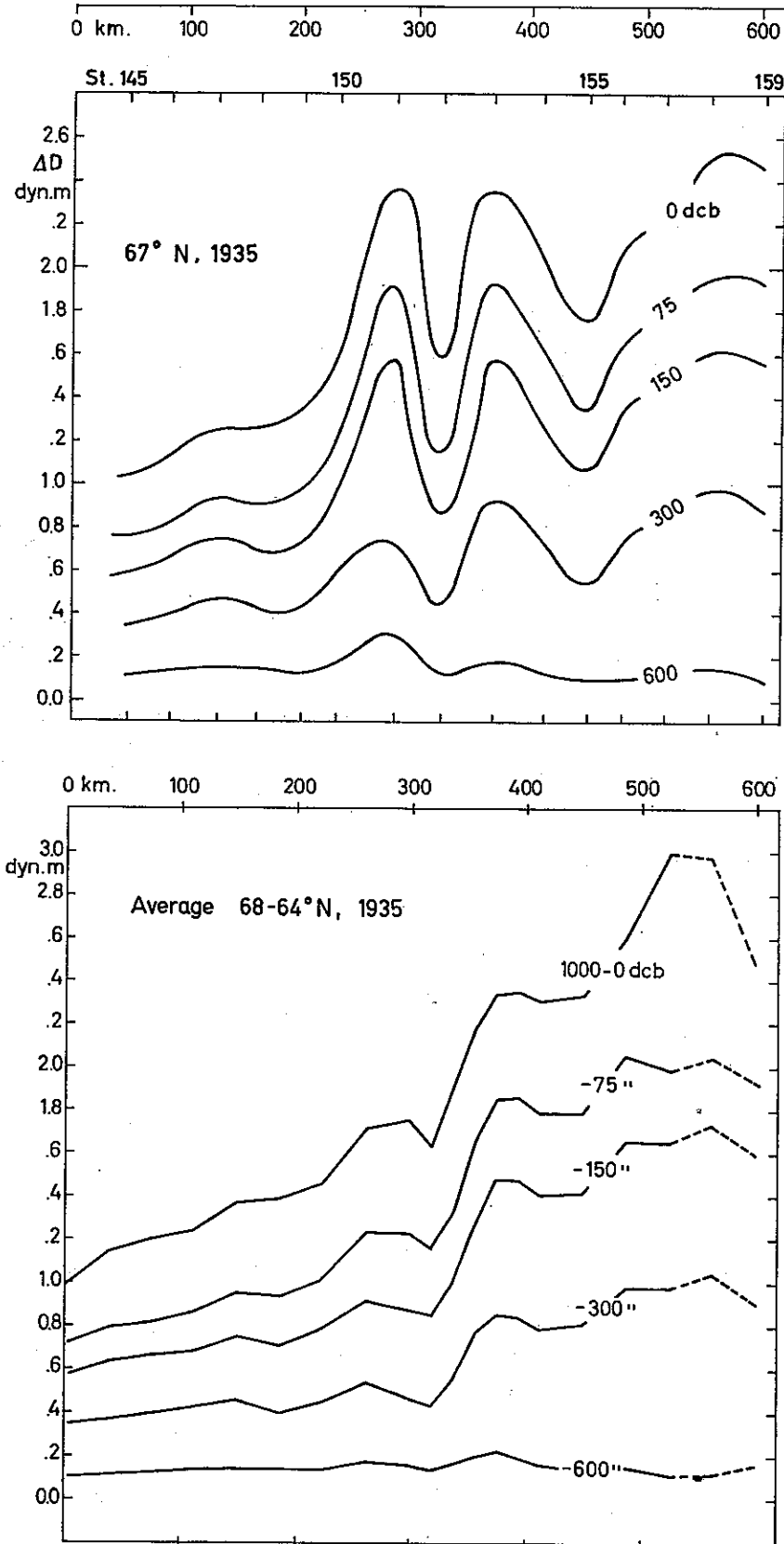


Fig. 9. Anomalies of dynamic depths along the sections.



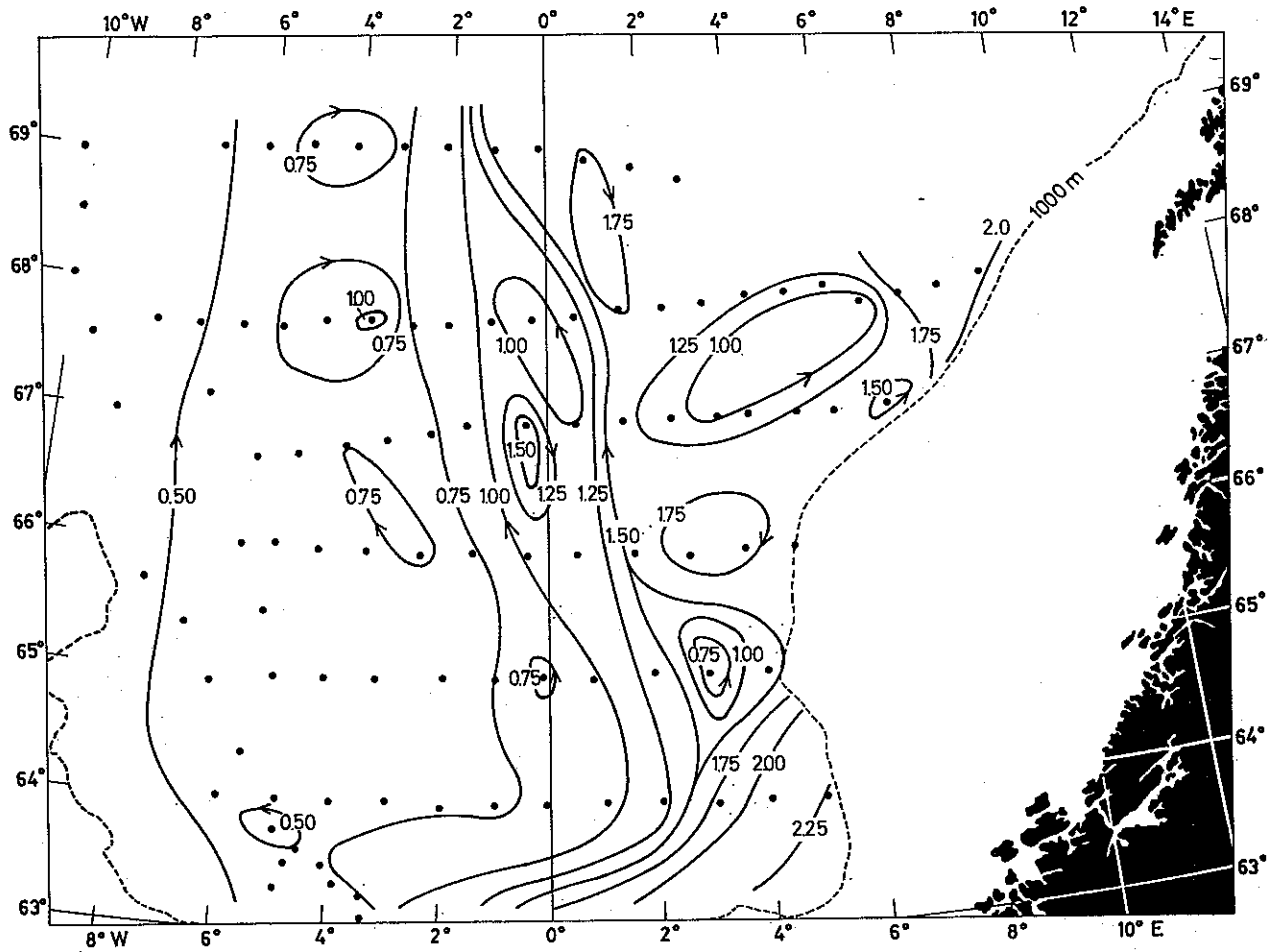


Fig. 10. Geostrophic current at 150 dc. in 1935.

far from synoptic; nearly a week elapsed between the working of one section and the next. If, for instance, a tolerably correct picture has been obtained for a local situation within one area, the situation may have been completely different earlier or later. As the curves in Figs. 8 and 10 indicate that the "waves" are shorter than the distance between the sections, it appears reasonable that so many isolated highs or lows have been located within each section. The maps in Figs. 8 and 10 can therefore be expected to represent a stationary situation only as far as the general features are concerned.

In Fig. 11 the topography of the sea surface relative to the 1000 decibar surface has been constructed on the basis of the 1936 observations. The net of stations is denser than in 1935, but it covers a smaller area. Again we find lows, of which one in latitude  $64\frac{1}{2}$  to  $65^\circ\text{N}$ , which may have remained there for the period of three days elapsed between the relevant observations in the two sections. When comparing with the corresponding map for 1935 (Fig. 8, bottom), it is seen that this low is located nearly in the same position in both years. The stations 352, 353, 354 of the section from the NW to the SE through the area in 1936 are out of step with the others; they have, therefore, been disregarded.

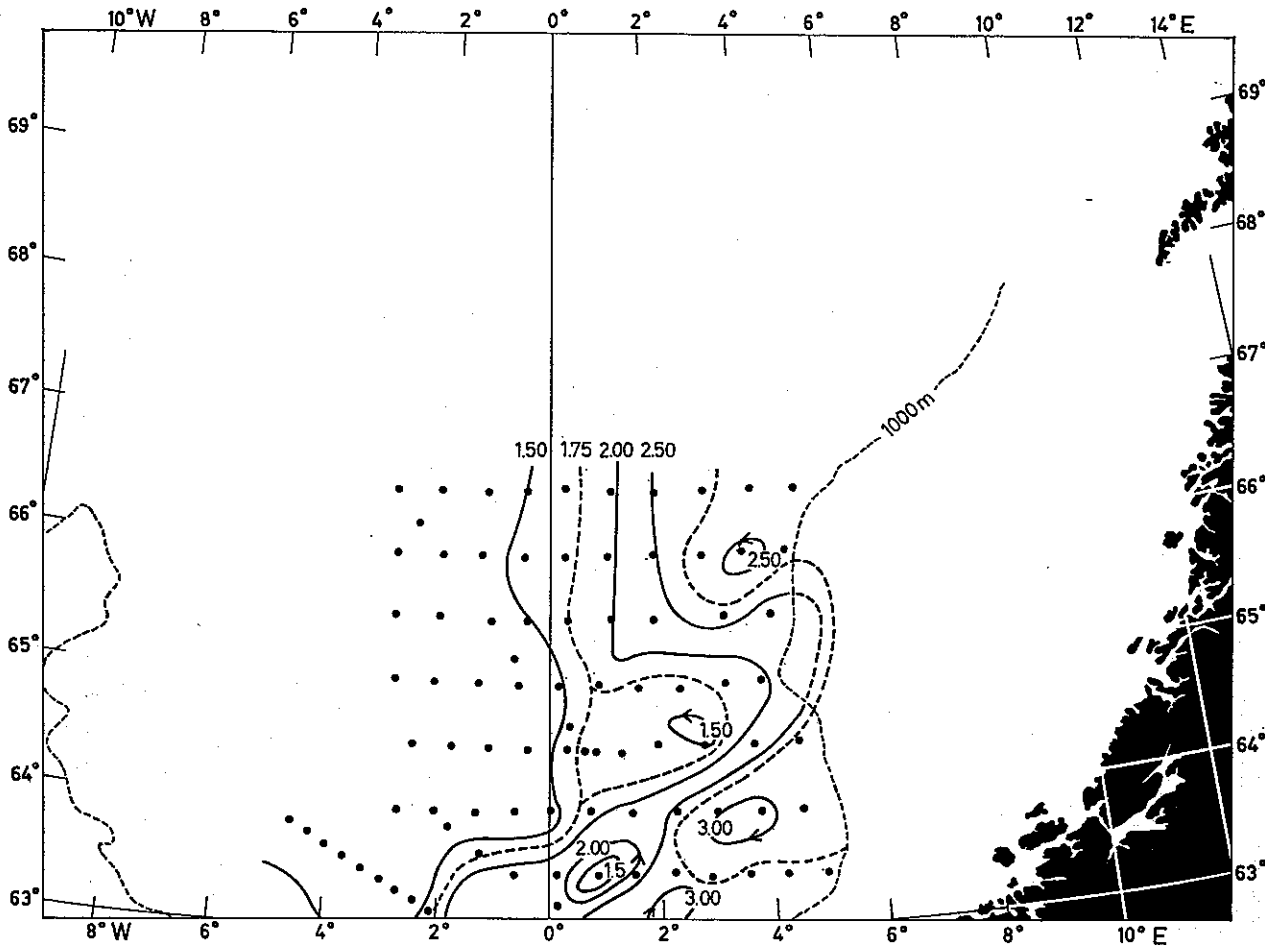


Fig. 11. Geostrophic surface current in 1936.

A special study of the two parallel southern sections of 1936 (stations 39 to 94), taken in six days at a distance of 50 to 60 km, stimulated the suspicion of the existence of large eddies, and in August 1954 the *Armauer Hansen* went out in search of such an eddy. During five days of systematic measurements with conventional equipment a mapping was made of the eddy illustrated in Fig. 12 by depth contours of the 4°-isothermal surface. Further investigations (see SÆLEN 1963) have shown that similar eddies are frequent in the area, eddies which may remain stationary for several days or move slowly or rapidly, usually in a north-easterly direction.

The "waves" of the sections need not in all cases be due to eddies. But if larger and smaller eddies are relatively abundant within the Atlantic current, they may have a considerable effect upon the horizontal mixing or large-scale diffusion within the Atlantic water. This conception will be applied in the next chapter of this paper.

7. *Atlantic water.* Since the early years of investigations (HELLAND-HANSEN and NANSEN 1909) this denomination has been used, within the Norwegian Sea, for waters of a salinity of 35.0‰ or more. In the following this definition will be retained, al-

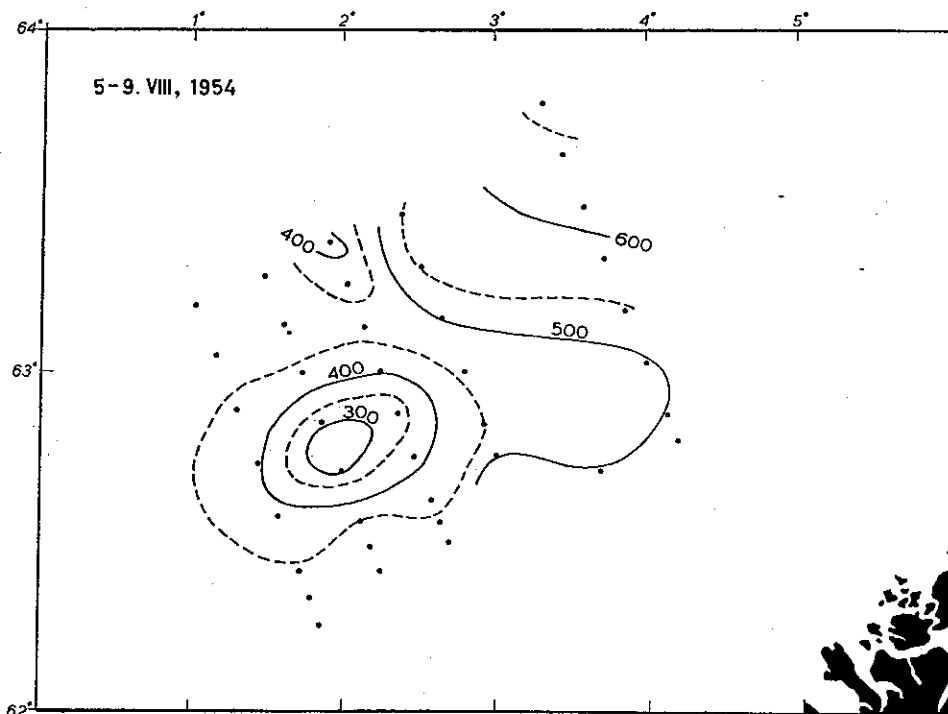


Fig. 12. Depth of the 4° surface in 1954.

though it should be kept in mind that an isohaline surface in the sea will usually move in relation to the water particles. In our case the vertical diffusion means that deep water is gradually transformed into Atlantic water.

In Fig. 13 the extension of the Atlantic water is illustrated by a bathymetric map of the lower 35.0‰ isohaline surface, i.e. the sub-surface of the Atlantic water, using, however, observations only within the sections from 64 to 68°. It is seen that there is a wedge of Atlantic water, limited in the west at an approximate longitude of 4 to 6 °W and extending eastwards to the continental shelf, where it reaches a depth of more than 500 m. Similar irregularities are encountered as in the maps of Figs. 8 to 11, but the main trends of the topography of the 35.0‰ isohaline surface are regular. Within this wedge we thus find the Atlantic current, the influence of which on the hydrography and climatology of the Norwegian Sea will be studied in some detail in the following.

## II. The Norwegian Atlantic current

1. *The Atlantic water* present in the Norwegian Sea is known to enter from the North Atlantic mainly through the Faroe-Shetland Channel, where it is characterized by 8.9°C and 35.3‰, values obtained as direct averages of the nearly 8000 sets of observations from the years 1927-52 published by TARR (1957). In the middle of the area covered by the stations of 1935, regular observations have been carried out from Weather Station M (66°N, 2°E). The "nucleus" of Atlantic water is here found at

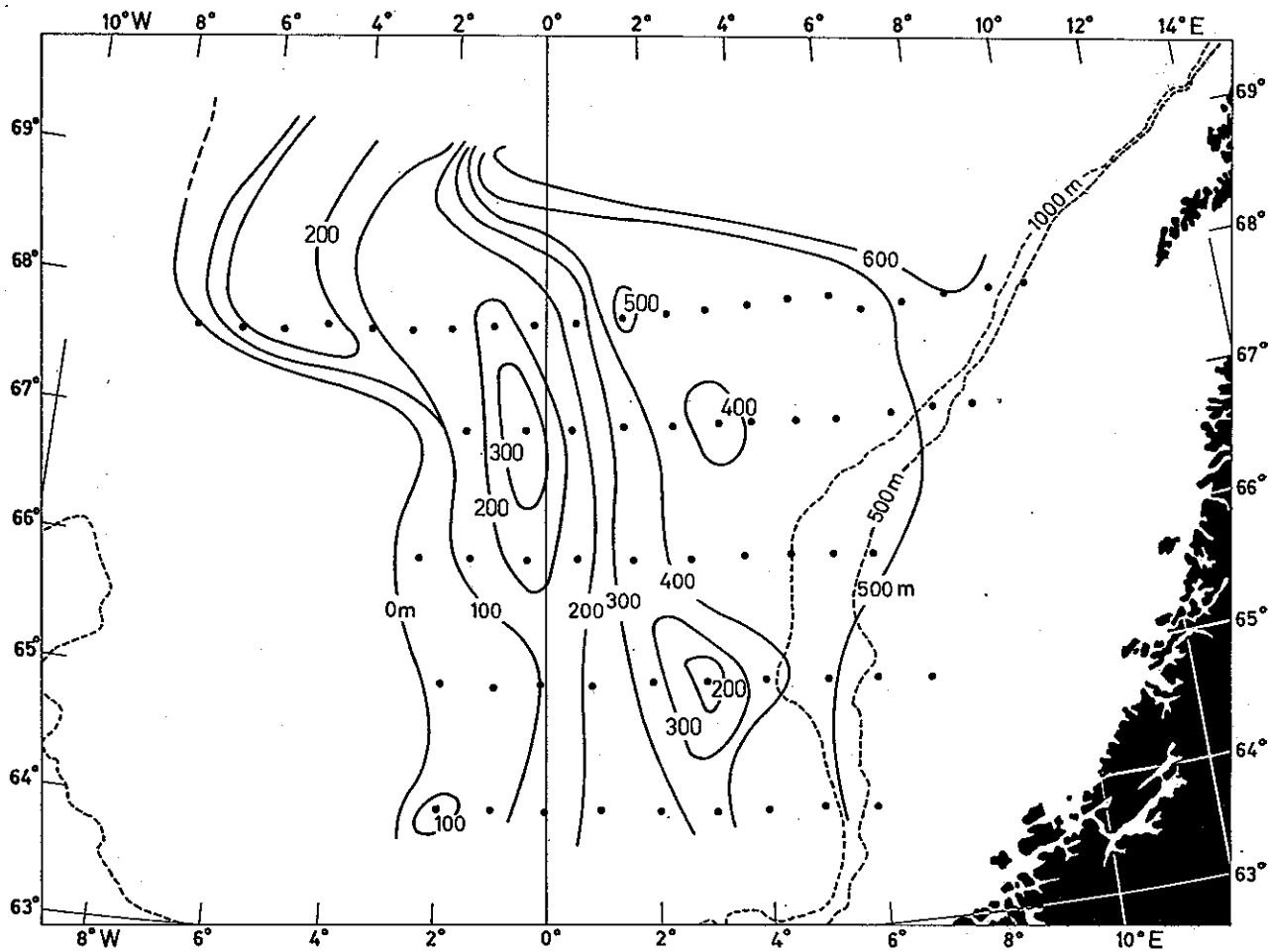


Fig. 13. Depth of the 35.0‰ surface in 1935.

50 to 57 m of depth. In the ten-year period 1948 to 1958 the temperatures were between 8.45 and 6.15°C and the salinities were  $35.20 \pm 0.05\text{‰}$  (HELLAND 1963).

On its way from the Faroe-Shetland Channel into the Norwegian Sea the Atlantic water is influenced in the surface layer by radiation, evaporation and precipitation, and in the sub-surface layer by mixing processes. The result is a gradual decrease of its temperature and salinity with latitude. Since early years the influx of heat from the North Atlantic into the Norwegian Sea has been considered the main cause of the abnormally mild climate of the area.

An attempt has been made (MosBY 1962) at a quantitative estimate of the water, salt and heat balance of the Norwegian Sea including the Greenland Sea and the Barents Sea. According to this estimate the amount of heat conveyed by the Atlantic current is more than half of the total amount of heat in play.

2. *Continuity conditions.* If all factors influencing the Atlantic water in the Norwegian Sea were known we might calculate the changes of characteristics of this water on its way towards the north. All effects could then be introduced into balance sheets, where

stationary conditions must lead to perfect balance due to the basic continuity conditions: the conservation of mass, of salt and of heat.

The continuity condition may be generally expressed by

$$\frac{\partial c}{\partial \tau} = \nabla \cdot c\mathbf{v} \quad (1)$$

where  $c$  is an arbitrary conservative concentration,  $\tau$  is time and  $\mathbf{v}$  is the velocity vector in the point considered. Under stationary conditions the above expression must disappear.

Imagine now  $\mathbf{v}$  consisting of a mean velocity and a turbulent velocity; we may then distinguish between advection and turbulent mixing. For the present purpose the seawater may be considered as incompressible, and equation (1) is therefore often written as follows (SVERDRUP 1946, p. 158)

$$\frac{\partial c}{\partial \tau} = \frac{\partial}{\partial x} \left( \frac{A_x}{\rho} \cdot \frac{\partial c}{\partial x} \right) + \frac{\partial}{\partial y} \left( \frac{A_y}{\rho} \cdot \frac{\partial c}{\partial y} \right) + \frac{\partial}{\partial z} \left( \frac{A_z}{\rho} \cdot \frac{\partial c}{\partial z} \right) - \left( v_x \frac{\partial c}{\partial x} + v_y \frac{\partial c}{\partial y} + v_z \frac{\partial c}{\partial z} \right) \quad (2)$$

If in the Norwegian Sea the hydrographic conditions were really stationary, equation (2) would have to be satisfied. With a relatively dense net of observations as those from 1935 or 1936 it would then be possible to determine all gradients. Applying equation (2) to mass, salt and heat would give three equations, the velocities would be found by dynamical computations and the coefficients  $A_x$ ,  $A_y$  and  $A_z$  could be determined for any point.

Such conditions are not present in the sea, but we shall assume that average conditions exist that may be considered as approximately stationary. This will mean that all "irregularities" are to be considered as "noise" or as "variability", the effects of which may be included in the definition of our coefficients. The stationary average conditions may then be sought by eliminating the "noise".

3. *An empirical model* may now be established as an average section based on the five sections in latitude 68 to 64°N. Having seen above that the main current is flowing north outside the slope of the continental shelf in a direction which is approximately parallel to the Greenwich meridian, we have in Fig. 14 divided the area by lines parallel to this meridian and at distances of 100, 200 etc. km. Within the five sections we then find from 9 to 11 individual stations in each 100 km broad strip. The resulting six groups of stations are now combined to "normal" stations as explained in an earlier paper (Mosby 1959). This way of averaging the stations is used in order to retain the vertical gradients. The average section (Figs. 15 and 16) has been constructed on the basis of the normal Stations I to VI, referring to 50, 150, 250, 350, 450 and 550 km of the kilometre scale in Fig. 14. It is seen to bear a general resemblance to the single sections, but to have a much simpler structure. The wedge of Atlantic water here appears very regular, with a 35.0‰ isohaline running smoothly from the slope of the shelf at 450 m depth near 580 of the kilometre scale, to the surface near 200 km. The highest salinities of 35.25‰ occur from 420 to 520 km at about 75 m depth.

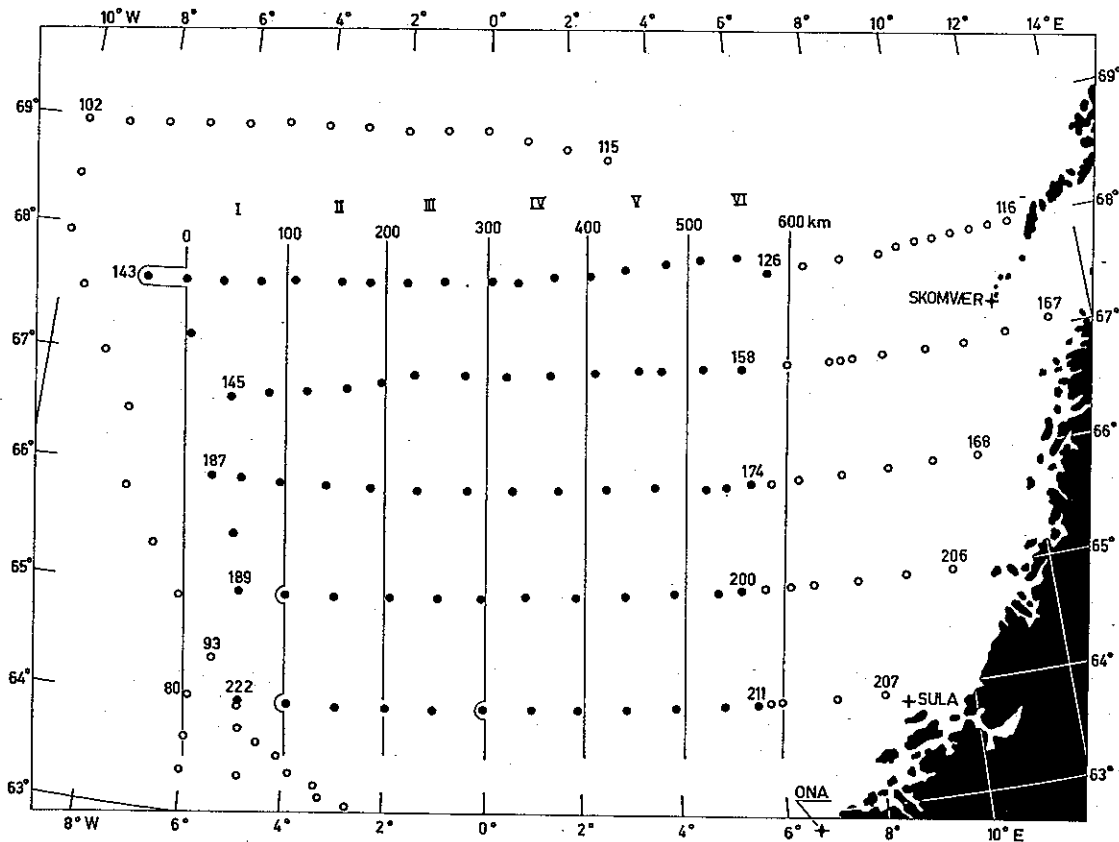


Fig. 14. Stations 1935.

The density distribution is shown in the upper part of Fig. 16, in the lower part of which are shown the isoveles as found by dynamical computations, this time using the 800 decibar level as reference. The speed of the current may appear astonishingly low, the highest value being only  $4 \text{ cm sec}^{-1}$ , and the average speed for the Atlantic water being  $2.1 \text{ cm sec}^{-1}$ . The total transport of Atlantic water still comes out equal to  $1.9 \cdot 10^6 \text{ m}^3 \text{ sec}^{-1}$ . This is of the order of magnitude usually assumed for this current, e.g. by HELLAND-HANSEN (1934) for the Sognefjord Section farther south, giving  $3 \cdot 10^6 \text{ m}^3 \text{ sec}^{-1}$ . SÆLEN (1959) computed the transport of Atlantic water within the Sognefjord Section from observations made on twenty-seven different occasions, and found values varying from  $1.8$  to  $6.4 \cdot 10^6 \text{ m}^3 \text{ sec}^{-1}$ , using the 1000 decibar surface as reference level.

In an attempt to determine horizontal gradients along the solenoids, average sections were established by means of the stations at  $64, 65, 66^\circ\text{N}$ , and at  $66, 67, 68^\circ\text{N}$ . These average sections appeared to be visibly influenced by the irregularities of the original sections, and the results are therefore perhaps in part unreliable. They showed in the east a northward decrease of temperature and salinity, also below the Atlantic water. But these gradients decrease towards the west, and are eventually replaced by opposite ones also above the  $35.0\text{‰}$  surface.

From the lower part of Fig. 16 it is seen that the speed of the current is lower in the east than in the west. The computed values are plotted in fine dotting against scales

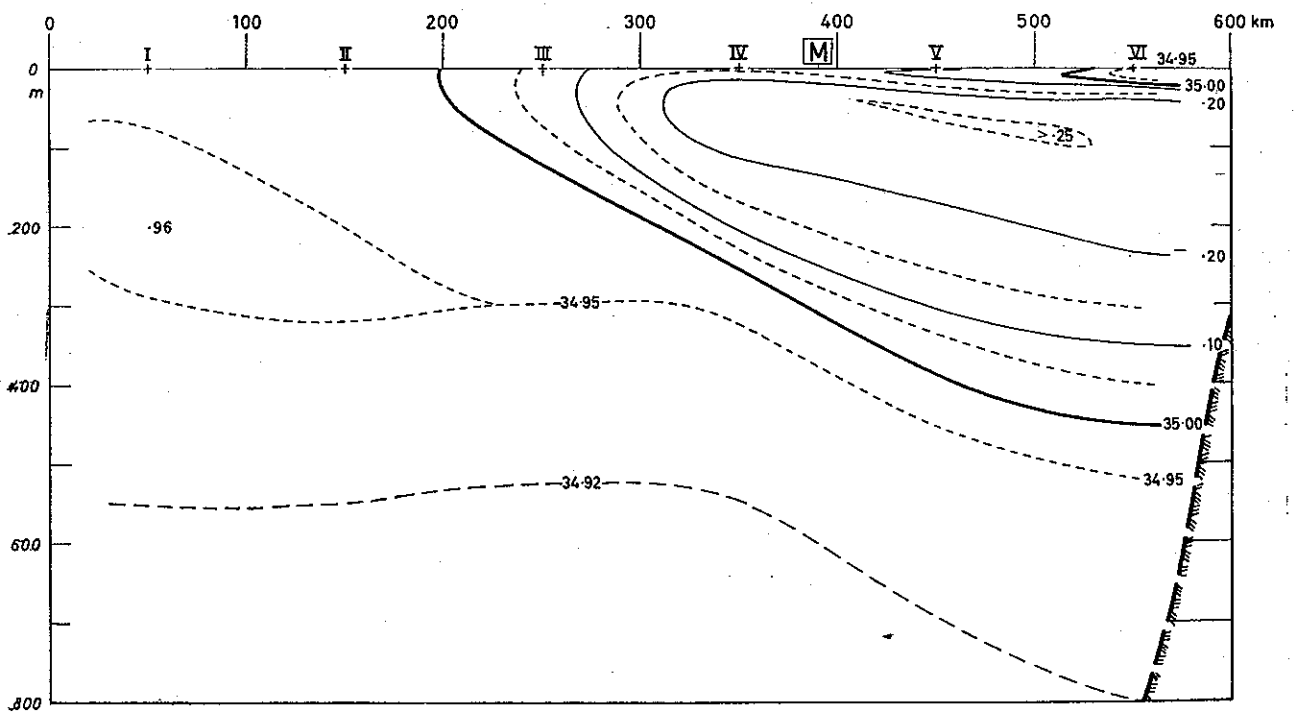
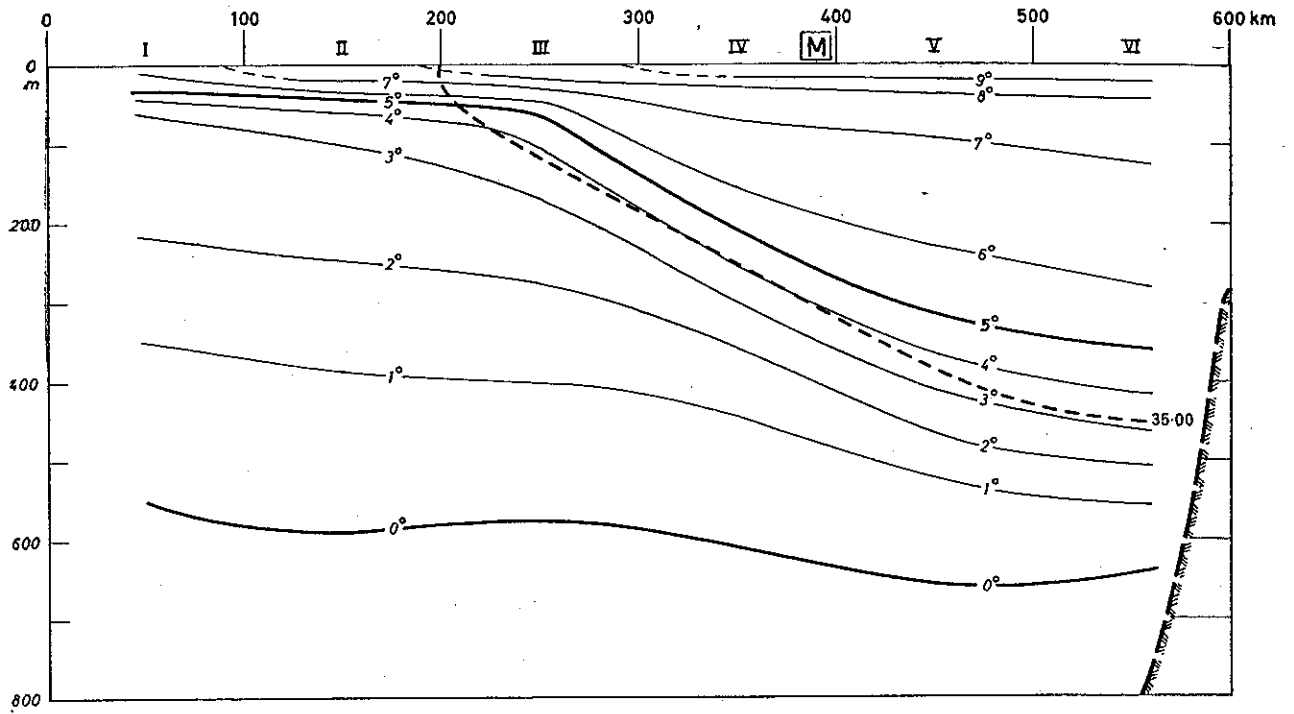


Fig. 15. Average section 1935, t°C and S ‰.

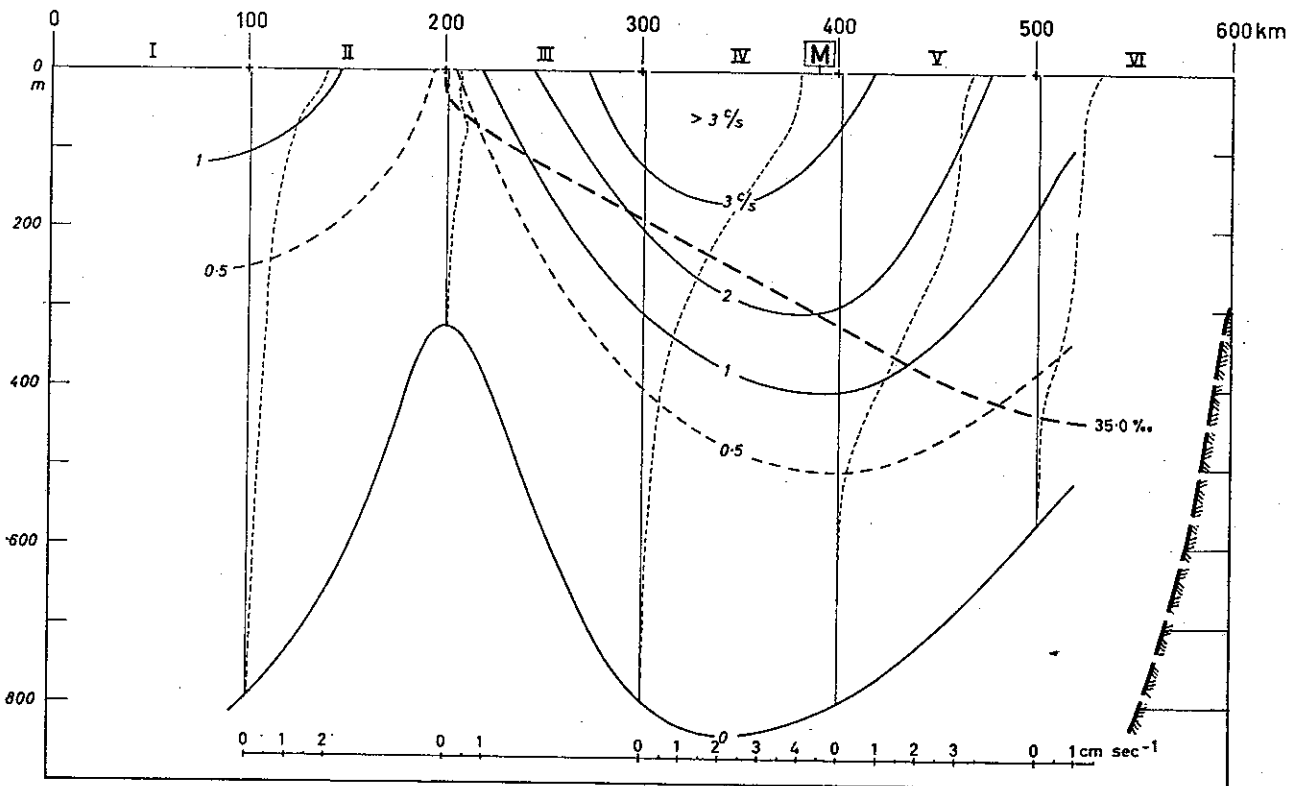
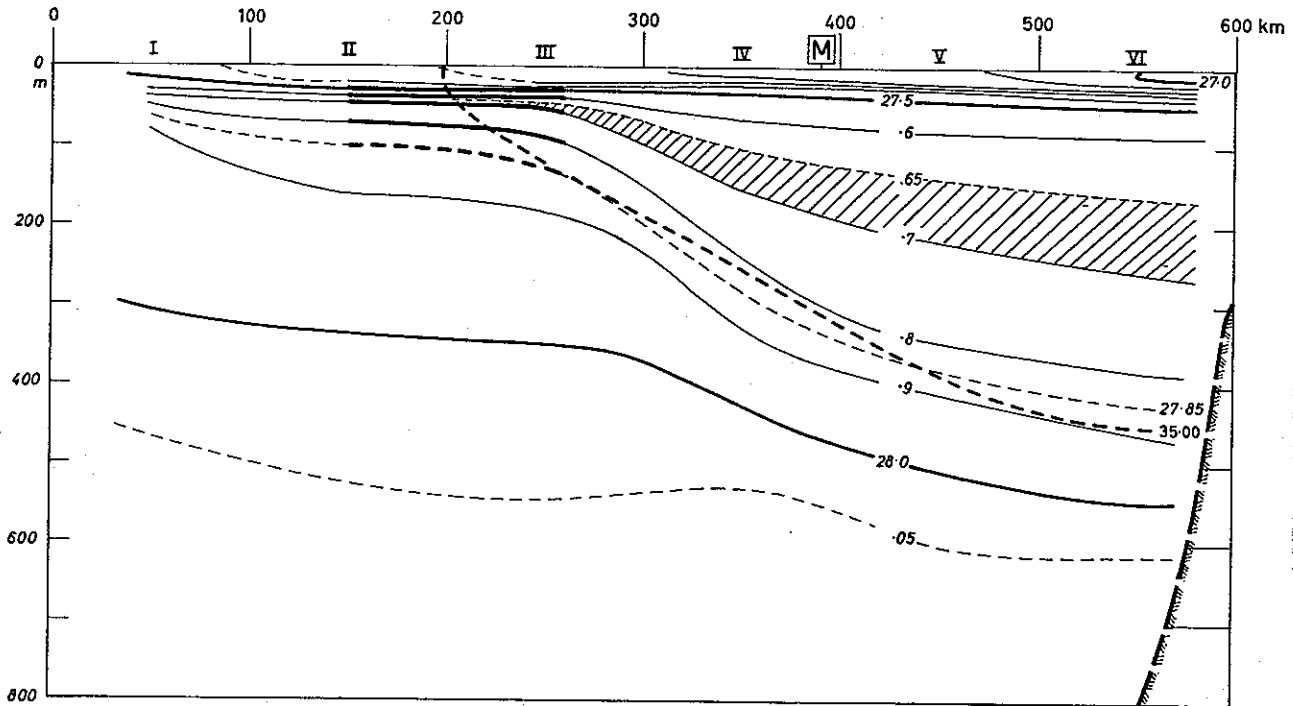


Fig. 16. Average section 1935,  $\sigma_t$  and  $v$   $\text{cm sec}^{-1}$ .



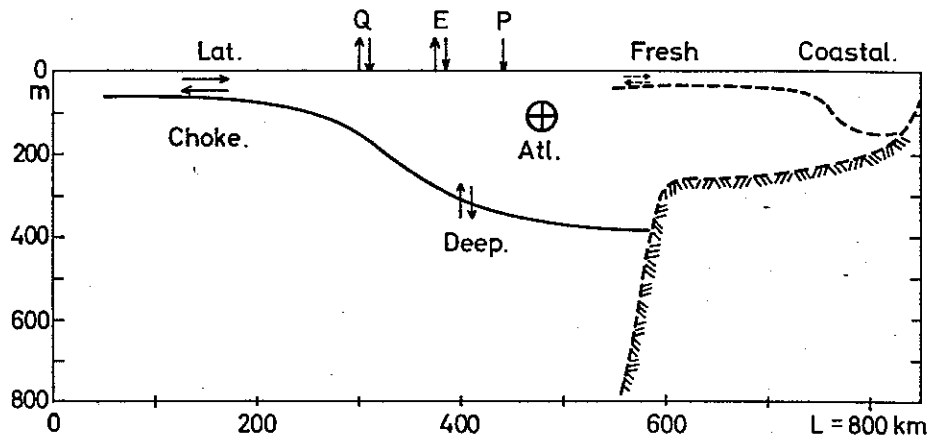


Fig. 17. Sketch diagram of thermohaline model.

at the bottom of the section. At 500 km, derived from normal Stations V and VI, the average speed of the Atlantic water, down to 435 m, is  $1.1 \text{ cm sec}^{-1}$ , while at 400 km we find  $3.45 \text{ cm sec}^{-1}$  down to 325 m. Per metre length of the section this means volume transport values of  $0.011 \cdot 435 = 4.8 \text{ m}^3 \text{ sec}^{-1}$  at 500 km and  $11.2 \text{ m}^3 \text{ sec}^{-1}$  at 400 km. However, when multiplying at every level by the horizontal gradients of temperature and salinity found from the two average sections 64, 65, 66°N and 66, 67, 68°N, we arrive at very nearly the same heat and salt transport at 500 km as at 400 km. Although based on perhaps not too well-established gradients, this result is of interest, particularly so because the situation at 400 km is very nearly as at Weather Station M, which is situated at 66°N and at about 390 km. This means that *Station M* is nearly representative of the whole of the average section in respect to heat and salt balance.

4. *A thermohaline model.* Starting from the average section, we may now try to establish a thermohaline model of the Atlantic current at 66°N (Fig. 17), claiming that the effects from the surface, from the sub-surface, from the east and from the west are keeping balance with the effects of the Atlantic water flowing through the section.

a. *The surface* receives heat by total radiation from sun and sky. For solar altitudes below  $60^\circ$  the amount of heat may be computed by the formula (Mosby 1936)

$$q_1 = 0.026[0.3 + 0.7(1 - C/100)]\bar{h} \text{ gcal cm}^{-2} \text{ min}^{-1}$$

in which  $\bar{h}$  is the average solar altitude above the horizon over 24 hours, and  $C$  is the mean cloudiness in per cent of the sky, while 0.026 is the probable value of a factor depending on the purity of the atmosphere, 6% being then subtracted due to reflection. Computing  $\bar{h}$  for the fifteenth of each month and introducing for  $C$  the mean monthly values of cloudiness observed at Weather Station M in the years 1954–58, we arrive at the values given in Table 1.

In the same table are given the corresponding values of heat lost through the surface by dark or long wave radiation as computed from the revised table by ÅNGSTRÖM

Table 1. Net heat received by radiation at St. M

Month	$\bar{h}^\circ$	C%	$q_1$	$t_s^\circ C$	$q_2$	Net radiation $q_1 - q_2$		330 m column
						gcal cm <sup>-2</sup> min <sup>-1</sup>	kcal cm <sup>-2</sup> month <sup>-1</sup>	
I	0.3	76.6	0.004	6.74	0.068	-0.064	-2.802	-0.085 °C
II	2.3	76.3	0.028	6.52	0.068	-0.040	-1.751	-0.053
III	6.5	79.7	0.074	6.39	0.063	0.011	0.482	0.015
IV	12.6	79.6	0.144	6.46	0.063	0.081	3.546	0.107
V	18.6	77.7	0.222	7.39	0.066	0.156	6.829	0.207
VI	22.1	84.2	0.236	8.68	0.055	0.181	7.923	0.240
VII	20.9	84.8	0.223	10.41	0.054	0.169	7.398	0.224
VIII	15.6	80.6	0.178	11.37	0.059	0.119	5.209	0.158
IX	9.2	82.1	0.103	10.77	0.057	0.046	2.014	0.061
X	4.0	79.5	0.046	9.09	0.062	-0.016	-0.700	-0.021
XI	0.8	77.1	0.010	7.89	0.066	-0.056	-2.451	-0.074
XII	0.0	74.5	0.000	7.16	0.070 <sub>5</sub>	-0.070 <sub>5</sub>	-3.086	-0.094
Mean			0.106		0.063	0.043	1.884	
Total			55.508		32.897		22.661 kcal cm <sup>-2</sup> year <sup>-1</sup>	

(1920) for a relative humidity of the air of 80% and after subtraction of 6% for reflexion, or approximately

$$q_2 = (0.194 - 0.0013 \cdot t_s)(1 - 0.83 C/100) \text{ gcal cm}^{-2} \text{ min}^{-1}$$

where  $t_s$  denotes sea temperature and  $C$  cloudiness. The net heat received by radiation  $q_1 - q_2$  is given in gcal cm<sup>-2</sup> min<sup>-1</sup> and in kcal cm<sup>-2</sup> month<sup>-1</sup> in Table 1.

Heat is also lost from the surface by evaporation. On the basis of observations from Weather Station M from October 1948 to September 1958, BØYUM (1966) has computed mean monthly values of heat lost as latent heat of evaporation and as "sensible" heat (convection to the atmosphere) on certain probable assumptions. These values are given in Table 4, p. 38.

As seen from Table 1 the total gain of heat by radiation is found to be  $Q = 22.611$  kcal cm<sup>-2</sup> year<sup>-1</sup>. If this heat is evenly distributed within a column of water of  $H$  m thickness, it will lead to an increase of temperature of this column of

$$\Delta t = 10 \cdot Q/H \text{ }^\circ\text{C year}^{-1} \quad (3)$$

when taking the heat capacity of the water to be  $\approx 1$ .

Assuming the ratio between sensible heat and latent heat to equal the values used by BØYUM, the total heat loss by evaporation will be (Table 4)

$$\Delta t = -879.9 \cdot E/H \text{ }^\circ\text{C year}^{-1} \quad (4)$$

where  $E$  denotes the total annual evaporation in metres.

Finally the average salinity of the water column will be slightly changed by evaporation, precipitation and fresh water from the coastal current. At Station M the mean annual salinity of the Atlantic water has been computed to be about 35.15‰, and the effect will be

$$\Delta S = +35.15 \cdot (E - P - F) / H \text{ ‰ year}^{-1} \quad (5)$$

where the evaporation  $E$ , the precipitation  $P$  and the fresh water effect  $F$  of the coastal current are all expressed in  $\text{m year}^{-1}$  and the average thickness of the Atlantic water  $H$  in m.

b. *The sub-surface* of the Atlantic water, which is characterized by  $S=35.00\text{‰}$ , is found in the pronounced transition layer between the Atlantic and the deep water (MosBY 1959, Fig. 32). Through this surface salt and heat are lost to the deep water by vertical turbulent diffusion, whereby the established distribution of temperature and salinity is moving downwards. This motion is balanced by the effects of the renewal of bottom and deep water, so that in the long run the transition layer is kept at a constant depth.

From the systematic observations at Station M, the changes in depth of the transition layer have been followed from 1948 to 1958. It then appeared (MosBY 1961, Fig. 8) that in some years the depth was reduced from about 360 to 305 m in spring, while in other years it first increased from 360 to 410 m in spring, and then was reduced to 305 m in the autumn. On the assumption that the reduction in spring is caused by formation of true bottom water, while the occurrence in the autumn is due to formation of intermediate layers of deep water, the average annual effect may be estimated at about 50 m for the years 1948–58.

Although the vertical diffusion in the transition layer is perhaps slightly disturbed by an advective effect, the above considerations provide a basis for an approximate determination of the diffusion coefficient. Plotting the normal temperatures and salinities for Station M, first directly against depth and then against depth minus 50 m, it is possible by integration of the curves to determine the losses of heat and salt. This integration was carried out from the depth of about 325 m to 0 m and to 25 m respectively. The ratio between the changes in average temperature and in average salinity came out equal to  $0.744^\circ : 0.0235\text{‰} = 31.7$  and  $0.775^\circ : 0.0293\text{‰} = 26.4$  respectively.

From the normal station curves the gradients at the level of 35.00‰ were found to be

$$\begin{aligned} dt/dz &= -2.3 \cdot 10^{-4} \text{ }^\circ\text{C cm}^{-1} \quad \text{and} \\ dS/dz &= -0.08 \cdot 10^{-4} \text{ ‰ cm}^{-1} \end{aligned}$$

The ratio between them is 28.75, or equal to the direction coefficient of the corresponding tangent to the  $t$ - $S$  curve. As this ratio falls between those just given for the layers 0–325 m and 25–325 m (31.7 and 26.4), we may apply the averages of the heat and salt losses, or  $0.760^\circ$  and  $0.0264\text{‰}$  to the layer from 13 to 325 m, which is 312 m thick.

Applying the above procedure for different values of the vertical motion  $h$ , e.g. 25, 50, 75 and 150 m, it is found that the losses in temperature and salinity vary nearly linearly with  $h$  and may be expressed

$$\begin{aligned}\Delta t &\approx -0.0152 \cdot h \text{ } ^\circ\text{C year}^{-1} \\ \Delta S &\approx -0.00053 \cdot h \text{ } \text{‰ year}^{-1}\end{aligned}\quad (6)$$

where  $h$  is given in metres.

This means that through its sub-surface the 312 m thick layer of Atlantic water loses an amount of heat of  $0.0152 \cdot h \cdot 31,200$  gcal in a year or in  $31.536 \cdot 10^6$  seconds if the heat capacity of the water is put equal to 1. With the above values of the gradients we then find

$$\begin{aligned}0.0152 \cdot h \cdot 31,200 &= 2.3 \cdot 10^{-4} \cdot 31.536 \cdot 10^6 \cdot A_t \\ 0.00053 \cdot h \cdot 31,200 &= 0.08 \cdot 10^{-4} \cdot 31.536 \cdot 10^6 \cdot A_s\end{aligned}$$

where  $A_t = A_s = A$  corresponds to  $A_z/\rho$  and  $h$  to  $v_z$  in equation (2) above. For  $h = 50$  m year<sup>-1</sup> we then find

$$A = 0.065 \cdot h = 3.2 \text{ cm}^2 \text{ sec}^{-1}$$

The corresponding stability is relatively low,  $d\sigma/dz \approx 1 \cdot 10^{-5}$ .

At the normal Stations IV, V, VI of the average section we find the same maximum gradients of temperature, and at the same depths slightly higher salinity gradients than those used above. A study of the data from St. M showed that there may be an annual variation of these gradients, with a minimum in spring and a maximum in autumn. But the effects of these variations in our final balance sheets appear to be negligible. For these reasons it will be sufficient to consider the effects of the deep water as constant both in time and within the section.

The sub-surface of the Atlantic water is found in the average section to fall at about 450 m of depth near the continental shelf and to reach the sea-surface about 400 km farther west. Still this surface is not far from horizontal, and the average thickness of the layer of Atlantic water is found to be 330 m. For the loss of heat and salt through the subsurface, we may therefore adopt the values

$$\begin{aligned}\Delta t &= -0.0152 \cdot 50 \cdot 312/330 = -0.719 \text{ } ^\circ\text{C year}^{-1} \\ &= -0.060 \text{ } ^\circ\text{C month}^{-1} \\ \Delta S &= -0.00053 \cdot 50 \cdot 312/330 = -0.0250 \text{ } \text{‰ year}^{-1} \\ &= -0.0021 \text{ } \text{‰ month}^{-1} \\ &= -0.020 \text{ m month}^{-1}\end{aligned}\quad (7)$$

(fresh water removed)

c. *In the west* the Atlantic water is in contact with the Norwegian Sea water of lower temperature and salinity; the average section (Fig. 16) shows how the  $\sigma_t$ -surfaces are here approaching the surface.

As mentioned in connection with the horizontal maps, large eddies appear to be frequent in the area considered. No explanation of their origin has so far been offered, but our measurements have shown that these eddies may remain for several days in approximately the same position or may be moving at a moderate speed. They are thus of a quasi-stationary nature, and the strong horizontal density gradients within the

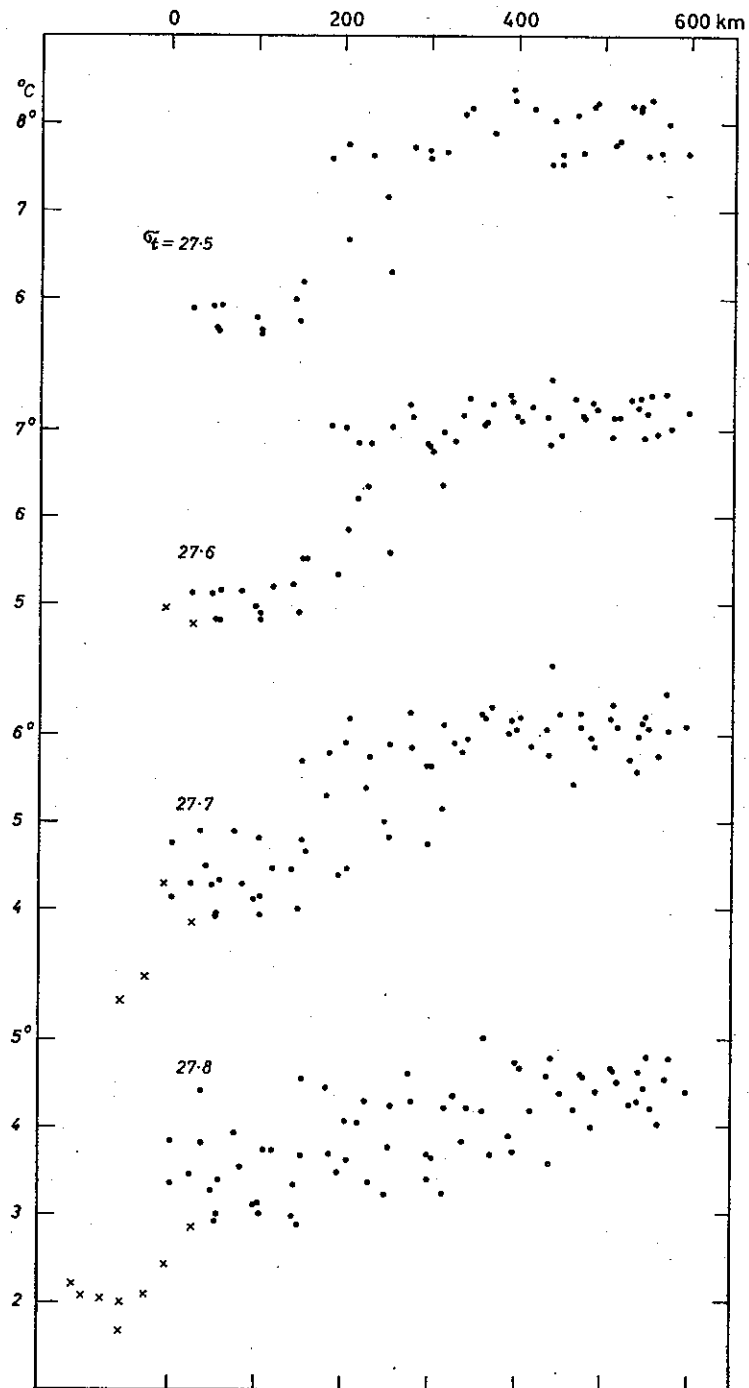


Fig. 18. Temperatures observed at different  $\sigma_t$ -surfaces.

average section must be assumed to be at least to some degree balanced by the effect of the earth's rotation. If this is correct, then the motions determined by dynamical computations should also be approximately correct.

The eddies must have a strong effect in mixing the water masses across the main direction of flow of the Atlantic water. The stability of the stratification will, however, prevent, or nearly prevent mixing across the density surfaces; in other words the motion must follow the quasi-isentropic  $\sigma_t$ -surfaces. If this is true, and if the mixing effect is sufficiently strong, then it must lead towards constant values of temperature and salinity along the  $\sigma_t$ -surfaces in our sections. By interpolation from the single station curves included in the average section all temperatures corresponding to the  $\sigma_t$ -values 27.5, 27.6, 27.7 and 27.8 were determined; they are plotted in Fig. 18 against the kilometre scale of the average section. With some scatter this diagram illustrates the expected constancy of temperature from the shelf at 600 km towards 200 km, from where a decrease towards the west is clearly seen. This decrease appears to be concentrated mainly between the normal Stations II and III, where the  $\sigma_t$ -curves in Fig. 16 have been made bolder, to mark the "choking area".

*The eddies may therefore have a considerable effect upon the macro-turbulence spectrum of the lateral mixing.* No detailed study of this spectrum has yet been undertaken, but it seems obvious that a strong tendency towards equalization of temperature and salinity across the main current is present. For this reason no attempt will be made to apply equation (2) in the direction across the current (i.e. east-west); instead we shall consider the bulk of Atlantic water as one water mass in our further considerations.

In the choking area, however, there are strong horizontal gradients of temperature and salinity, and here a lively exchange of heat and salt must be going on as a lateral mixing between the Atlantic water and the Norwegian Sea water in the west. The  $\sigma_t$ -surfaces are here very nearly horizontal, and the gradients may be determined along these surfaces or in the horizontal without great differences in the result. From the normal stations II and III, valid in summer, we find the following values

$$\begin{array}{lll}
 0-30 \text{ m} & 1.5 \cdot 10^{-7} \text{ }^\circ\text{C cm}^{-1} & 0.17 \cdot 10^{-7} \text{ }_{\text{‰}} \text{ cm}^{-1} \\
 30-50 \text{ m} & 1.1 \cdot 10^{-7} \text{ }^\circ\text{C cm}^{-1} & 0.12 \cdot 10^{-7} \text{ }_{\text{‰}} \text{ cm}^{-1} \\
 50-80 \text{ m} & 1.1 \cdot 10^{-7} \text{ }^\circ\text{C cm}^{-1} & 0.11 \cdot 10^{-7} \text{ }_{\text{‰}} \text{ cm}^{-1}
 \end{array} \quad (8)$$

or as averages from the surface to  $D_\sigma=80$  m, the approximate lower limit ( $\sigma_t=27.8$ ) of the Atlantic water in the choking area

$$\begin{aligned}
 g_t &= 1.25 \cdot 10^{-7} \text{ }^\circ\text{C cm}^{-1} \\
 g_s &= 0.135 \cdot 10^{-7} \text{ }_{\text{‰}} \text{ cm}^{-1}
 \end{aligned}$$

The exchange through the choke of a thickness of  $D_\sigma=80$  m affects the bulk of Atlantic water, which has a horizontal extension along the section of  $L=400$  km and an average thickness of  $H=330$  m.

Denoting now by  $B$  (corresponding to  $A_x/\rho$  and  $A_y/\rho$  of equation (2) above)

the coefficient of lateral turbulent diffusion, the annual effect (if constant) on the average temperature and salinity of the Atlantic water may be written

$$\begin{aligned}\Delta t &= -365 \cdot 24 \cdot 60 \cdot 60 \cdot BD_{\sigma g_i} / LH = -789 \cdot 10^{-8} \cdot B/H \\ \Delta S &= -365 \cdot 24 \cdot 60 \cdot 60 \cdot BD_{\sigma g_s} / LH = -85.2 \cdot 10^{-8} \cdot B/H\end{aligned}\quad (9)$$

d. *In the east* the Atlantic current will be diluted by fresh water originating from run-off from land through the Norwegian coastal current. In summer this water will go into the surface layer, while in winter the vertical convection may bring it into deeper layers. This will be dealt with later.

e. *The Atlantic current* according to the average section is a wedge of water moving northwards along the slope of the continental shelf. From the isoveles of Fig. 16 it is found that from the outer border at 200 km the speed of the current at all depths first increases to a maximum at about 320 km, then more slowly decreases towards the shelf at 590–600 km. The thickness of the current increases from some 50 m at 200 km to 450 m on the shelf; the result of this is a nearly symmetrically distributed volume transport with a maximum amounting to 10% of the total transport between 360 and 420 km, or around the position of Station M, at 390 km. Multiplication by temperatures and by salinities reveals a distribution of the heat and of the salt transport similar to that of the volume transport.

The total volume transport is found to be about  $1.9 \cdot 10^6 \text{ m}^3 \text{ sec}^{-1}$  through an area of the section of  $90 \cdot 10^6 \text{ m}^2$ . The average speed of the whole current is  $v = 2.1 \text{ cm sec}^{-1}$ , and the average speed within the column of Atlantic water at St. M is  $v_M = 2.74 \text{ cm sec}^{-1}$ .

In an earlier paper it has been shown that the extremes, i.e. the highest corresponding values of temperature and salinity, decrease northwards by  $0.35^\circ\text{C}$  and  $0.026\text{‰}$  per degree latitude (Mosby 1959, Figs. 30 and 31). Also the average temperatures and salinities decrease northwards. This has been found by planimeter from the original sections, limiting by the 300 m isobath of the bottom, the  $35\text{‰}$  isohaline or the  $4^\circ$  isotherm, and in neglecting first the surface layer down to 40 m depth. When plotting against temperature and salinity respectively the areas between successive  $1^\circ$  isotherms or  $0.1\text{‰}$  isohalines, all expressed in percentages of the total area, it was seen that they were distributed around one area of maximum extension, whose percentage decreased

Table 2. *Decrease of  $t$  and  $S$  with latitude*

Lat. N	Days	$\bar{t}$	$\bar{S}$	$\bar{t}$ corr.	$\bar{S}$ corr.
64°		7.17° C	35.186‰	7.08° C	(35.185)‰
65°	4½	7.08	.212	7.04	.212
66°	4½	6.66	.180	6.66	.180
67°	5	5.91	.149	5.96	.150
68°	8	5.50	.123	5.63	.124

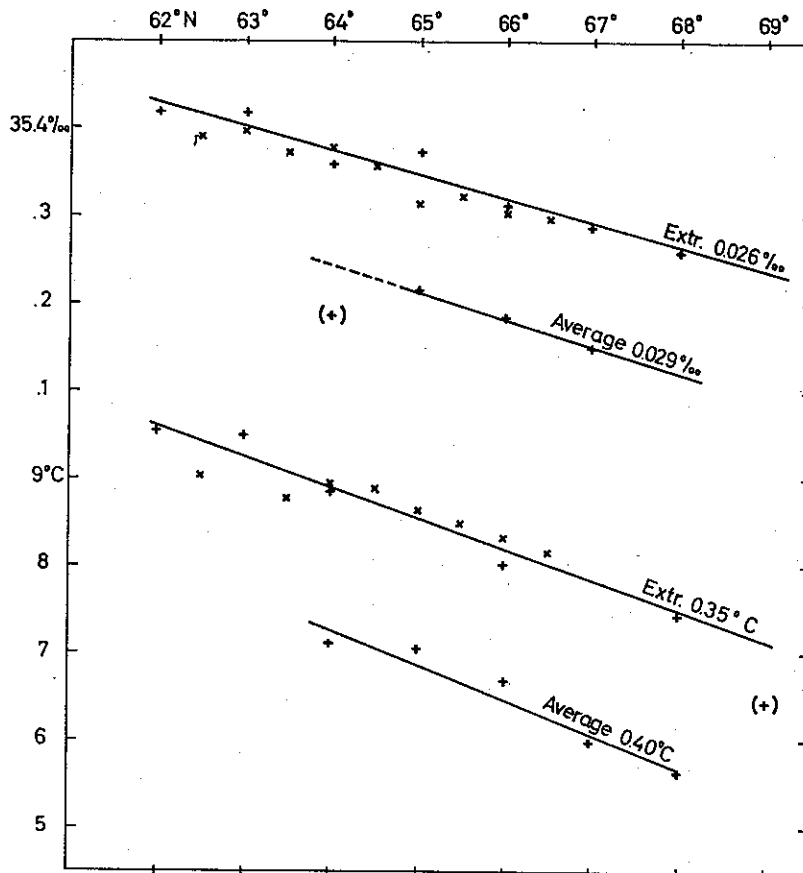


Fig. 19. Decrease with latitude of  $t^\circ$  and  $S \text{ ‰}$ .

northwards, its temperature or salinity also decreasing northwards. These statistical details seem to indicate the existence of a very coherent system of distribution.

The surface layer was treated separately in estimating the average values of temperature and salinity of the upper 40 m within each 20 km, in the original section, taking into account only areas where  $S > 35.0 \text{ ‰}$ . The result was a regular decrease of the average temperature of about  $0.5^\circ \text{ C}$  per degree latitude northwards and an irregular variation of the average salinity.

The values obtained for the whole of the Atlantic water are given in Table 2.

From the observations at St. M it is found that in June–July there is in the Atlantic water an average increase of the temperature of  $0.308^\circ \text{ C}$  per month, and of the salinity of  $0.003 \text{ ‰}$  per month. Applying these as corrections by means of the number of days between the sections, we arrive at the values given in the last two columns of the table. These values are plotted on Fig. 19, in which are also indicated the average decrease of the extreme values. The average values are of course the lower ones, but the decrease is about the same. The average salinity at  $64^\circ \text{ N}$  is out of track with the others. Leaving this value out of consideration we find by the method of least squares

$$\begin{aligned}\bar{t}_{\text{corr.}} &= 32.742 - 0.398\varphi \\ \bar{S}_{\text{corr.}} &= 37.122 - 0.0294\varphi\end{aligned}$$



where  $\varphi$  denotes latitude, and the horizontal gradients are

$$\begin{aligned} G_t &= 0.40^\circ \text{ C per degree latitude} \\ G_s &= 0.03\text{‰ per degree latitude} \end{aligned}$$

It will be noticed that the ratio  $G_t : G_s = 13.3$  corresponds to the slope of the approximately straight line obtained when plotting into a  $t$ - $S$  diagram all couples of temperature and salinity from the Atlantic water within any one of the sections.

The advective effect of the Atlantic current may now be expressed by

$$\begin{aligned} \Delta t &= G_t \cdot v \cdot 365 \cdot 24 \cdot 60 \cdot 60 / 11'111'111 \\ &= 2.838 \cdot G_t \cdot v = 1.135 \cdot v^\circ \text{ C year}^{-1} \\ \Delta S &= 2.838 \cdot G_s \cdot v = 0.085 \cdot v\text{‰ year}^{-1} \end{aligned} \quad (10)$$

f. For balance within the Atlantic current we now must claim (eqs. 3, 4, 5, 6, 9, 10)

$$\begin{aligned} \Sigma \Delta t &= 10 \cdot Q/H - 879.9 \cdot E/H - 0.0152 \cdot h - 789 \cdot 10^{-8} \cdot B/H + 2.838 \cdot G_t \cdot v = 0 \\ \Sigma \Delta S &= 35.15 \cdot (E - P - F)/H - 0.00053 \cdot h - 85.2 \cdot 10^{-8} \cdot B/H + 2.838 \cdot G_s \cdot v = 0 \end{aligned}$$

where  $B$  is the coefficient of lateral diffusion within the layer from 0 to 80 m in the choking area. Introducing now  $Q = 22.61 \text{ kcal cm}^{-2} \text{ year}^{-1}$  (Table 1),  $h = 50 \text{ m year}^{-1}$  and  $H = 330 \text{ m}$ , we find

$$\begin{aligned} E &= -0.029 + 0.426 \cdot v - 0.897 \cdot 10^{-8} \cdot B \\ P + F &= -0.289 + 1.228 \cdot v - 3.051 \cdot 10^{-8} \cdot B \end{aligned} \quad (11)$$

g. In summer the surface layer is light due to high temperatures and low salinities, and it is separated from the Atlantic water below by a transition layer of great stability. This stability hampers the vertical mixing and the two layers have little influence upon each other. Our two equations may therefore be split up into four.

The annual variation of temperature at Station M is illustrated in a paper by HELLAND (1963, Fig. 2). At 0, 10 and 25 m the increase of temperature in summer is much greater than at 50 m and deeper. From December to May the salinity is seen to increase at all depths, but from May on there is a decrease at 0, 10 and 25 m; this is an effect of the coastal current, whose less salty water can now spread out near the surface. But while the salinity of the surface layer decreases rapidly from May to August, the salinity at 50 m and more continues to increase. This increase, which started in December can only be explained as an effect of the Atlantic current. Another effect at 50 m and more is an increase of temperature, and the ratio between the two must be approximately as between the longitudinal gradients or as  $G_t : G_s = 0.40 : 0.03 = 13.3$ . An influence from the surface layer here means an additional increase of temperature and a reduction of the increase of salinity. If at any time we find the above-mentioned ratio, this indicates that no such influence is present. When plotting the ten-day means in  $t$ - $S$  diagrams, this ratio is found at 150 m from 25 May to 15 July, at 100 m from 15 May to 5 July, at 75 m from 15 June to 5 July, but not at 50 m.

From the ten-day means of the above paper (HELLAND 1963) we have computed averages for the periods 20 May to 30 June and 1 July to 10 August (Table 3). Each

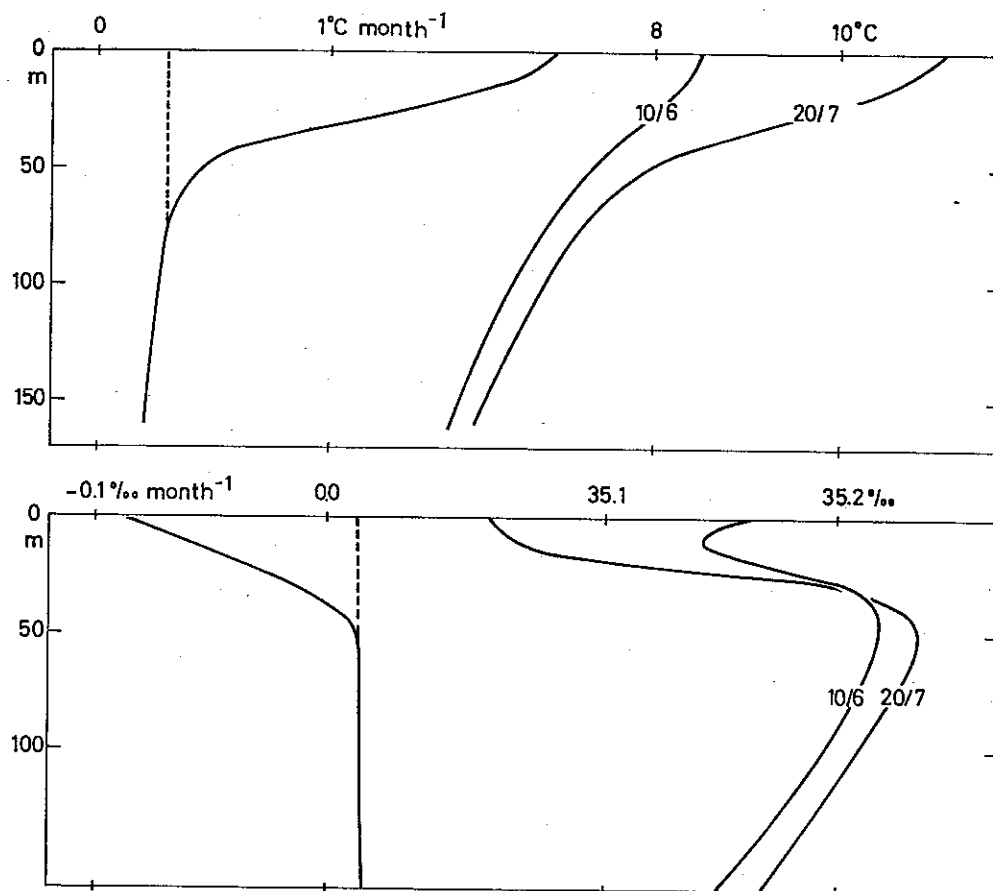


Fig. 20. Accumulation of heat and salt in summer at St. M.

of these periods is covered by about 150 stations. The vertical distribution of the averages is shown in Fig. 20 (top) to the right; the average changes per month are plotted to the left. From these curves we find the accumulation of heat between 0 and 40 m to be  $4.58 \text{ kcal cm}^{-2} \text{ month}^{-1}$ .

The corresponding salinities are shown in Fig. 20 (bottom) to the right and the average changes per month to the left. We find the reduction of the content of salt between 0 and 40 m to be  $0.0509\text{‰}$  per month.

Table 3. Changes at St. M in June-July

m	20/5-30/6		1/7-10/8		per month	
	t °C	S ‰	t °C	S ‰	°C	‰
0	8.48	35.165	11.10	35.050	1.96	-0.086
10	8.40	.142	10.84	.060	1.83	-0.062
25	8.02	.192	9.80	.162	1.31	-0.022
50	7.28	.218	7.87	.235	0.44	0.013
75	6.81	.208	7.21	.225	.30	.013
100	6.45	.195	6.80	.210	.26	.011
150	5.90	.157	6.17	.175	.20	.014

The distribution of salinity is shown in Fig. 15. It is seen that the Atlantic water reaches the surface between 200 and 500 of the kilometre scale. The surface values are highest about 350 km — between 35.10 and 35.15‰ — decreasing in both directions. In the east they go down to 34.86‰ on the approaches to the coastal current.

When plotting the average salinities for 0, 10 and 25 m on a map (not reproduced), it is seen that the western border, 35.0‰, of the Atlantic water is not a straight line, but a curve bending towards the west at 66°N and towards the east at 68°N. From the 28 stations taken between this border and the 800 km line an average salinity of 34.80‰ is found, while 35.18‰ is the average obtained from the 32 stations between the border and 200 km.

From Fig. 15 it is seen that the temperature of the surface layer is approximately constant from 600 km (in fact even from 800 km) in the east to between 200 and 300 km, from where decreasing values are found towards the west in the choking area. As the currents on the shelf seem to be weak (SÆLEN 1959, p. 27), the lateral mixing here may also be less effective, and we shall consider the edge of the shelf at 600 km as the probable eastern limit of the surface layer in our model. For the thermal effect of the lateral mixing we then have with  $D_\sigma=30$  m,  $G_t=1.5 \cdot 10^{-7} \text{ }^\circ\text{C cm}^{-1}$  (eq. 8),  $L \approx 350$  km and the average thickness of the surface layer  $H=39$  m

$$31.536 \cdot 10^6 \cdot D_\sigma g_t / HL = 10.4 \cdot 10^{-8}$$

and the loss of heat

$$10.4 \cdot 10^{-8} \cdot B / 12 = 0.867 \cdot 10^{-8} \cdot B$$

Both temperature and salinity gradients are large between the surface layer and the Atlantic water, viz. between 25 and 50 m on

10 June	$-3.0 \cdot 10^{-4} \text{ }^\circ\text{C cm}^{-1}$	$0.10 \cdot 10^{-4} \text{ } \text{‰ cm}^{-1}$
20 July	$-7.7 \cdot 10^{-4} \text{ }^\circ\text{C cm}^{-1}$	$0.29 \cdot 10^{-4} \text{ } \text{‰ cm}^{-1}$
average	$-5.3 \cdot 10^{-4} \text{ }^\circ\text{C cm}^{-1}$	$0.20 \cdot 10^{-4} \text{ } \text{‰ cm}^{-1}$

Denoting by  $A$  the coefficient of vertical heat conduction, the heat loss may be expressed

$$A \cdot 5.3 \cdot 10^{-4} \cdot 31.536 \cdot 10^6 / 12 \cdot 3900 = 0.357 \cdot A \text{ }^\circ\text{C month}^{-1}$$

where 3900 is the average thickness of the layer in cm.

From the average values of the above salinity gradients, we find the salt gain from below to be

$$A \cdot 0.20 \cdot 10^{-4} \cdot 31.536 \cdot 10^6 / 12 \cdot 3900 = 0.0135 \cdot A \text{ } \text{‰ month}^{-1}$$

where  $A$  denotes the coefficient of vertical salt diffusion.

The net gain of heat by radiation (Table 1) in June–July is  $7.66 \text{ kcal cm}^{-2} \text{ month}^{-1}$ , sufficient for an average increase of the temperature of the 39 m thick layer by  $1.964 \text{ }^\circ\text{C month}^{-1}$ . The heat lost by evaporation (Table 4) is  $3.422 \text{ kcal cm}^{-2} \text{ month}^{-1}$  if the annual evaporation is  $E=1.0 \text{ m year}^{-1}$ ; this means a decrease of temperature of

$0.877 \cdot E^\circ \text{ C month}^{-1}$ . The heat accumulated was found from Fig. 20 to be  $4.58 \text{ kcal cm}^{-2} \text{ month}^{-1}$ , which corresponds to  $1.174^\circ \text{ C month}^{-1}$ . The heat gain by advection is

$$2.838 \cdot 0.40 \cdot v / 12 = 0.0946 \cdot v$$

For heat balance we then have

$$1.964 - 0.877 \cdot E = 1.174 + 0.867 \cdot 10^{-8} \cdot B + 0.357 \cdot A - 0.946 \cdot v$$

or

$$E = 0.901 + 0.108 \cdot v - 0.407 \cdot A - 0.990 \cdot 10^{-8} \cdot B \quad (12)$$

When plotting the average salinities within the surface layer for every 50 km interval of the section, we find in the west a gradient  $0.17 \cdot 10^{-7} \text{‰ cm}^{-1}$  and in the east  $0.07 \cdot 10^{-7} \text{‰ cm}^{-1}$ . These gradients are active to a depth of about 40 m in the west and to 30 m in the east; the average thickness of the layer is about 60 m. With  $L = 500 - 200 = 300 \text{ km}$  between the horizontal gradients in the east and in the west we now have in  $\text{‰}$  per month:

in the west

$$-31.536 \cdot 10^6 \cdot 40 \cdot 0.17 \cdot 10^{-7} \cdot B / 12HL = -0.149 \cdot 10^{-8} \cdot B$$

in the east

$$-31.536 \cdot 10^6 \cdot 30 \cdot 0.07 \cdot 10^{-7} \cdot B / 12HL = -0.046 \cdot 10^{-8} \cdot B$$

at St. M

Advection	=	$2.838 \cdot G_s \cdot v / 12 = +0.0071 \cdot v$
Accumulation	=	$+0.0509$
Precipitation	June-July =	$-0.0542 \cdot P$
Evaporation	June-July =	$+0.0391 \cdot E$
Diffusion	June-July =	$+0.0135 \cdot A$

where  $P$  and  $E$  are annual totals in  $\text{m year}^{-1}$ .

For balance this gives

$$0.0071 \cdot v + 0.0509 + 0.0135 \cdot A + 0.0391 \cdot E - 0.0542 \cdot P - 0.195 \cdot 10^{-8} \cdot B = 0$$

or

$$P = 0.721 \cdot E + 0.131 \cdot v + 0.939 + 0.249 \cdot A - 3.598 \cdot 10^{-8} \cdot B$$

Introducing  $E$  by eq. (12), we find

$$P = 1.585 + 0.208 \cdot v - 0.044 \cdot A - 4.312 \cdot 10^{-8} \cdot B$$

From a study of vertical diffusion in the Byfjord near Bergen (not yet published), where the stability below the surface layer was as high as at St. M ( $d\sigma/dz \approx 1 \cdot 10^{-4}$ ), it appears that a value about  $A = 0.4$  may be expected for the *summer surface layer*. Introducing this, we obtain for this layer

$$\begin{aligned} E &= 0.738 + 0.108 \cdot v - 0.990 \cdot 10^{-8} \cdot B \\ P &= 1.571 + 0.208 \cdot v - 4.312 \cdot 10^{-8} \cdot B \end{aligned} \quad (13)$$

h. *Intermediate layer in summer*. Immediately below the extreme Atlantic water there is a water layer which is hardly influenced from above (hatched in Fig. 16). When plotting all ten-day means in  $t$ - $S$  diagrams, for 50, 75, 100 and 150 m, the lowest

values of the ratio  $t : S$  are found in summer. As will be remembered the ratio between the corresponding advective effects of the Atlantic current is  $G_t : G_s = 0.40 : 0.030 = 13.3$ . Similar values are found at 150 and 100 m, for a brief period also at 75 m. By some smoothing we find

100 m	25/5–25/6	0.180°	0.014‰	ratio	12.9
	5/6–5/7	0.210	0.017		12.4
	15/6–15/7	0.250	0.017		14.7
150 m	25/5–25/6	0.126	0.010		12.6
	5/6–5/7	0.128	0.010		12.8
	15/6–15/7	0.195	0.015		11.7
	25/6–25/7	0.165	0.008		20.6

The lower values, slightly below 13.3, are found at both of these levels in the periods 25/5–25/6 and 5/6–5/7. Limiting to these, we find the average values

100 m	0.195°	0.015‰
150 m	0.127°	0.010‰
0.161°		0.0127‰ per month

Although the amounts of heat and salt entering from above at the 50 m level are again leaving the intermediate layer at the 150 m level because the vertical gradients are approximately equal, the general reduction of temperature and salinity of the bulk of Atlantic water by diffusion to the deep water must be felt in the intermediate layer (as eq. 7 or a little more).

Also the effect of the lateral mixing is felt in the intermediate layer (100–150 m at St. M), which is found in June–July to correspond very nearly to the layer between the  $\sigma_t$ -surfaces 27.65 and 27.70 (hatched in Fig. 16). These surfaces are found in the choke at about 40 and 45 m at St. II, and at 46 and 55 m at St. III, or at a vertical distance of  $\Delta D_\sigma \approx 7$  m. The gradients are  $g_t = 1.10 \cdot 10^{-7} \text{ C cm}^{-1}$  at  $\sigma_t = 27.6$  and  $g_s = 0.86 \cdot 10^{-7} \text{ C cm}^{-1}$  at  $\sigma_t = 27.7$ ; as an average between 27.65 and 27.70 we thus find  $g_t = 0.9 \cdot 10^{-7} \text{ C cm}^{-1}$ . In the relevant intervals the ratio between temperature and salinity at constant  $\sigma_t$  is as  $\Delta t : \Delta S = 20 : 3$ ; accordingly we may put  $g_s = 3 \cdot 0.9 \cdot 10^{-7} / 20 = 0.135 \cdot 10^{-7} \text{‰ cm}^{-1}$ . From the average section it is seen that the  $\sigma_t = 27.7$  surface approaches the shelf edge at about 260 m depth near the 600 km, while the 27.65 surface continues onto the shelf to at least 800 km. The lateral extension of this water layer may thus be estimated at about  $L = 500$  km, and its average thickness is found from the section to be approximately  $\Delta H \approx 37$  m. We then find

$$\begin{aligned} 31.536 \cdot 10^6 \cdot \Delta D_\sigma g_t / \Delta H L &= 1.1 \cdot 10^{-8} \\ 31.536 \cdot 10^6 \cdot \Delta D_\sigma g_s / \Delta H L &= 0.16 \cdot 10^{-8} \end{aligned}$$

Limiting arbitrarily to  $L = 340$  km, the average thickness of the layer becomes  $\Delta H \approx 54$  m, and the result becomes the same.

For balance we now have for the *intermediate layer* ( $27.65 < \sigma_t < 27.70$  or 100–150 m at St. M) by eq. (10)

$$12 \cdot 0.161 + 0.719 + 1.1 \cdot 10^{-8} \cdot B = 1.135 \cdot v$$

$$12 \cdot 0.0127 + 0.0250 + 0.16 \cdot 10^{-8} \cdot B = 0.0851 \cdot v$$

from which

$$B = 0.3 \cdot 10^8, \quad v = 2.7 \text{ cm sec}^{-1}$$

At St. M the geostrophic speed between 100 and 150 m of depth is  $2.9 \text{ cm sec}^{-1}$ .

Introducing next into the equations (13) for the *summer surface layer* the same value  $B = 0.3 \cdot 10^8$  and the geostrophic speed in this layer at St. M or  $v = 3.2 \text{ cm sec}^{-1}$ , we obtain

$$E = 0.79 \approx 0.8 \text{ m year}^{-1}$$

$$P = 0.95 \approx 1.0 \text{ m year}^{-1}$$

Introducing finally into the equations (11) for the whole of the Atlantic current  $B = 0.3 \cdot 10^8$  and the average geostrophic speed between 0 and 330 m at St. M or  $v = 2.7 \text{ cm sec}^{-1}$ , we find for the whole year

$$E = 0.85 \text{ m year}^{-1}$$

or slightly higher than just obtained from the surface layer, and

$$P + F = 2.11 \text{ m year}^{-1}$$

whereby

$$F = 2.11 - 0.95 = 1.16 \approx 1.1 \text{ m year}^{-1}$$

We may thus adopt as probable values

$$E = 0.8 \text{ m year}^{-1}$$

$$P = 1.0 \text{ m year}^{-1}$$

$$F = 1.1 \text{ m year}^{-1}$$

i. *The evaporation* was found by BØYUM (1966, Table 7) to vary between 0.9 in 1950–51 and  $1.2 \text{ m year}^{-1}$  in 1954–55, with an average of 1.08 for the years 1948–58. He also quotes the values 0.96 given by BUDYKO (1963) and 0.71 given by ZAITZEV (1960). Our value 0.8 thus appears quite reasonable, remembering that our hydrographic observations were made in 1935.

The relative values of BØYUM for the ten-year period October 1948 to September 1958 are used in Table 4 to compute the total heat loss and the corresponding temperature reduction of a 330 m column of water on the assumption of an evaporation of  $E = 0.8 \text{ m year}^{-1}$ . The drop from October to November occurs in seven out of the ten years and is thus probably representative. The last column of the table gives the averages of every two consecutive monthly values; these averages are used in Table 11 below.

j. *The precipitation* at sea is difficult to measure. After thorough experiments 1950–1954 SKAAR (1955) found an average annual value for St. M of about  $\frac{1}{3} \text{ m year}^{-1}$ . SPINNANGR (1958) compared with coastal stations, at which it was possible to estimate

the orographical effect and arrived at the result that a more reasonable value would be the double or three times that of SKAAR. The above value  $1.0 \text{ m year}^{-1}$  is in agreement with the latter estimate.

Table 4. *Evaporation at St. M (after Bøyum)*

Month	1948-1958		gcal $\text{cm}^{-2} \text{ day}^{-1}$			$E = 1.0 \text{ m year}^{-1}$ kcal $\text{cm}^{-2}$	For a total of $E = 0.8 \text{ m year}^{-1}$			
	mm day $^{-1}$	mm month $^{-1}$	Latent	Sensible	Total		kcal $\text{cm}^{-2}$	330mcolumn	mm	mm
I	4.56	141	271	161	432	12.758	10.206	-0.309°C	107.8	101
II	4.41	124	261	154	415	11.070	8.856	.268	94.2	89
III	3.53	109	209	130	339	10.011	8.009	.243	83.4	74
IV	2.78	83	166	90	256	7.316	5.853	.177	63.6	57
V	2.10	65	132	57	189	5.582	4.466	.135	49.6	44
VI	1.63	49	97	34	131	3.744	2.995	.091	37.3	35
VII	1.42	44	84	21	105	3.101	2.481	.075	33.6	38
VIII	1.83	57	107	23	130	3.839	3.071	.093	43.2	48
IX	2.26	68	133	36	169	4.830	3.864	.117	51.7	63
X	3.18	99	189	75	264	7.797	6.238	.189	75.2	72
XI	3.04	91	180	83	163	7.516	6.013	.182	69.6	80
XII	3.84	119	228	125	353	10.425	8.340	.253	90.8	99
Total		1049				87.989	70.392	-2.132	800.0	800

From the mean monthly values of precipitation for the ten-year period October 1948 to September 1958 (*Norsk Meteorologisk Årbok* 1949-1960) we have computed the averages given in Table 5 for the coastal stations Ona, Sula and Skomvær (see Fig. 14), while data from Hoyvik in the Faroe Islands were taken from *Dansk Meteorologisk Aarbog* (1950-64). The annual mean values are very different, varying from  $0.546 \text{ m year}^{-1}$  at Skomvær to  $1.453 \text{ m year}^{-1}$  at Hoyvik. But the annual variation is very similar, exception being made only for the high October values observed on the Norwegian coast but not in the Faroe Islands. It therefore appears reasonable to assume for the sea area in question a similar annual variation, using approximately the averages of the values from the stations mentioned. These are given in the sixth column of Table 5, and after reduction to  $P=1 \text{ m year}^{-1}$  in the seventh column. Consecutive means over three months are given in the last column. The monthly values for June and for July are both near to 0.054 of the total for the year.

k. *The fresh water F* shall here include all fresh water originating from land, mainly from Norway, but also from other areas such as through the Baltic current. All of this water must be conveyed into the Atlantic current *via* the coastal current, which is certainly variable, but which is present all the year round. It therefore appears reasonable to assume that most of the changes in run-off, such as the flooding in spring, are felt in the Atlantic current as smoothed effects.

Table 5. *Precipitation in mm*

Month	Ona	Sula	Skomvær	Hoyvik	Mean	$P = 1.0 \text{ m year}^{-1}$	
I	131	100	67	168	116	110	102
II	92	74	41	124	83	79	88
III	80	69	45	108	76	72	71
IV	77	56	32	99	66	63	64
V	70	55	29	82	59	56	57
VI	69	49	38	61	54	51	54
VII	78	51	32	75	59	56	57
VIII	78	50	37	98	66	63	70
IX	132	67	49	144	98	93	96
X	200	128	66	161	139	132	111
XI	145	95	56	165	115	109	119
XII	155	112	54	168	122	116	112
Year	1307	906	546	1453	1053	1000	1001

A quantitative estimate of the run-off is difficult. For the relevant coastal areas of Norway the following values are based on records and estimates by TOLLAN (1968):

Møre-Trøndelag	$2425 \text{ m}^3 \text{ sec}^{-1}$
Nordland	$2363 \text{ m}^3 \text{ sec}^{-1}$
	$4788 \text{ m}^3 \text{ sec}^{-1}$

With an average speed of about  $2 \text{ cm sec}^{-1}$  the Atlantic current will need more than a year to pass from Stad to Lofoten, a distance corresponding approximately to these two coastal areas. If the nearly  $5000 \text{ m}^3 \text{ sec}^{-1}$  were disposed regularly over an area, such as from  $63$  to  $69^\circ\text{N}$  and within  $500 \text{ km}$  from the coast, it would provide some  $0.45 \text{ m year}^{-1}$ . This water would have to pass the Norwegian coastal current, a continuation of the Baltic current. As stressed already by HELLAND-HANSEN and NANSEN (1909) the latter current is the only way out for the surplus of fresh water from the Baltic, the Kattegat, the Skagerrack and the North Sea. From the Baltic alone this current carries some  $16'000 \text{ m}^3 \text{ sec}^{-1}$  of brackish water of  $8\%$  salinity (JACOBSEN 1925).

From these considerations it seems justified to conclude that the total effect, denoted in this paper by  $F$ , may be expected to be somewhere between  $0.5 \text{ m year}^{-1}$  and the value  $1.1 \text{ m year}^{-1}$  computed above (p. 37).

5. *Seasonal variations.* Table 6 gives for each month the effect upon the average temperature of the total column of Atlantic water (average thickness  $330 \text{ m}$ ): of the net radiation income (from Table 1), of the total loss of heat for an annual evaporation of  $E=0.8 \text{ m year}^{-1}$  (from Table 4), of the heat loss to the deep water (from eq. 7), and of the turbulent lateral mixing in the west (from eq. 9 with  $B=0.3 \cdot 10^8$ ). Columns 6–7 give the total  $\Sigma$  of these temperature changes in each month and the corresponding values after interpolation for the last day of each month. From average



Table 6. Heat balance of the Norwegian Atlantic current at 66° N, expressed in °C of a 330 m column of water

1 Month	2 Radiat.	3 Evapor.	4 Deep w. 50 m	5 Lateral	6 $\Sigma$	7 $\Sigma_{\text{interp.}}$	8 $\Delta \bar{t}_{0-330m}$	9 $\bar{t} - \Sigma_{\text{interp.}}$	10 Conv.	11 cm sec <sup>-1</sup>
I	-0.085	-0.309	-0.060	-0.060	-0.514	-0.495	-0.257	0.238		2.52
II	-0.053	-0.268	.060	.060	-0.441	-0.400	-0.144	.256		.71
III	0.015	-0.243	.060	.060	-0.348	-0.277	-0.012	.265		.80
IV	0.107	-0.177	.060	.060	-0.190	-0.125	0.129	.254		.69
V	0.207	-0.135	.060	.060	-0.048	0.006	0.259	.253	0.260	.67
VI	0.240	-0.091	.060	.060	0.029	0.035	0.301	.266		.81
VII	0.224	-0.075	.060	.060	0.029	0.000	0.286	.286		3.02
VIII*	0.158	-0.093	.060	.060	-0.055	-0.108	0.158	.266		2.81
IX	0.061	-0.117	.060	.060	-0.176	-0.258	-0.013	(.245)	0.260	(.59) 2.75
X	-0.021	-0.189	.060	.064	-0.334	-0.360	-0.159	(.201)	.260	(.12) 2.75
XI	-0.074	-0.182	.060	.064	-0.380	-0.415	-0.273	(.142)	.260	(1.50) 2.75
XII	-0.096	-0.253	.060	.064	-0.473	-0.505	-0.276	(.229)	.260	(2.42) 2.75
Year	0.683	-2.132	-0.720	-0.732	-2.901	-2.902	-0.001	(2.901)	3.124	-0.223

temperatures from 0 to 330 m, obtained by a careful study of the observations from Weather Station M (1948–1954), were found the changes from month to month. As these values show some irregularities, they have been smoothed by forming means of three consecutive values in column 8. In column 9 are given the differences between these latter changes and the values  $\Sigma_{\text{interp.}}$ . These differences correspond to the advective effect of the Atlantic current, i. e. the term  $2.838 \cdot G_t / 12v$ , where  $G_t = 0.40^\circ \text{C}$  per degree latitude. In column 11 are given the values of  $v$  obtained on the assumption of a complete heat balance in each month.

The contents of Table 6 are presented in Fig. 32 (p. 55), from which it is seen that the advective effect of the Atlantic current is keeping a nearly constant value of  $0.26^\circ \text{C month}^{-1}$  ( $v = 2.75 \text{ cm sec}^{-1}$ ) throughout 8–10 months, while in autumn it decreases, so that from the middle of November to the middle of December the average is only  $0.142^\circ \text{C}$ , corresponding to a speed of the current of  $1.5 \text{ cm sec}^{-1}$ . It is hardly possible to ascribe this irregularity to inaccuracies in any of the above adopted patterns of annual variation. We know very little about variations in the speed of the Atlantic current; the studies by TAIT (1957) indicate an increase in the autumn, if any. It is hard to imagine a corresponding change of the horizontal gradient  $G_t$ , which was in fact found also in the December measurements. The computed values of the net radiation are fairly reliable and in particular so as far as the annual variation is concerned. This may be said also about the evaporation. The effect of the deep water must be very nearly constant throughout the year, since the vertical gradients in the transitional layer are nearly constant. But the lateral mixing in the west may change; this will be investigated in the following, where the changes in autumn are to be related to the vertical convection created by the cooling of the surface. However, if an independent reason for the decrease of  $\Delta \bar{t} - \Sigma$  in the autumn is found, then heat balance must prevail through the rest of the year, or from the middle of December to the middle of October. For this period we find from Table 6 that with the average geostrophic current speed at St. M, 0–330 m, or  $v = 2.74 \text{ cm sec}^{-1}$ , there is a perfect heat balance if  $E = 0.8 \text{ m year}^{-1}$ .

6. *Winter conditions.* After the disturbance of the heat balance in autumn had been found\*, supplementary measurements were carried out in December 1965 along 67,  $66\frac{1}{2}$ , 66,  $65^\circ \text{N}$  as seen from Fig. 21. The observations have been sent to the ICES Data Centre in Copenhagen; they are also available (MosBY 1969) on request together with the observations from two sections in latitudes 64 and  $66^\circ \text{N}$ , taken in March 1965, also used in the present paper to illustrate the seasonal changes. The December section from  $66^\circ \text{N}$  is seen in Fig. 22 to be more irregular than that from the summer of 1935 (MosBY 1959, Figs. 6, 7). This may perhaps help to explain why the horizontal gradients  $G_t$  and  $G_s$  also appear more uncertain in December. Using planimeter within the limits  $35\%$ ,  $4^\circ$  and  $3^\circ$ , and using the extreme values, we find the averages  $G_t = 0.34^\circ \text{C per degree latitude}$  and  $G_s = 0.040\%$  per degree latitude between

\* Presented on 13/11–64 at the Saclant Centre, La Spezia, on 21/8–65 to the Association of Norwegian Oceanographers, and on 17/9–65 to the Norwegian Geophysical Society.

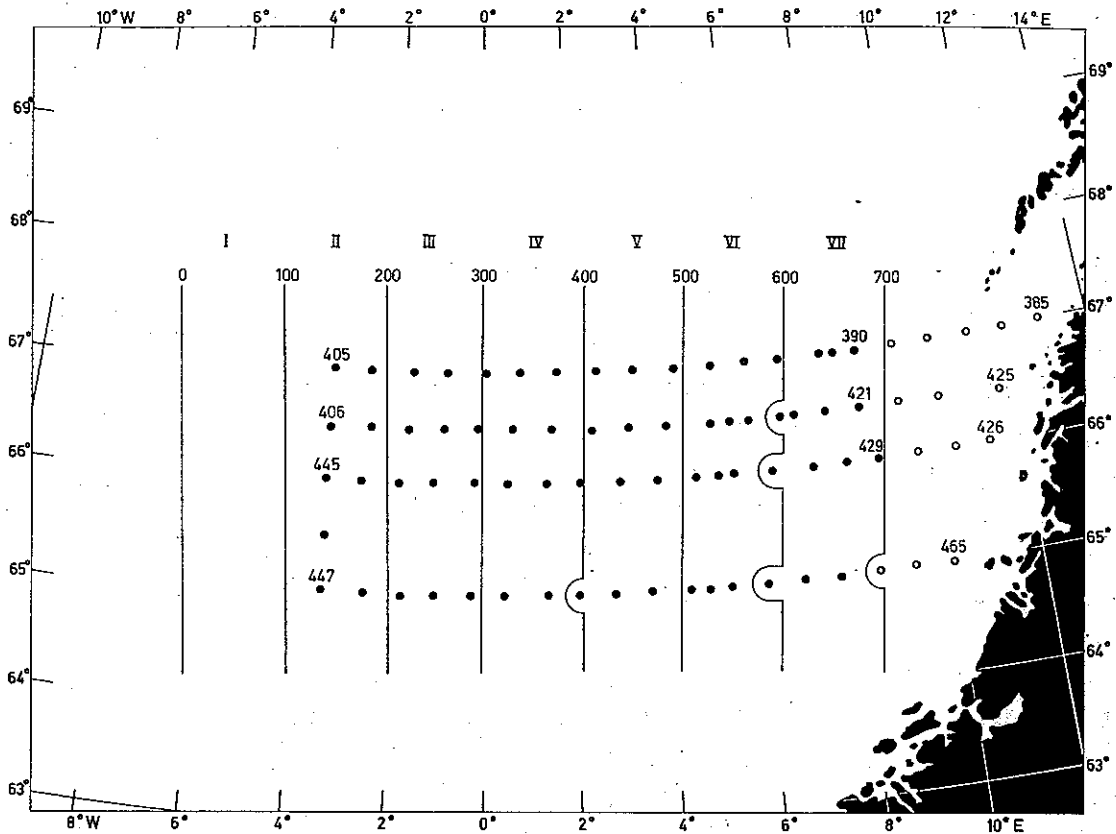


Fig. 21. Stations December 1965.

65 and 67° N. But both of these averages are based on rather different values between two and two sections. From the two sections in latitudes 64 and 66° N in March 1965 the number of observations is even more unsatisfactory. We find by planimeter  $0.12^\circ$ ,  $0.012\%$ , but by extreme values  $0.36^\circ$ ,  $0.025\%$ . The situation in winter seems to be characterized by a higher degree of large-scale heterogeneity, and a larger number of observations will therefore be needed for a statistically reliable determination. But there can hardly be any doubt that the horizontal gradients are being preserved throughout the winter, it being difficult to understand how the vertical convection could destroy them, and even more difficult to explain how they could reappear after the New Year.

The four sections from December 1965 were used for construction of the average section Figs. 23 and 24. By dynamical computations we find between Stations III and IV a mean geostrophic speed of the current between 0 and 330 m depth, of  $2.55 \text{ cm sec}^{-1}$ , or slightly less than  $2.74 \text{ cm sec}^{-1}$ , as found from the corresponding part of the average section from the summer of 1935. The main difference is found between 0 and 150 m depth.

When studying the observations for the years 1948–1958 for St. M, HELLAND (1963) showed that the thickness of the homogeneous surface layer increased nearly linearly

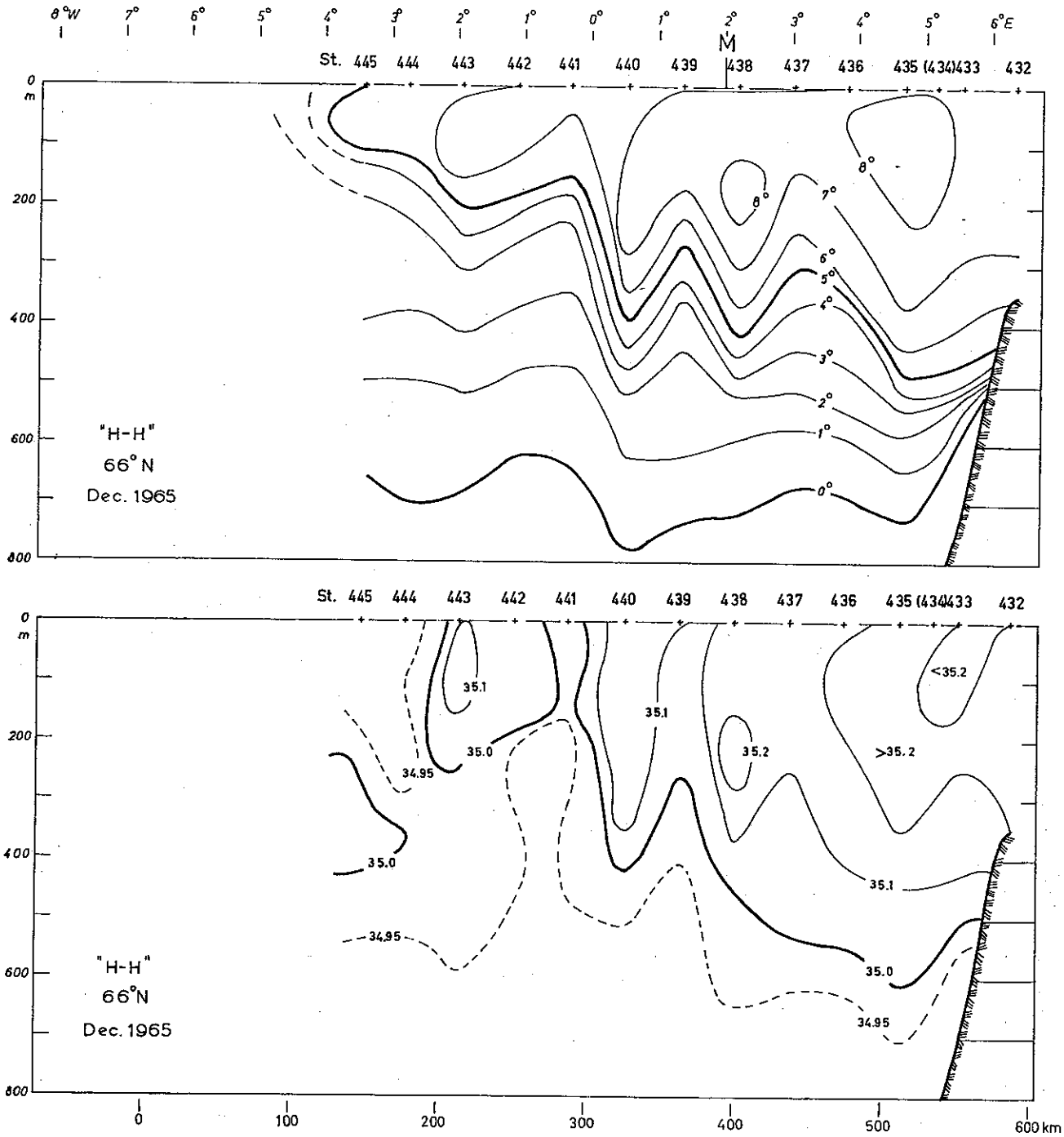


Fig. 22. Section 66°N, December 1965, t°C and S ‰.

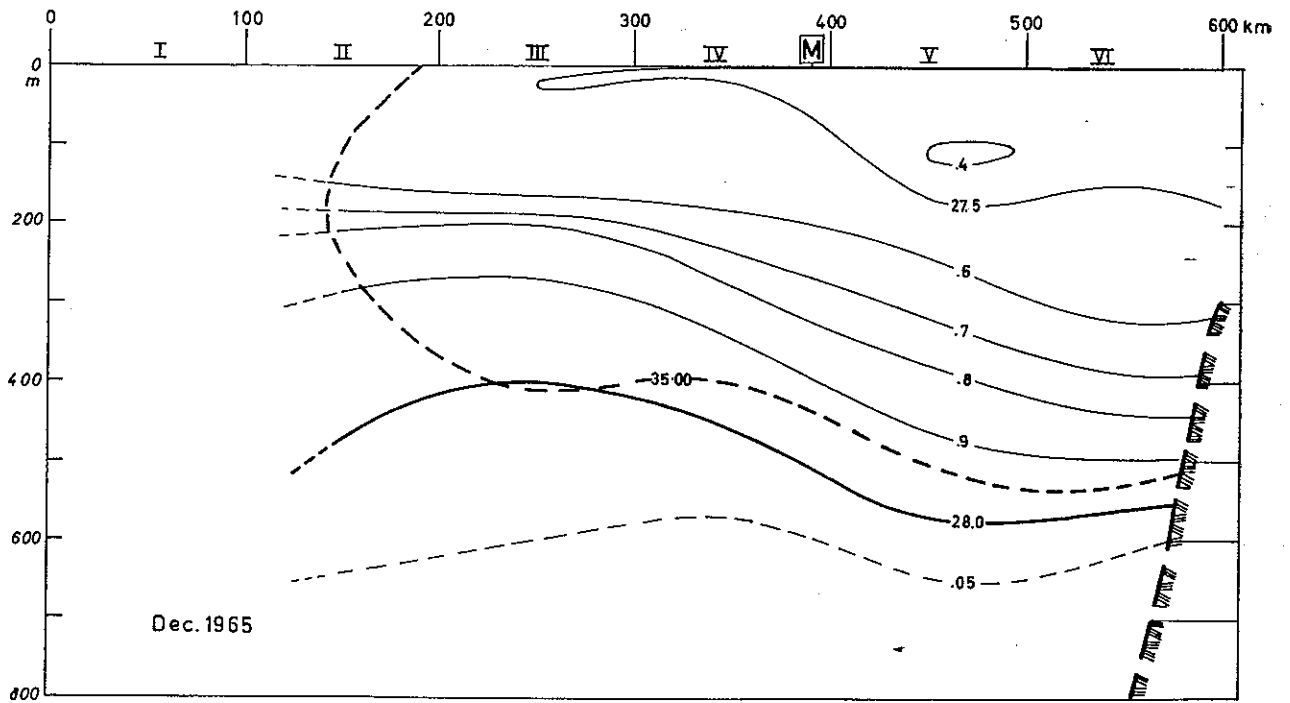
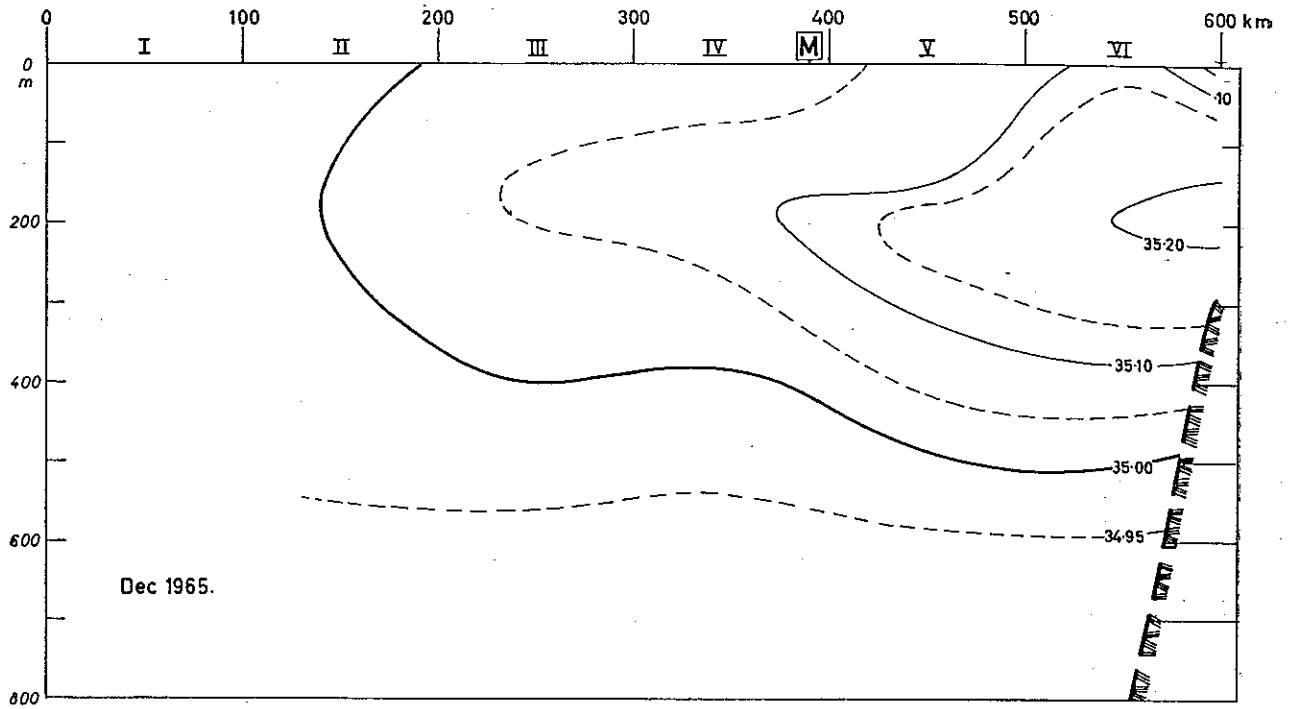


Fig. 23. Average section December 1956,  $S \text{ ‰}$  and  $\sigma_t$ .

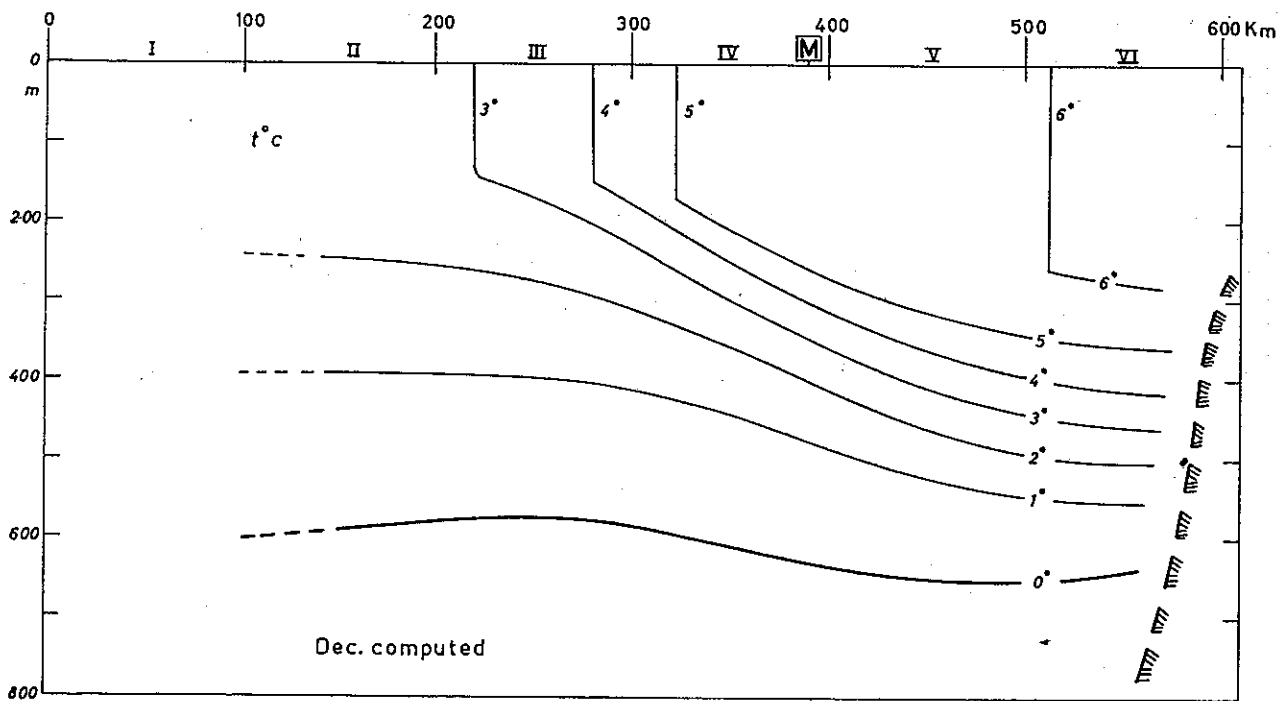
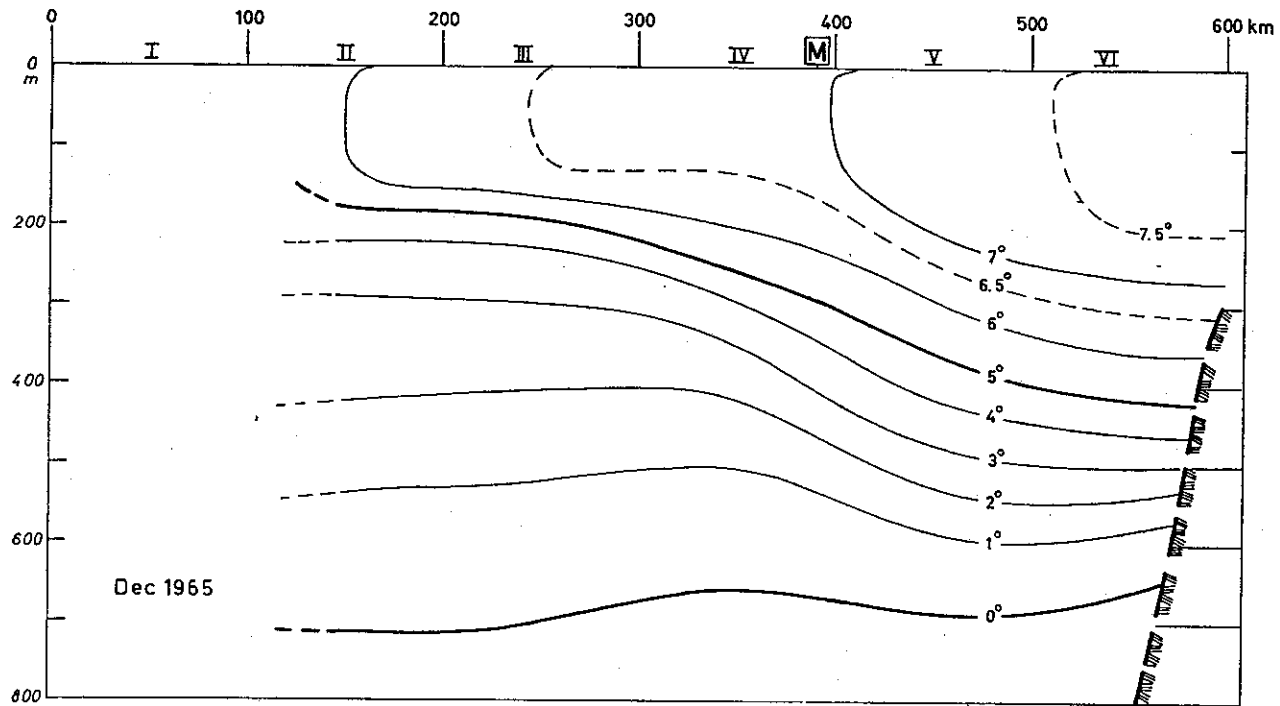


Fig. 24. Average section December 1965, t°C observed and computed.

with time from the beginning of October to the end of December. Taking into consideration all observations from the years 1948–1963, we find a nearly homogeneous surface layer, the thickness of which varies with time as seen from Table 7. Taking into consideration the amount of heat lost by radiation and by evaporation, it is easy to compute the depth to which a column of water as observed for the middle of September would be homogenized if it were kept isolated from the surrounding water masses. The values are given in the third column of Table 7; they are seen to agree well with the observed ones until February. Starting from the normal stations of the average section from July 1935 we have now in the same way established the section Fig. 24 (bottom) for the 8th of December. It is not quite correct to do this since the sections were run between the 19th of June and the 14th of July. From this time to the middle of September, when cooling of the surface starts, the temperature of the water at St. M is known to increase considerably. The average increase in the uppermost 100 m is about 1.5° C, with a maximum of 1.84° C at 25 m; it is about 0.6° between 100 and 200 m and decreases with depth. Similar changes might have been applied to the normal stations, so as to refer these first to the middle of September. However, as the final result is nearly the same, we have used the original normal stations. It must be admitted that the crudely computed section resembles that in Fig. 24 (top), which was based on the five sections from 2–15 December 1965. Absolute values of temperature should not be compared, as the situation below the effect of the vertical convection was not the same in July 1935 as in December 1965. A discrepancy is also found in the eastern part of the section, where the convection has not reached the computed depth.

Table 7. *Homogeneous surface layer at St. M*

Date	Obs.	Comp.
15.IX	30 m	36 m
15.X	40 m	58 m
15.XI	80 m	90 m
15.XII	122 m	145 m
15.I	160 m	183 m
15.II	180 m	(223 m)
15.III	190 m	(246 m)

A similar computation was carried out also on the basis of the two sections from the middle of March (see Fig. 25). Comparing with the normal temperature curves in Fig. 26, a considerable agreement is found; but it is also seen that the upper water layer is not really homothermal. In fact, it is seen from Fig. 25 that the isotherms are sloping towards the surface in the west; this is true also of the  $\sigma_t$ -curves. It is seen from

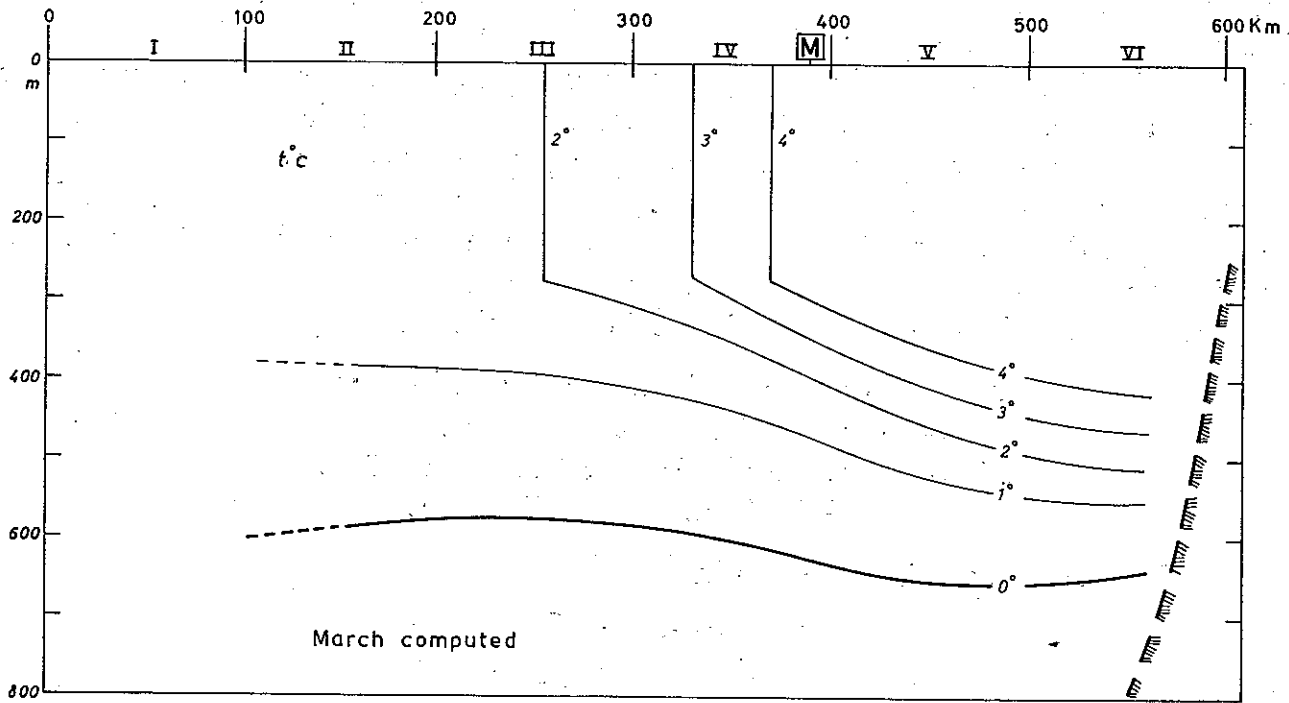
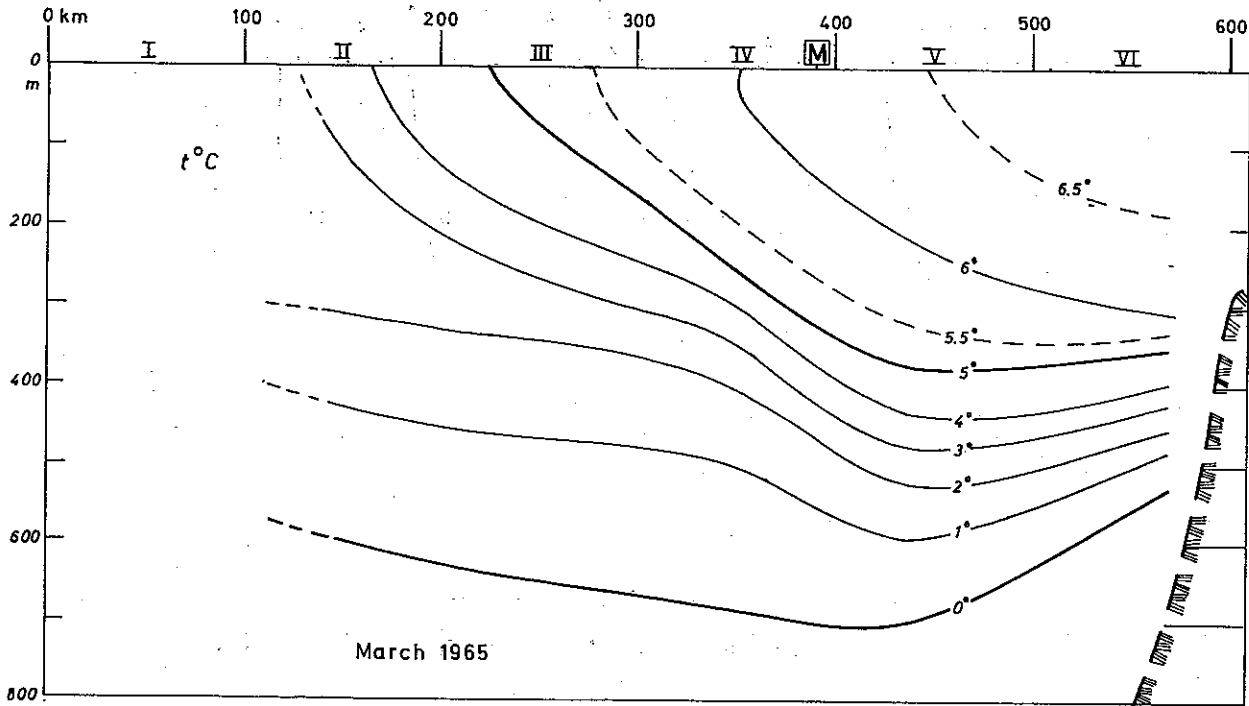


Fig. 25. Average section March 1965,  $t^{\circ}\text{C}$  observed and computed.



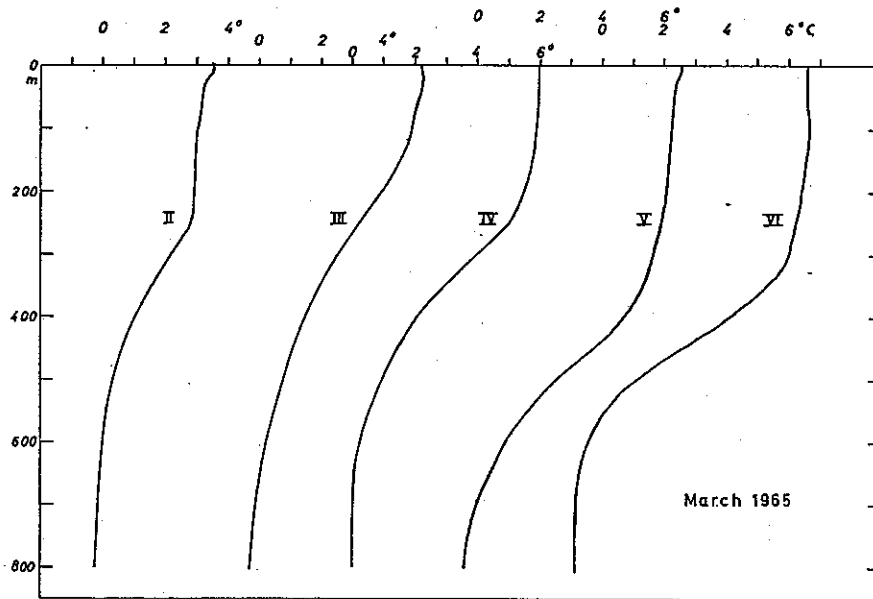


Fig. 26. Temperature distribution at average stations March 1965.

the diagrams that the cooling in autumn has produced a surface layer which is very nearly homothermal down to about 150 m depth, although it is of different temperatures in different parts of the section. The salinity is not constant within the vertical, and also the density decreases a little towards the surface. But the stability of the upper layer is weak and the depth or the thickness of the upper layer within the choking area is now some 160 m, or nearly twice the summer value. From the average section we find between the Stations II and III an average difference in temperature of  $0.67^{\circ}\text{C}$  and in salinity of  $0.044\text{‰}$ ; these values are nearly the same from the surface down to 150 or 160 m, while at greater depths the differences are much smaller.

The lateral mixing will now for December have the following effects:

$$\begin{aligned}\Delta t &= -160 \cdot 0.67 \cdot 10^{-7} \cdot 31.536 \cdot 10^6 \cdot B/H \cdot 400 \cdot 10^5 \\ &= -845 \cdot 10^{-8} \cdot B/H = -2.56 \cdot 10^{-8} \cdot B \\ \Delta S &= -160 \cdot 0.044 \cdot 10^{-7} \cdot 31.536 \cdot 10^6 \cdot B/H \cdot 400 \cdot 10^5 \\ &= -55.54 \cdot 10^{-8} \cdot B/H = -0.168 \cdot 10^{-8} \cdot B\end{aligned}$$

With  $B=0.3 \cdot 10^8$ , as before, we find in

$$\begin{aligned}\text{winter } \Delta t &= -0.064^{\circ}\text{C month}^{-1} \\ \Delta S &= -0.0042\text{‰ month}^{-1}\end{aligned}$$

Comparing with our values (eq. 7) for the

$$\begin{aligned}\text{summer } \Delta t &= -0.060^{\circ}\text{C month}^{-1} \\ \Delta S &= -0.0064\text{‰ month}^{-1}\end{aligned}$$

we find that the heat loss is slightly higher and the salt loss lower than in summer. This has been taken into consideration in our heat balance sheet Table 6.

In our salt balance sheet Table 11 with units  $\text{m month}^{-1}$  this means that  $330 \cdot \Delta S / 35.15 = 9.39 \cdot \Delta S = 0.060$  from the middle of January to the middle of September, while for the following three months we may introduce a linear decrease to  $9.39 \cdot 0.042 = 0.039$ , i.e. the values 0.053, 0.045, 0.039  $\text{m month}^{-1}$ .

7. *Vertical convection.* When cooling of the surface of an isolated column of water in the sea leads to vertical convection, it is easy by integration of the original temperature curve to compute the depth  $D$  to which the convection will reach when an amount of heat of  $Q \text{ kcal cm}^{-2}$  has been removed (Fig. 27). If an additional amount of heat  $\Delta Q$  is removed, this will suffice to reduce the temperature of the column  $D$  by  $\Delta Q / cD^\circ \text{C}$ , where  $c$  is the specific heat of the water. And it would suffice to give the same layer a temperature gradient of  $\Delta t / \Delta z = 2 \cdot \Delta Q / cD^2^\circ \text{C cm}^{-1}$ . Within a wide interval ( $-1 < t^\circ < 16$ ) the following relation is valid

$$\sigma_t = 0.130 + 0.8 \cdot S - (0.061 + 0.0054 \cdot t)t \quad (14)$$

from which

$$\Delta \sigma / \Delta z = 0.8 \cdot \Delta S / \Delta z - (0.061 + 0.0108 \cdot t) \cdot \Delta t / \Delta z,$$

and on the assumption of homohalinity we therefore have

$$\Delta \sigma / \Delta z = - (0.061 + 0.0108 \cdot t) \cdot 2 \Delta Q / cD^2$$

Within the surface layers in question  $d\sigma/dz$  is a sufficient measure of stability, and  $\Delta \sigma / \Delta z$  therefore may be said to measure the degree of instability which might be established by the removal of  $\Delta Q \text{ kcal cm}^{-1}$ . The expression  $\Delta \sigma / \Delta z$  will here be called the *destabilization*.

At St. M the vertical convection was seen until the end of January to reach approximately the same depths as if the water column had been isolated from the surroundings (Table 7). These depths have therefore been computed for the normal stations for the last day of each of the months September to February; they are shown in Fig. 28 together with the  $\sigma_t$ -curves for June–July 1935. It is seen that the smallest depths are reached in the choking area, a little to the west of St. III.

Fig. 29 illustrates a classical case from the theory of geophysics, namely the special case of the circulation theorem of Bjerknes known as the theorem of Sandström. Imagine two neighbouring water columns, e.g. those at two of the normal stations, to be isolated while cooled at the surface. At a certain time the vertical convection will have created two homogeneous water columns of different temperatures, salinities and—accordingly—densities. Let the two columns reach to approximately the same depth.

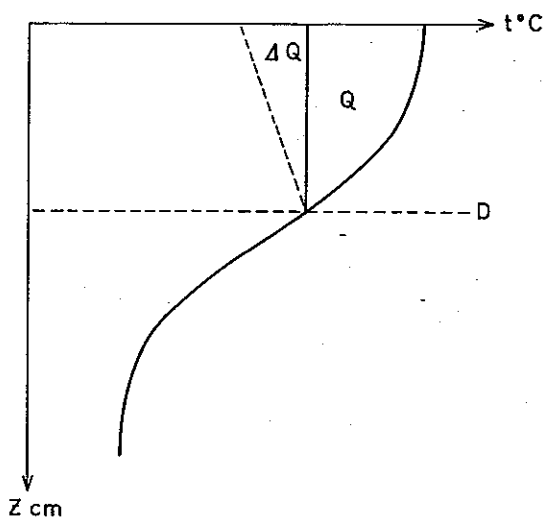


Fig. 27. Cooling of an isolated column.

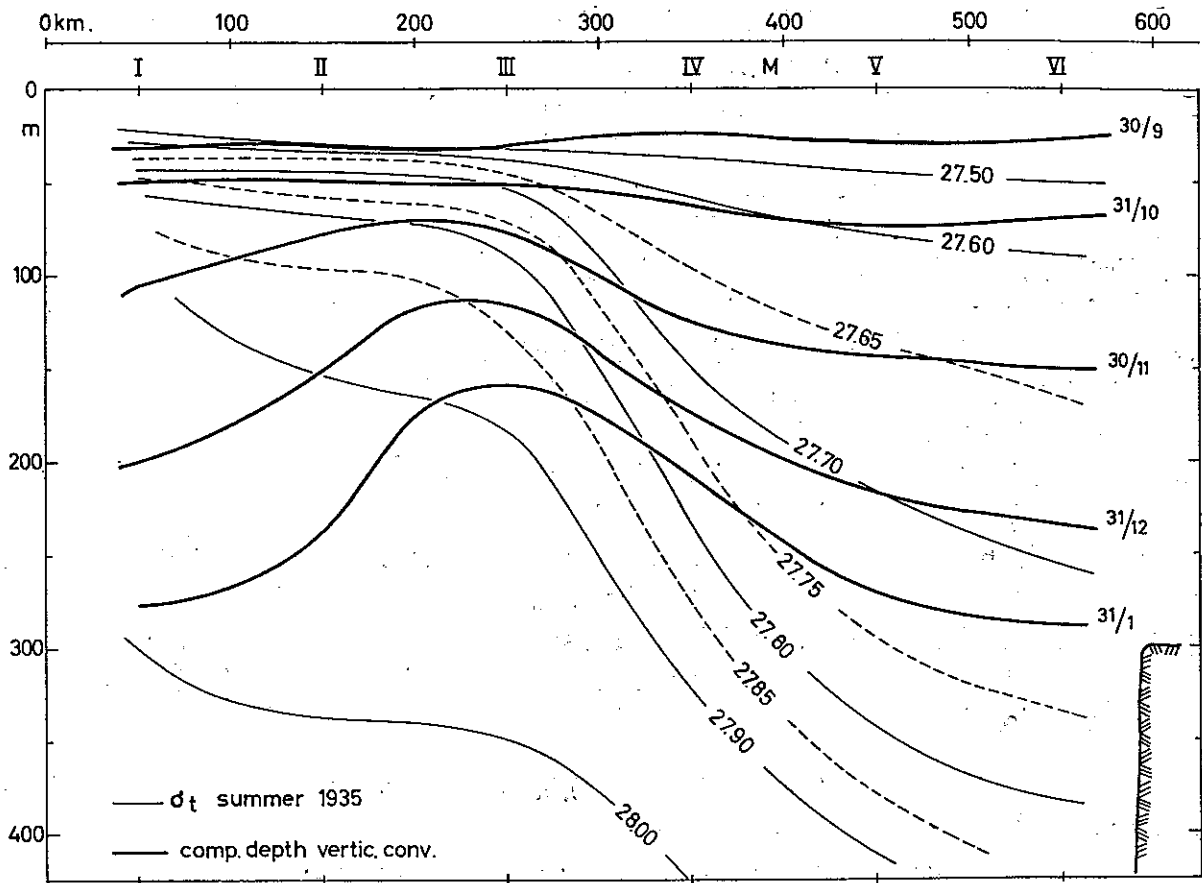


Fig. 28. Computed depth of vertical convection in the autumn (heavy) and distribution of  $\sigma_t$  in the summer of 1935 (light).

Removing now the isolating “wall” between them, we have a section characterized by horizontal isobars and vertical isosteres. The pressure gradient  $-\nabla p$  is directed upwards and the ascendant of the specific volume  $\nabla s$  is directed towards the east, since in the Atlantic current we find the lighter water in the east. In the theorem of Bjerknes we may now neglect the term for the rotation of the earth, and the effect will be an counterclockwise circulation, as indicated in the diagram. Or we may interpret the situation as done by Sandström for the land- and seabreeze, with the “cold source” on top. The intensity of the circulation is measured by the number of solenoids, which in this case means the horizontal density gradient of  $\Delta\sigma/\Delta x$ , where  $x$  is directed towards the east along the section. A theoretical solution to our problem appears difficult; in the following we shall use, for the said intensity, the name *stabilization*, which may then be expressed by  $\kappa(\Delta\sigma/\Delta x)$  where  $\kappa$  is a factor of proportionality.

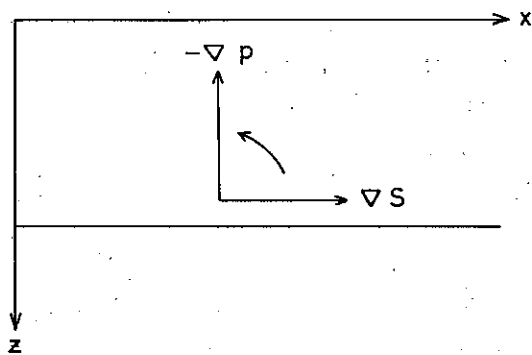


Fig. 29. The theorem of Sandström.

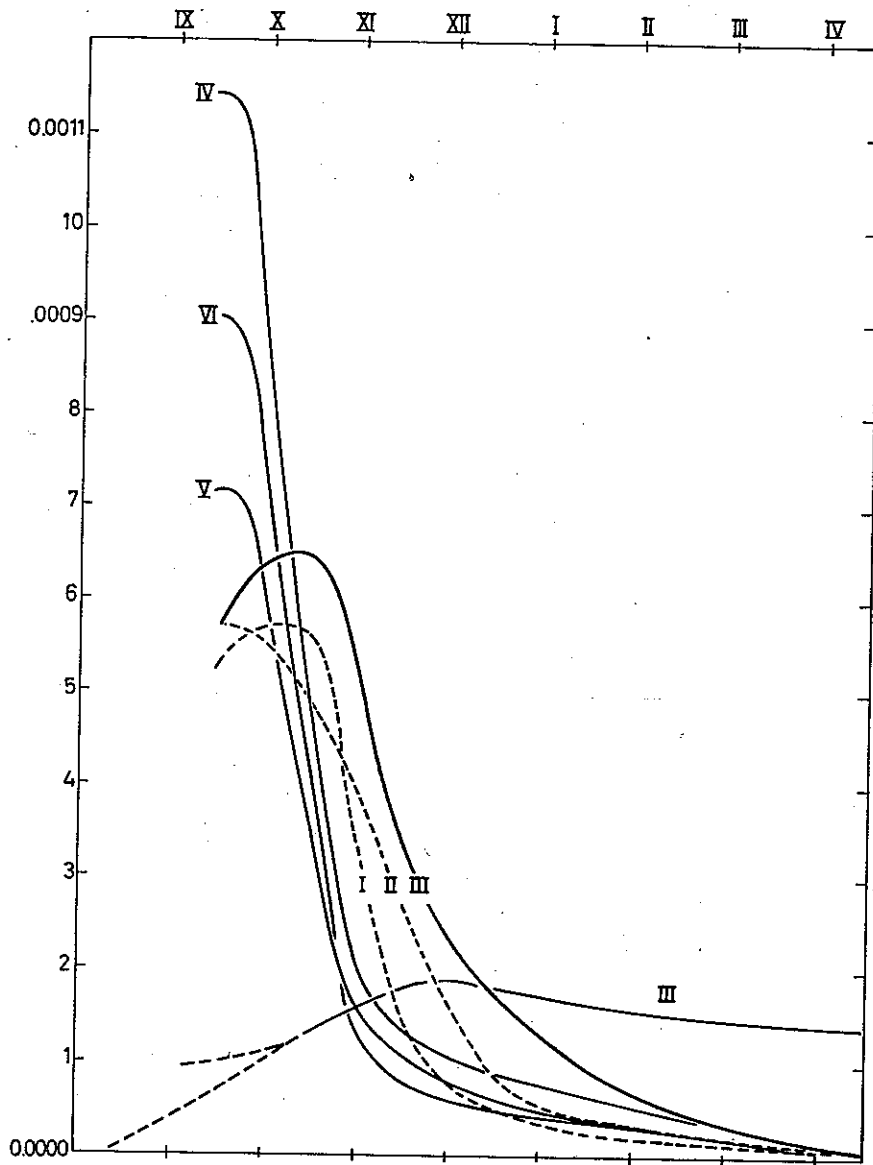


Fig. 30. Destabilization at normal stations and stabilization at St. III.

The intensity of the vertical convection may now be expressed as the difference between the intensities of destabilization and of stabilization, or

$$\text{Conv.} = \Delta\sigma/\Delta z - \kappa(\Delta\sigma/\Delta x) = -(0.061 + 0.0108 \cdot t) \cdot 2\Delta Q/cD^2 - \kappa(\Delta\sigma/\Delta x)$$

where  $t$  and  $\sigma$  are averages for the two homogeneous water columns considered.

When determining the destabilization  $\Delta\sigma/\Delta z$ , we have proceeded as follows. On the temperature curves for the normal stations the depths of every  $0.5^\circ \text{C}$  were read and from these depths it was easy to find the temperature limits for different amounts of heat contained above the same limits. Plots of heat contents *versus* temperature were used to find the temperature limit corresponding to the heat losses at the end of each month in autumn. From the station curves of temperature the depths  $D$  could now be

found directly. Introducing next into the expression for the destabilization the average temperature  $t$  of the column and its thickness  $D$  as well as the heat losses from month to month, and putting  $c \approx 1$ , we found the values plotted in Fig. 30. For each station we find a maximum value shortly after the cooling has started, at the beginning (Sts. II, IV, V, VI) or near the end (Sts. I, III) of October. The maxima are followed by values which are first decreasing rapidly, later more slowly. It is seen that from the end of October Station III shows higher values than any other station. At this station, therefore, any stabilizing effect will be balanced for the longest period.

The normal station curves for salinity were now used to find the approximate average salinity for each 25 m layer. From these the average salinity of each homogeneous layer  $D$  was easily found, and the average values of density were computed from eq. (14). The result is shown in Fig. 31. As the critical part of the section is at Station III, it may suffice to determine the horizontal density gradient in this position. Taking simply the differences  $\sigma_{II} - \sigma_{IV}$  divided by  $200 \text{ km} = 2 \cdot 10^7 \text{ cm}$ , we find for the stabilization the relative values given in Table 8.

Table 8. *Stabilization*

Date	$\frac{1}{2}(\sigma_{II} - \sigma_{IV}) \cdot 10^{-7}$	$\kappa \frac{\Delta\sigma}{\Delta x}$
30.IX	0.055 $10^{-7}$	0.000'104
31.X	.062	118
30.XI	.094	179
31.XII	.094	179
(1.I	.0905	172)
31.I	.087	165
28.II	.080	152
31.III	.076	144
30.IV	.075	142

In studying the heat balance, we found that the divergency obtained in the autumn seemed to disappear about the middle of January. Claiming now that at this time  $\text{Conv.} = 0$ , we find

$$0.090_5 \cdot 10^{-7} \cdot \kappa = 0.000'172$$

$$\kappa = 19'000$$

The values given in the last column of Table 8 are found on the basis of this value of  $\kappa$ . They are plotted on Fig. 30, in which it is seen that the stabilization increases in the autumn to a maximum in December, coming to an intersection with the destabilization curve for Station III in January. From this moment the stabilization is dominating.

The circulation arising through the establishment of a solenoidal field must have an effect of importance to our studies of heat and salt balance. As seen from the December measurements, Figs. 23 and 24, both temperature and salinity of the homogeneous layer decrease towards the west. The circulation therefore leads to a net transport

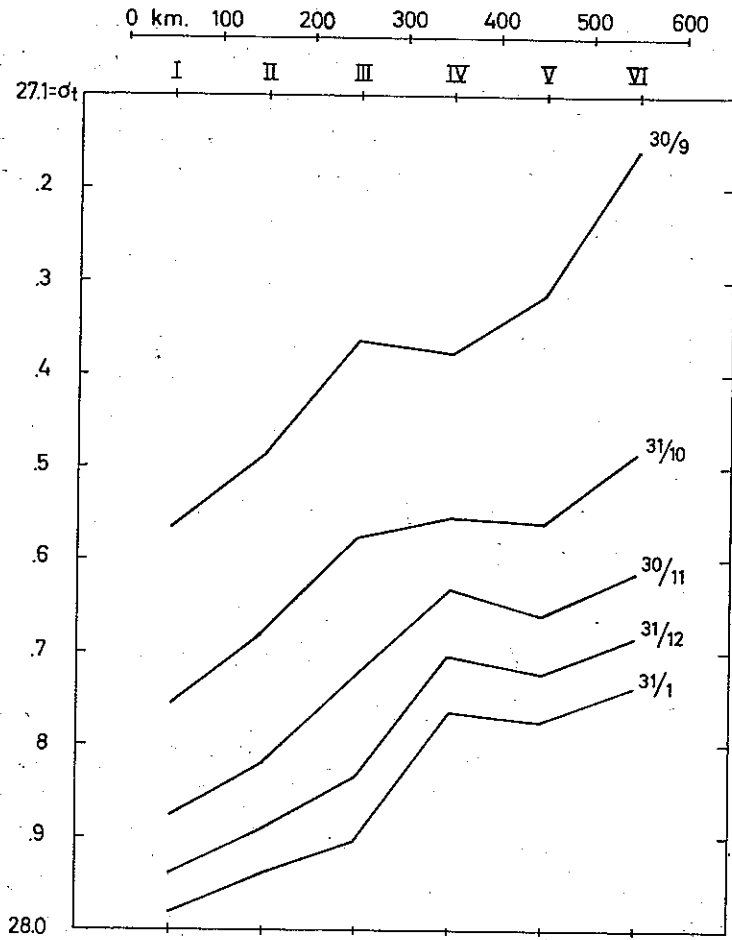


Fig. 31. Computed density distribution.

of both heat and salt westwards. This transport must be proportional to the circulation as well as to the horizontal gradients of temperature and salinity.

From the computed values of temperature and salinity of the isolated homogeneous water columns we find (Table 9) the following gradients between Stations IV and II (distance 200 km).

Table 9. Gradients between Stations IV and II

	$\frac{\Delta t}{\Delta x}$	$\frac{\Delta S}{\Delta x}$	$\frac{\Delta \sigma}{\Delta x}$	$\frac{\Delta t}{\Delta S}$
30.IX	$1.09 \cdot 10^{-7}$	$0.124 \cdot 10^{-7}$	$-0.055 \cdot 10^{-7}$	8.8
31.X	1.16 »	.104 »	.062 »	11.2
30.XI	1.46 »	.090 »	.099 »	16.2
31.XII	1.55 »	.087 »	.144 »	17.8
Mean	$1.32 \cdot 10^{-7}$	$0.101 \cdot 10^{-7}$	$-0.090 \cdot 10^{-7}$	13.1
1965	0.35 »	0.030 »	0.025 »	11.7
Ratio	0.27	0.30	0.28	

It is seen that  $\Delta t/\Delta x$  is increasing and  $\Delta S/\Delta x$  is decreasing with time; the ratio  $\Delta t/\Delta S$  is increasing. For the mean values the ratio is 13.1 or about the same as found for the gradients along the Atlantic current  $G_t: G_s = 0.40: 0.030 = 13.3$ . This means that the relative effects in temperature and salinity of the convection within the average section are as those of the Atlantic advection. This will facilitate our introduction of the convection in the following.

The values of Table 9 are based on computations for isolated water columns. In the last line but one of the table are given the corresponding values as deduced from the measurements in December 1965. They are considerably lower, less than one-third of the mean values; they give a ratio of 11.7 or not too far from 13.

The convective circulation is measured by the stabilization or by  $\Delta\sigma/\Delta x$  and gives rise to losses of heat and salt towards the west. These losses are proportional to the depth  $D$  of the homogeneous layer and further to the gradients  $-\Delta t/\Delta x$  and  $-\Delta S/\Delta x$ . They may therefore be expressed by

$$\begin{aligned}\Delta t &= K \cdot D \cdot \Delta\sigma/\Delta x \cdot \Delta t/\Delta x \\ \Delta S &= K \cdot D \cdot \Delta\sigma/\Delta x \cdot \Delta S/\Delta x\end{aligned}$$

where  $K$  is unknown but may be determined if the loss of heat or salt is known. As was seen above the assumption of no decrease of the effect of the Atlantic advection leads to the heat losses given in Table 6, column 10. These are introduced in Table 10, where the depths  $D_{\text{III}}$  are those computed for Station III, in the choke. The last value of  $K$  for December–January is low due to the small heat loss this month; it should be discarded since the convective process comes to an end within this period, and since before that one may expect a slow-down. The other values are of the same order of magnitude, giving an average  $\bar{K} \approx 1.1 \cdot 10^{10}$ . Using this value, we find—for comparison—the values of the heat losses  $\Delta t'$  given in the last column. By this  $\bar{K}$  or the above values of  $K$  we may compute the losses of salt to be expected. For our present use, however, this may be done in a simpler way, as will be shown later.

Table 10. Heat loss by convective circulation

Month	$\Delta t$	$D_{\text{III}}$ cm	$\frac{\Delta t}{\Delta x}$	$\frac{\Delta\sigma}{\Delta x}$	$K$	$\Delta t'$
IX–X	$-0.015^\circ\text{C}$	3200	$1.09 \cdot 10^{-7}$	$-0.055 \cdot 10^{-7}$	$0.78 \cdot 10^{10}$	$-0.02_1$
X–XI	.059	5200	.16	.062	1.58	.04 <sub>1</sub>
XI–XII	.118	7700	.46	.099	1.06	.12 <sub>2</sub>
XII–I	.031	11500	.55	.144	(0.12 <sub>1</sub> )	.28 <sub>2</sub> )

8. *Final balance.* As explained already, the heat balance of the Atlantic current was established (Table 6, Fig. 32) by claiming that the Atlantic advection, which appeared to keep constant within 10% ( $0.260 \pm 0.024^\circ\text{C month}^{-1}$ ) from January to September, should continue to do so for the rest of the year, the computed divergency

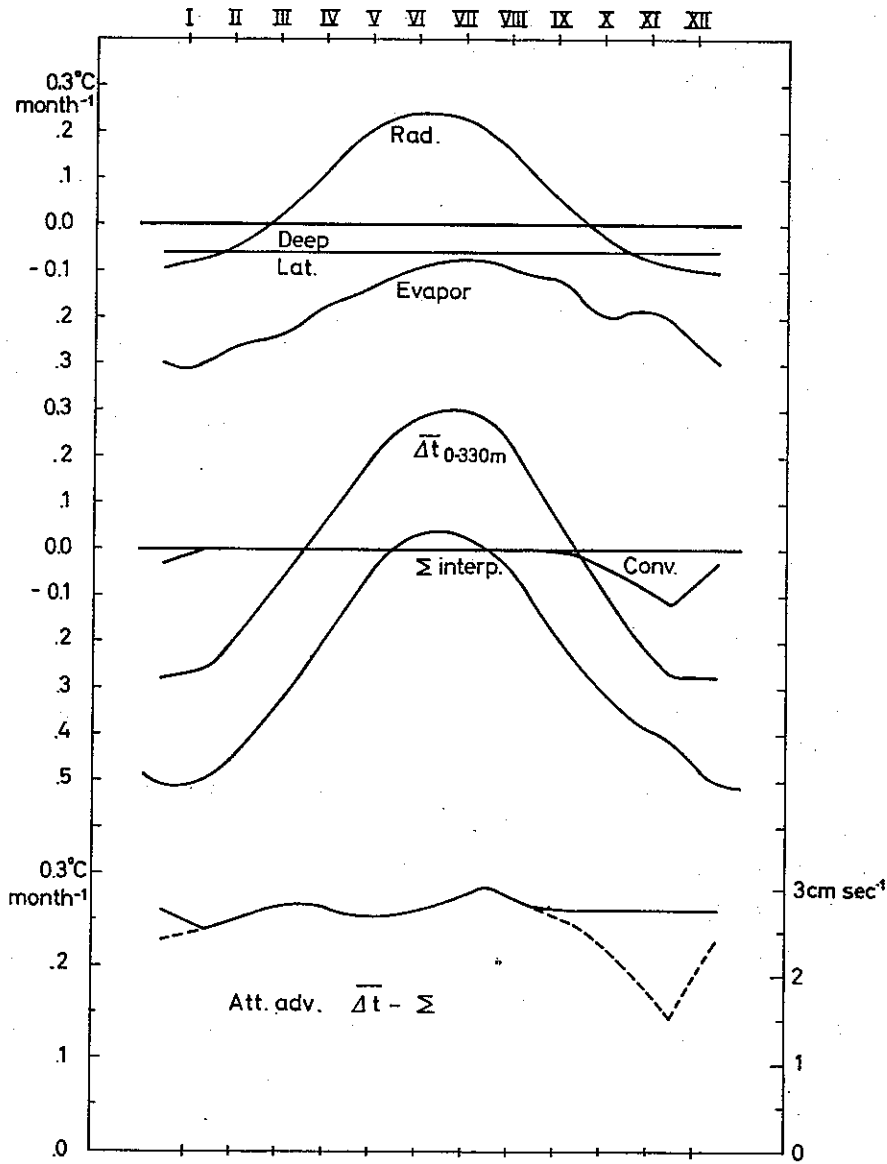


Fig. 32. Heat balance of the Atlantic current.

being assumed to be due to the convection in the autumn. For the salt balance, we have introduced the values corresponding to the total effect of advection and convection demonstrated in the lower part of Fig. 3. They are given in Table 11, and were found from the values of the ninth column of Table 6 by multiplication by

$$G_s H / G_s \bar{S} = 0.03 \cdot 330 / 0.40 \cdot 35.15 = 0.704$$

giving the amount of salt received, expressed in terms of the height of fresh water (metres per month) to be removed if the same result should be effected. Expressed in the same way are given, in the following columns of the table: the evaporation (annual total  $E=0.8 \text{ m year}^{-1}$ ), the diffusion through the sub-surface (vertical motion due to bottom water formation  $50 \text{ m year}^{-1}$ ), the lateral mixing and the precipitation (annual



total  $P=1.0$  m year<sup>-1</sup>). Finally the accumulation of salt has been taken into consideration as follows. From the average monthly values of salinity at St. M the mean values of salinity between the surface and 330 m (the level of 35.00‰) were first determined by integration. As apparent irregularities remained, these values were smoothed by taking the means of five consecutive months. From the smoothed curve the changes of  $\bar{S}_{0-330m}$  from month to month were determined; they are given (with negative values for increasing salinity and *vice versa*) in the last column but one of Table 11.

Table 11. Salt balance of the Norwegian Atlantic current at 66° N, expressed in equivalent metres of fresh water removed

Month	Atl. adv.	Evapor.	Deep	Lat.	Precip.	-Accum.	$\Sigma = -F$
I	+0.168	+0.101	-0.021	-0.060	-0.102	-0.023	0.063
II	.180	.089	.020	.060	.088	.030	.071
III	.187	.074	.021	.060	.071	.032	.077
IV	.179	.057	.021	.060	.064	.028	.063
V	.178	.044	.021	.060	.057	.017	.067
VI	.187	.035	.020	.060	.054	.017	.071
VII	.201	.038	.021	.060	.057	+0.009	.110
VIII	.187	.048	.021	.060	.070	.026	.110
IX	(.172) .183	.063	.020	.060	.096	.036	(.095) .106
X	(.142) .183	.072	.021	.053	.111	.034	(.063) .104
XI	(.100) .183	.080	.021	.046	.119	.036	(.030) .113
XII	(.161) .183	.099	.021	.039	.112	.006	(.094) .116
	(2.042) 2.199	+0.800	-0.249	-0.678	-1.001	0.000	(0.914) 1.071

All elements of this table are plotted in Fig. 33, in the lower part of which are seen the total effects of all the factors mentioned; they are to be balanced by the fresh water  $F$  from the Norwegian and other coasts through the coastal current. The annual total is found to be 1.07 m, in fair agreement with the value 1.15 m, which was obtained above. The curve shows a nearly constant value of 0.07 m month<sup>-1</sup> from January to June, followed by 0.11 m month<sup>-1</sup> from July to December. This may be understood as follows.

From observations from St. M for 1948-1958 (HELLAND 1963, Table 2) it is found that the increase of temperature from May to August at 0, 10 and 25 m depth is 4.49, 4.49 and 3.75°, while at 50 to 150 m we find between 1.61 and 0.60°. A considerable amount of the accumulated heat is thus stored in the uppermost layer, in which the salinity decreases by 0.20, 0.17 and 0.09‰, while in the lower layer it increases by 0.01 to 0.03‰. In the increasingly stabilized surface layer the low salinity water of the coastal current spreads relatively freely from the shelf into the area around St. M, leading after two months to the sudden increase shown by the lower curve in Fig. 33.

The vertical convection in autumn leads to a net loss of heat and salt towards the west. The loss of heat is compensated for by the higher amounts of heat conveyed by

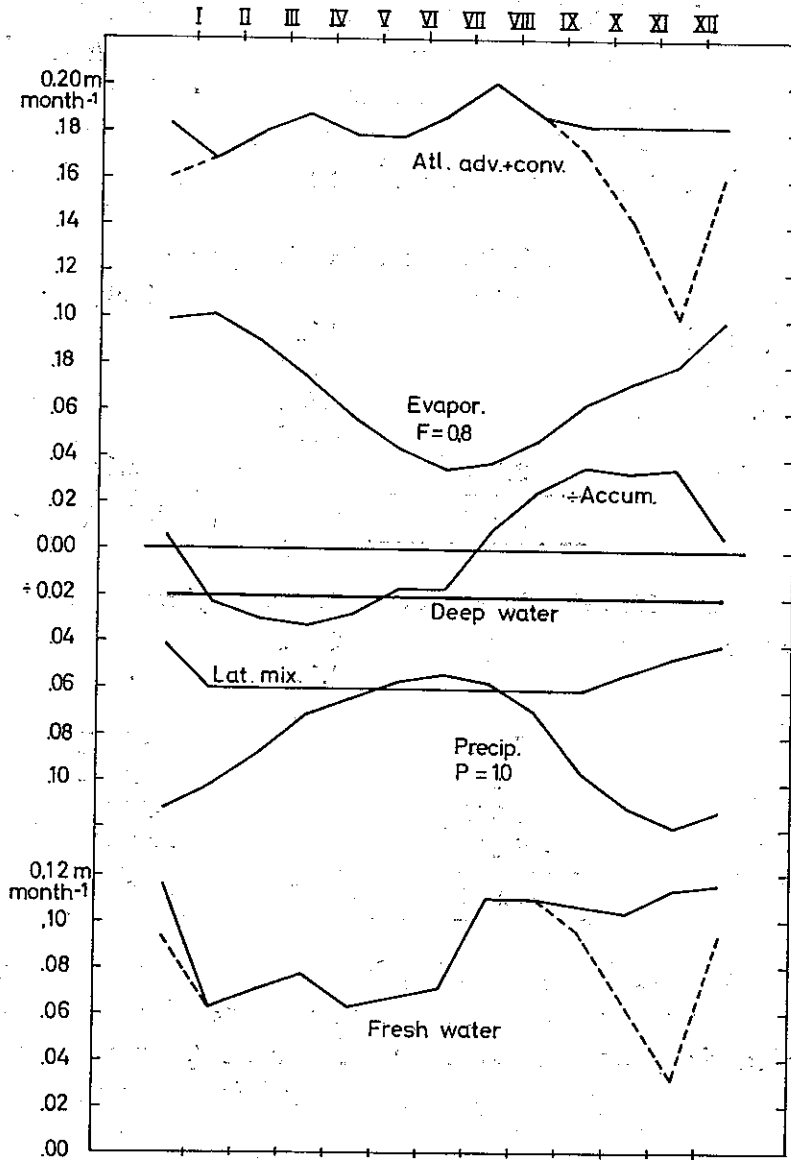


Fig. 33. Salt balance of the Atlantic current.

the Atlantic advection (Fig. 32, lower curve). Similarly the loss of salt is compensated for by the higher amounts of salt also conveyed by the Atlantic advection (Fig. 33, upper curve), whereby the computed amounts of fresh water removed (Table 11, last column giving  $\Sigma = -F$ ) and accordingly conveyed through the coastal current become higher in autumn (Fig. 33, lower curve). The drop of the values does not follow until January, at the time when the choke is closed.

This indicates the existence of a sensitive mechanism, by which the opening and closing of the choke may seem to control the speed of absorption of coastal water by the Atlantic current. A more reasonable assumption would be that the absorption of coastal water has an influence upon the whole system so as to determine the time for closing the choke. In summer the coastal water enters the Atlantic current in the surface

layer, while in autumn it is absorbed into an increasingly thick layer due to the vertical convection. The amount of coastal water conveyed into the Atlantic current must necessarily affect the whole stratification and thus also the choke.

From the last lines of Tables 6 and 11 we have finally compiled the balance for the whole year in Tables 12 and 13. These tables show that 82% of the heat is received

Table 12. *Heat balance in °C year<sup>-1</sup>*

Net radiation	0.683		17.9%	
Evaporation (0.8 m)		-2.132		-56.0%
Deep water (50 m)		-0.720		-18.9%
Lateral mixing		-0.732		-19.2%
Convection		-0.223		-5.9%
Atlantic advection	3.124		82.1%	
	3.807	-3.807	100.0%	-100.0%

Table 13. *Salt balance in equivalent m year<sup>-1</sup> of fresh water*

Atlantic advection		2.042		68.1%
Convection		0.157		5.2%
Evaporation		0.800		26.7%
Deep water	-0.249		-8.3%	
Lateral mixing	-0.678		-22.6%	
Precipitation	-1.001		-33.4%	
Fresh water	-1.071		-35.7%	
	-2.999	2.999	-100.0%	100.0%

through the Atlantic advection, only 18% from the net radiation, while 56% is lost by evaporation. Of the salt received 68% is due to the Atlantic advection and 27% to evaporation; of the fresh water needed for balance, 36% is run-off, 33% precipitation and 31% is due to loss of salt mainly by lateral mixing, but also to the deep water.

## REFERENCES

- ÅNGSTRÖM, A. (1920): Applications of heat radiation measurements to the problems of the evaporation from lakes and the heat convection at their surfaces. *Geogr. Ann.* H. 3. Stockholm.
- BALAKSHIN, L. L. (1959): The water circulation and bottom contour of the northern part of the Greenland Sea. *Intern. Ocean. Congr.* N.Y. Sept. Preprints. Washington D.C. p. 430.
- BUDYKO, M. L. (1963): Atlas of heat balance. (In Russian) Leningrad.
- BØYUM, G. (1966): The energy exchange between sea and atmosphere at ocean Weather Stations M, I and A. *Geof. Publ.* XXVI, No. 7.
- DANSK METEOROLOGISK AARBOG (1948-1958): København 1950-1964.
- EGGVIN, J., H. KISMUL and S. LYGREN (1963): *Bathymetric chart of the Norwegian Sea.* Bergen.
- HELLAND, P. (1963): Temperature and salinity variations in the upper layers at ocean Weather Station M. *Univ. Bergen Arb. mat.-naturv. R.* No. 16.
- HELLAND-HANSEN, B. (1934): The Sognefjord Section. *James Johnstone Memorial Volume.* Liverpool. pp. 257-274.
- HELLAND-HANSEN, B. (1935): *Årsberetn. Geof. inst.* 1934-35.
- HELLAND-HANSEN, B. (1936): *Årsberetn. Geof. inst.* 1935-36.

- HELLAND-HANSEN, B. (1937a): New investigations in the Norwegian Sea. *Assoc. d'Océanogr. Phys. Proc. Verb.*, No. 2.
- HELLAND-HANSEN, B. (1937b, 1938): *Årsberetn. Geof. inst.* 1936-37, 1937-38.
- HELLAND-HANSEN, B. (1939): Untersuchungen über örtliche und zeitliche Schwankungen des "Golfstroms" im Norwegischen Meer, und Planlegung einer internationalen Golfstromuntersuchung im Nordatlantischen Ozean. *Norsk geogr. Tidsskrift VII*, Hefte 5-8.
- HELLAND-HANSEN, B. (1940): The international survey of the Gulf Stream Area. Presidential Address. *Assoc. d'Océanogr. Phys. Proc. Verb.*, No. 3.
- HELLAND-HANSEN, B. and F. NANSEN (1909): The Norwegian Sea. Its physical oceanography based upon the Norwegian Research 1900-1904. *Rep. Norw. Fish. Mar. Inv. II*, No. 2.
- JACOBSEN, J. P. (1925): Die Wasserumsetzung durch den Öresund, den Grossen und den Kleinen Belt. *Medd. fra Komm. for Havunders.*, Serie: Hydrogr. II, No. 9.
- MOSBY, H. (1936): Verdunstung und Strahlung auf dem Meere. *Ann. d. Hydrogr. u. Mar. Met. Juli*.
- MOSBY, H. (1954): Oceanographical investigations at Weather Station M. *Univ. Bergen Årb. naturv. R.*, No. 10.
- MOSBY, H. (1959): Deep water in the Norwegian Sea. *Geof. Publ. XXI*, No. 3.
- MOSBY, H. (1961): Recording the formation of bottom water in the Norwegian Sea. *Proc. Symp. Mat.-Hydrodyn. Meth. Phys. Oceanogr. Hamburg*.
- MOSBY, H. (1962): Water, salt and heat balance of the North Polar Sea and of the Norwegian Sea. *Geof. Publ. XXIV*, No. 11.
- MOSBY, H. (1967): Bunnvannsdannelse i havet. The Nansen Mem. Lecture Oct. 11, 1965. The Norwegian Academy of Science and Letters, Oslo.
- MOSBY, H. (1969): Norwegian Atlantic current. March and December 1965. Tables. *Geoph. Inst. Stensil*, No. 17.
- NORSK METEOROLOGISK ÅRBOK 1948-1958. Oslo 1949-1960.
- SANDSTRØM, J. W. and B. HELLAND-HANSEN, (1903): Über die Berechnung von Meeresströmungen. *Reports on Norw. Fish. and Mar. Inv. II*, 1902, No. 4.
- SKAAR, J. (1955): On the measurement of precipitation at sea. *Geof. Publ. XIX*, No. 6.
- SPINNANGR, F. (1958): Some remarks on precipitation measurements at sea. *Met. Ann. IV*, No. 7. Oslo.
- SVERDRUP, H. U., M. W. JOHNSON, and R. H. FLEMING, (1946): *The oceans, their physics, chemistry and general biology*. New York.
- SÆLEN, O. H. (1959): Studies in the Norwegian Atlantic current. Part I, the Sognefjord section. *Geof. Publ. II*, No. 13.
- SÆLEN, O. H. (1963): Studies in the Norwegian Atlantic current, Part II, investigations during the years 1954-59 in an area west of Stad. *Geof. Publ. XXIII*, No. 6.
- TAIT, J. B. (1957): Hydrography of the Faroe-Shetland Channel, 1927-1952. Scottish Home Dept. *Mar. Res. No. 2*. Edinburgh.
- TOLLAN, A. (1968): Vannbalansen i Norden. Rapport til 5. Nordiska Hydrologkonferensen 23-27. August 1967, Helsingfors. (Stencil).
- ZAITZEV, E. N. (1960): The heat balance of the Norwegian and Greenland Seas and factors governing its formation. *Soviet Fisheries Investigations in North European Seas*. (In Russian), Moscow.

## APPENDIX

Corrections to HÅKON MOSBY: "Deep water in the Norwegian Sea". *Geof. Publ.* Vol. XXI, No. 3, Oslo 1959.

1. In this paper the deep water in the Norwegian Sea was carefully studied on the basis of the observations from Weather Ship Station M from October 1948 to June 1956. From Table 13 and Fig. 21 on pp. 34–35 the changes of salinity are seen to be small, with the main exception that the values for the period from December 1948 to May 1950 are clearly higher than the others. No explanation of this was found until 1964, when Mr. R. LEINEBØ, at that time one of my students, went very carefully into the details of the original journals. He found that a small error had been made when correcting the titration results by means of Standard Sea Water. The conclusion was that *all salinities for the period mentioned, were 0.013‰ too high*. When subtracting this value from the salinities in question, the sudden rise in December 1948 and the drop in 1950 disappears, and only minor changes are found from 1948 to 1968. This correction does not effect any of the conclusions otherwise drawn in the paper.

2. The oxygen values from the *Armauer Hansen* in 1935 were only briefly treated in the paper referred to. The samples had to be stored on board until they could be brought ashore for titration, and the results may be subject to some doubt. It has been demonstrated that all oxygen values from Stations 182 and 184 are about 0.2 ml/l lower than those from all other stations. It therefore seems probable that the *vertical distribution demonstrated in Fig. 8, p. 16 is misleading*.